This is to certify that the

dissertation entitled

Interactions Between Stream-Wetland Boundaries and an Aquifer Stressed by a Pumping Well

presented by

Yakup Darama

has been accepted towards fulfillment of the requirements for

PhD degree in Civil and Environmental Engineering

Roger B. Wallace
Major professor

Date 7/6/91

INTERACTIONS BETWEEN STREAM-WETLAND BOUNDARIES AND AN AQUIFER STRESSED BY A PUMPING WELL

By

Yakup Darama

A DISSERTATION

Submitted to
Michigan State University
in partial fulfillment of the requirements
for the degree of

DOCTOR OF PHILOSOPHY

Department of Civil and Environmental Engineering

1991

ABSTRACT

INTERACTIONS BETWEEN STREAM-WETLAND BOUNDARIES AND AN AQUIFER STRESSED BY A PUMPING WELL

By

Yakup Darama

The rates of stream depletion (q_r) and captured wetland evapotranspiration (q_a) caused by a pumping well located in a connecting water table aquifer are studied.

An analytical model is developed to predict q_r caused by cyclic pumping from a deep phreatic aquifer. Equations and dimensionless plots are developed for the volume of stream depletion over a pumping cycle (v_{cyc}) and for the maximum rate of stream depletion at dynamic equilibrium. These plots provide a way to determine the time required to reach equilibrium and the error in q_r produced by neglecting the nonuniform pumping rate within a pumping cycle. Analysis showed that v_{cyc} ending at time t, is equal to the volume of stream depletion between the start of pumping and time t by continuous pumping and under some circumstances, approximating the effects of cyclic pumping by a continuous pumping at the equivalent cycle-average rate is not adequate.

A second analytical model is developed to predict q_r and q_a caused by a continuously pumping well located in a shallow phreatic aquifer. Linear variation of q_a as a function of the drawdown of the water table is incorporated to the model. Scaled plots of q_r are developed for transient and for steady

state conditions. Analysis showed that as the pumping distance increases, q_a increases, while q_r decreases, and the system reaches equilibrium faster. Analysis also showed that linear ET assumption can produce errors in q_r, and q_a.

A third model is developed to predict the steady state q_r by a pumping well including the effects of the nonlinear variation of q_a as a function of water table depth. Dimensional analysis is used to determine the relationship between the scaled q_r, the scaled pumping distance (a/h_d), the scaled hydraulic conductivity (K_S/PET), and the scaled initial depth to the water table $((d_i/h_d)^n)$. Families of scaled graphs are developed for a wide range of these parameters. Analysis showed that (1) $(d_i/h_d)^n$ has an increased effect on q_r as K_S/PET increases, and (2) q_r decreases as K_S/PET decreases while $(d_i/h_d)^n$, and a/h_d increase.

This dissertation is dedicated to my wife Mahkame for her continuous support and deep love.

ACKNOWLEDGEMENTS

The author wishes to express his deep appreciation and gratitude to his advisor Dr. Roger B. Wallace for his continuous encouragement, assistance and useful suggestions throughout this study.

He also wishes to thank for interest and cooperation of the other committee members, Dr. David C. Wiggert of the Department of Civil and Environmental Engineering, Dr. George Merva of the Department of Agricultural Engineering and Dr. Raymond Kunze of the Department of Crop and Soil Sciences.

He is particularly grateful to the Ministry of Education of the Republic of Turkey for awarding him a National Science Scholarship. Also, Division of Engineering Research and Institute of Water Research are acknowledged for the partial financial support of this research.

The author also wishes to express his appreciation to his colleague and friend Michael D. Annable for his valuable suggestions during this study.

Valuable suggestions of Dr. Arthur T. Corey in development of the last stage of this dissertation are appreciated.

The author also wishes to express his appreciation to the reviewers of Water Resources Research, AGU who reviewed

earlier versions of the third and the fourth chapters and provided helpful comments.

Most of all, the author would like to express his sincere gratitude to his beloved parents for whom he has deep respect and love.

TABLE OF CONTENTS

CHAPTER ..... PAGE

LIST OF FIGURES ix

LIST OF TABLES xii

NOMENCLATURE xiii

CHAPTER I. INTRODUCTION 1

1.1. Objective and Scope of the Study 3

1.1.1. Objective 3
1.1.2. Scope 4

CHAPTER II. LITERATURE REVIEW 6

2.1. Introduction 6

2.2. Stream Depletion by Pumping Wells 6

2.3. Steady State Evaporation from the Water Table 11

2.4. Summary 15

CHAPTER III. STREAM DEPLETION BY CYCLIC PUMPING OF WELLS 17

3.1. Introduction 17

3.2. Stream Depletion During a Single Pumping Cycle 19

3.2.1. Stream Depletion During Pumping 19
3.2.2. Stream Depletion After Pumping Stops 21

3.3. Rate of Stream Depletion During Cyclic Pumping 23

3.3.1. Conceptual Description 23
3.3.2. Analytical Solution for Stream Depletion 23

3.4. Volumetric Stream Depletion During One Cycle of Pumping 27

3.4.1. Graphical Interpretation 27
3.4.2. Analytical Solution 29

3.5. The Approach to and the Conditions at Dynamic Equilibrium 31

3.5.1. Conceptual Description 31
3.5.2. Dependence of τ on the Pumping Cycle Characteristics, Aquifer Response Time, and Time 31
3.5.3. Accuracy of Stream Depletion Rates Calculated with the Cycle-Average Pumping Rate 40

3.6. Summary and Conclusions 42

CHAPTER IV. STREAM DEPLETION BY A PUMPING WELL INCLUDING THE EFFECTS OF LINEAR VARIATION OF CAPTURED WETLAND EVAPOTRANSPIRATION 47

4.1. Introduction 47

4.2. Analytical Model Development 49

4.2.1. Model Assumptions 49
4.2.2. Flow Equation 51
4.2.3. The Relationship Between d_o, *PET*, and Soil Properties 57
4.2.4. Solutions for Drawdown, Stream Depletion Mined Water, and Captured ET 62
4.2.5. Discussion of the Solution 72

4.3. Solution of Partial Differential Equation Using A 2-D Finite Element Model 75

4.3.1. Formulation and Description of the Hypothetical Aquifer for 2-D Finite Element Model Application 75
4.3.2. Comparison of the Analytical Model and 2-D Finite Element Model Results 80

4.4. Summary and Conclusions 81

CHAPTER V. STREAM DEPLETION BY A PUMPING WELL INCLUDING THE EFFECTS OF NONLINEAR VARIATION OF CAPTURED WETLAND EVAPOTRANSPIRATION 87

5.1. Introduction 87

5.2. Model Development 90

5.2.1. Model Assumptions 90
5.2.2. Flow Equation 91
5.2.3. The Nonlinear Relationship for q_e as a function of the depth to water table 96
5.2.3. Scaling the Flow Equation 98

5.3. Numerical Solution of Flow Equation for Hypothetical Situation 105

5.3.1. The Hypothetical Aquifer 106
5.3.2. Accuracy of the Solution 108
5.3.3. Discussion of Scaled Families of Curves for Stream Depletion 118

5.4. Summary and Conclusions 124

CHAPTER VI. SUMMARY AND CONCLUDING REMARKS 128

APPENDICES 136

APPENDIX A: Solution of Equation 4.8 by Laplace Transformations 137

APPENDIX B: Listing of Computer Program for Stream Depletion Caused by Cyclic Pumping of Wells 141

APPENDIX C: Listing of Computer Program for Stream Depletion by a Pumping Well Including the Effects of Linear Variation of Wetland ET 151

LIST OF REFERENCES 160

LIST OF FIGURES

Figure 3.1. Cross section of the aquifer described by analytical method 18

Figure 3.2. Stream depletion during constant-steady pumping 21

Figure 3.3. Stream depletion during and after pumping 22

Figure 3.4. Construction of total stream depletion with the method of superposition for series of cyclic pumping 24

Figure 3.5. Example calculation of the rate of stream depletion Equation 3.6 at t = 450 days 26

Figure 3.6. (a) Construction of total stream depletion for cyclic pumping when t_p and t_d are constant and (b) detail of Figure 3.6a between t-t_d and t 28

Figure 3.7. (a) Total stream depletion during the cycle ending at t and (b) alternate representation of Figure 3.7a 30

Figure 3.8. The dependence of τ, the dimensionless volume of stream depletion during one cycle on the scaled times α and γ 33

Figure 3.9. Comparison of stream depletion rate caused by cyclic pumping and the equivalent cycle-average rate of steady-continuous pumping when γ = 900 39

Figure 3.10. The accuracy of stream depletion rates calculated with the cycle-average pumping rate 43

Figure 3.11. Comparison of stream depletion rate caused by cyclic pumping and the equivalent cycle-average rate of steady-continuous pumping when γ = 0.5 and τ = 0.95 44

Figure 4.1. Cross section of the semi-infinite stream-wetland aquifer system during pumping 48

Figure 4.2. Cross section of the leaky water table aquifer during pumping (After Hantush, 1964a) 54

Figure 4.3. Cross section of the semi-infinite stream-wetland aquifer system before pumping 55

Figure 4.4. Dependence of evapotranspiration on depth to water table when K_s = 3000 cm/day 59

Figure 4.5. Linear and nonlinear dependence of captured ET, q_{et}, on the depth to water table 61

Figure 4.6. Transient behaviour of stream depletion and captured ET rates when pumping is continuous 65

Figure 4.7. The dependence of τ_{et} and τ_{em} during continuous pumping on ϵ, the scaled pumping distance, and α, the scaled time 68

Figure 4.8. Dependence of τ_{et}, the scaled steady state stream depletion on ϵ, the scaled pumping distance when ET varies as a linear function of water table depth 71

Figure 4.9. Comparison of steady state stream depletion rates obtained from the nonlinear ET model (AQUIFEM) when d_C=0.151 m, with the depletion rates obtained from the linear ET model for different values of d_0 (Analytical model) 74

Figure 4.10. (a) Plan view of the hypothetical aquifer, (b) cross section II - II′, (c) cross section I - I′ 77

Figure 4.11. Comparison of the boundary fluxes produced by the analytical model and by the 2-D finite element model 79

Figure 4.12. Water table profile computed by the 2-D finite element model along the cross section II - II′ at t = 2000 days 82

Figure 4.13. Water table profile computed by the 2-D finite element model along the cross section I - I'at t = 2000 days 83

Figure 5.1. Cross section of the semi-infinite stream-wetland aquifer system described by Equation 5.1 92

Figure 5.2. Cross section of the semi-infinite stream-wetland aquifer system prior to pumping 94

Figure 5.3. (a) Dependence of steady state ET flux on the depth to water table, (b) Dependence of steady state captured ET flux on the depth to water table 97

Figure 5.4. Comparison of the stream depletion rates obtained from the linear ET, the nonlinear ET, the step ET, and no ET models when a = 500 m, K_s=43.2 m/d, and d_i= 0.01 m 110

Figure 5.5. Comparison of the stream depletion rates obtained from the linear ET, the nonlinear ET, the step ET, and no ET models when a = 500 m, K_s=8.64 m/d, and d_i= 0.01 m 111

Figure 5.6. Comparison of the stream depletion rates obtained from the linear ET, the nonlinear ET, the step ET, and no ET models when a = 500 m, K_s=.864 m/d, and d_i= 0.01 m 112

Figure 5.7. Variation of captured boundary fluxes obtained from the nonlinear ET model when a=1000 m, K_s=8.64 m/d, d_i=0.1 m 116

Figure 5.8. Dependence of the scaled steady state stream depletion on the scaled pumping distance and the scaled initial depth to water table when $K_s/PET = 10^4$ 121

Figure 5.9. Dependence of the scaled steady state stream depletion on the scaled pumping distance and the scaled initial depth to water table when $K_s/PET = 10^3$ 122

Figure 5.10. Dependence of the scaled steady state stream depletion on the scaled pumping distance and the scaled initial depth to water table when $K_s/PET = 10^2$ 123

LIST OF TABLES

Table 3.1. Data for dimensionless volume of stream depletion, τ, corresponding to selected values of α and γ 34

Table 3.2. Range of values of hydraulic conductivity, specific yield, aquifer thickness, transmissivity, and γ 36

Table 3.3. Values of time to practical state of dynamic equilibrium, t_e, at τ=0.95 for corresponding values of γ 38

Table 3.4. Values of β corresponding to selected values of λ and γ 41

Table 4.1. Characteristics of the hypothetical aquifer 78

Table 4.2. Characteristics of the grid configurations used in the 2-D finite element model 78

Table 5.1. Range of values of aquifer parameters used in the nonlinear ET model 107

Table 5.2. Comparison of the scaled steady state q_r obtained from configurations 2 and 3 118

NOMENCLATURE

a perpendicular distance from the pumped well to the stream, [L].

a_0 the first term in the summation of infinite series in Equation 4.5, [1].

a_s soil parameter in Gardner's unsaturated hydraulic conductivity function.

A_n soil parameter function in Warrick's equation, [1].

b aquifer thickness, [L].

$\bar{b}$ average saturated thickness, [L].

b' thickness of the semi permeable layer, [L].

b_s soil parameter in Gardner's unsaturated hydraulic conductivity function.

B evapotranspiration capture coefficient, [L].

C coefficient to determine the value of d_0 in Equation 4.14, [1].

d depth to the water table at time t, [L].

d_c depth where evapotranspiration is less than potential evapotranspiration, [L].

$\bar{d}_c$ average critical depth where evapotranspiration flux is zero, [L].

d_i initial depth to water table, [L].

d_0 water table depth where linear ET is approximately zero, [L].

ET evapotranspiration rate, [L/T].

F flux per unit area that leaves or enters the aquifer, [L/T].

h piezometric head in the aquifer at $t > 0$, [L].

h_b depth of water in a piezometer that is open at the base of the aquifer, [L].

h_d displacement head at imbibition cycle, [L].

h_i required elevation of the piezometric surface for evapotranspiration to be equal to the potential rate, [L].

h_0 initial head in the aquifer at $t = 0$, [L].

$\bar{h}$ average piezometric head in the aquifer at $t > 0$, [L].

i index that counts the number (less one) of pumping periods each of duration t_p.

j index that counts the number of terms in the summation of the terms in Warrick's equation for steady state ET flux.

K' hydraulic conductivity of the semi-permeable layer, [L/T].

K_C unsaturated hydraulic conductivity, [L/T].

K_S saturated hydraulic conductivity, [L/T].

n pore-size distribution parameter in Anat et al.'s and Warrick's equation.

N total number of pumping periods in time t.

P_C capillary pressure, [M/LT^2].

PET potential evapotranspiration rate, [L/T].

q steady state evaporation flux in Gardner's equation, [L/T].

q_0 stream depletion rate produced by the first pumping cycle at $t > 0$, [L^3/T].

q_1 stream depletion rate produced by the second pumping cycle at $t > 0$, [L^3/T].

q_b groundwater flow to the stream before pumping, [L^3/T].

q_{br} groundwater flow to the stream during pumping, [L^3/T].

q_C rate of stream depletion caused by continuous steady pumping at dynamic equilibrium where the effects of captured evapotranspiration are not accounted, [L^3/T].

q_e evapotranspiration flux at a point calculated by Warricks and Anat et al relationships, [L/T].

q_{et} captured evapotranspiration flux at a point, [L/T], or captured evapotranspiration rate from the entire surface area at time $t > 0$, [L^3/T].

q_l rate of leakage from the lower confined aquifer to the phreatic aquifer, [L^3/T].

q_m rate of mined water from the aquifer storage at time $t > 0$, [L^3/T].

q_{max} maximum rate of stream depletion caused by cyclic pumping at dynamic equilibrium, [L^3/T].

q_r rate of stream depletion at time $t > 0$, [L^3/T].

q_s horizontal boundary flux, [L/T].

Q pumping rate, [L^3/T].

Q_{td} cycle-average pumping rate, [L^3/T].

r radial distance between the pumping well and an arbitrary point P, [L].

r' radial distance between the image well and an arbitrary point P, [L].

s drawdown in the aquifer produced by pumping well, [L].

sdf Jenkins' stream depletion function, [T].

S suction head, [L]

S_y specific yield of the aquifer.

t time since pumping started, [T].

t_a aquifer response time, [T].

t_e time to practical condition of dynamic equilibrium, [T].

t_d time for one complete cycle of pumping (on and off), [T].

t_p time for period of pumping during one cycle, [T].

$t_{\alpha i}$ $t-t_d i$, time parameter to simplify Equation 3.6, [T].

t_{ni} $t-t_p-t_d i$, time parameter to simplify Equation 3.6, [T].

T aquifer transmissivity, [L^2/T].

$U_{\alpha i}$ $\sqrt{t_a/[4(t-t_d i)]}$, scaled time to simplify Equation 3.6.

U_{ni} $\sqrt{t_a/[4(t-t_p-t_d i)]}$, scaled time to simplify Equation 3.6,

v_1 volume of stream depletion by continuous pumping from a deep water table aquifer starting time at time zero, [L^3].

v_2 volume of stream depletion by continuous pumping from a deep water table aquifer starting time at time t_p, [L^3].

v_{cyc} volume of stream depletion by cyclic pumping during the period $t-t_d$ to t, [L^3].

v_a volume of evapotranspiration captured by continuous pumping during time t, [L^3].

V_m volume of water mined from aquifer storage by continuous pumping during time t, [L^3].

V_r volume of stream depletion produced by continuous pumping during time t, [L^3].

$W()$ well function for leaky aquifers.

x rectangular coordinate system perpendicular to the river, [L]

y rectangular coordinate system along the river boundary, [L].

z depth to water table in Gardner's equation for steady state evaporation flux, [L]

Z parameter to simplfy Equations 4.5 and 5.5, [L^2].

Greek Letters

α t/t_a, scaled time

β error produced by approximating the effects of cyclic pumping by continuous-steady pumping at the equivalent cycle-average rate.

β_c $(0.5/\sqrt{\alpha}-\epsilon\sqrt{\alpha})$, scaled aquifer response time with inclusion of linear variation of wetland ET.

γ t_p/t_a, scaled pumping period

$\delta()$ unit step function.

ϵ scaled distance between the well and the stream.

ζ $1/4\alpha$, scaled time.

η α/γ, scaled time without inclusion of linear variation of wetland ET.

η_c $(0.5/\sqrt{\alpha}+\epsilon\sqrt{\alpha})$, scaled aquifer response time with inclusion of linear variation of wetland ET.

λ t_d/t_p, scaled cycle length.

ξ $1/[4(\alpha-\gamma)]$, scaled time without inclusion of linear variation of wetland ET.

τ scaled stream depletion volume during cyclic pumping.

τ^* criteria for the practical state of dynamic equilibrium during cyclic pumping.

τ_{cr} scaled stream depletion with inclusion of wetland ET.

τ_{cm} scaled mined water from the aquifer storage.

τ_{cm} criteria for steady state condition for continuous pumping from a shallow water table aquifer.

CHAPTER I.

INTRODUCTION

Groundwater is one of the major water resources in the United States as well as around the world. In the past and present, groundwater has been a major source of fresh water for many municipalities, industries and irrigation. In the United States alone, groundwater is estimated to supply water for about half of the population and about one-third of all irrigation water (Bouwer, 1978). Reports (William et al., 1973; Henningsen, 1977; Bedell and Van Til, 1979; Fulcher et al., 1986) indicate that groundwater usage for irrigation purposes has been increasing tremendously over the past two decades and will be increasing in the future. Since groundwater supplies are not unlimited, adequate management of groundwater is essential to keep the groundwater resources usable for this and future generations.

It is well known that surface water features are hydraulically connected to the groundwater in the adjacent aquifers. Because of the hydraulic connection between the surface water features and the groundwater in the aquifer, water removed from the aquifer to irrigate crops reduces the flow available to support habitats in streams, lakes, and

wetlands. Reduction of streamflow and/or evapotranspiration (ET) for phreatophyte use occurs because the irrigation water is returned to the atmosphere rather than to the aquifer. This depletion rate is often referred to as capture (Bredehoeft et al., 1982) that can be considered as reduced groundwater flow to surface water features or increased flow from the surface water features toward the pumping well. This capture often adversely effects the quantity and the quality of water in wetlands, lakes and streams during drought periods. The magnitude and timing of the capture caused by pumpage are transmitted through the aquifer to the surface water features and depend upon the aquifer properties (storativity or specific yield and transmissivity), the hydraulic connection between the aquifer and stream and/or wetland, and the distance between the pumping well and the stream. Numerous problems, past and present, have illustrated the excessive reduction in the quantity of streamflow and wetland evapotranspiration caused by excessive pumping for irrigation purpose. In order to reduce the adverse impacts of pumping on streamflow, legislation was created in Massachusetts (Mueller and Male, 1990) to regulate pumping rates at certain times.

To determine the reduction in wetland ET due to drawdown of the water table by a pumping well, it is necessary to recognize the importance of the unsaturated zone. The unsaturated zone is near the ground surface and plays a critical role in the determination of evaporation or the ET

rate from the ground surface to the atmosphere. Several investigators (Gardner, 1958; Anat et al., 1965, Ripple et al., 1972; Skaggs, 1978; Markar and Mein, 1987; Warrick, 1988) indicated that the rate of actual ET is limited by the soil water distribution in the unsaturated zone when the ET rate is less than the potential rate. They concluded that the distribution of soil water in the unsaturated zone strongly depended on the unsaturated soil properties and the depth to water table.

1.1. Objective and Scope of the Study

1.1.1. Objective

The overall objective of this research is to gain an improved understanding of the transient and steady state behavior of stream depletion caused by wells that pump water (1) from a deep water table aquifer where there is no ET loss and (2) from a shallow water table aquifer where there is ET loss from the ground surface. The specific objectives involved in this study are:

1. To develop an analytical model to predict stream depletion caused by nonuniform cyclic pumping during the period when flow in the aquifer establishes a condition of dynamic equilibrium.
2. To develop an analytical solution that predicts stream depletion and captured wetland ET that varies as a linear

function of water table depth in a semi-infinite wetland area where water is pumped from a shallow phreatic aquifer.

3. To investigate the adequacy of the analytical solution for stream depletion where the effects of linear variation of captured wetland evapotranspiration are included.
4. To develop a method that can approximate the nonlinear variation of wetland ET accurately.
5. To develop a method that can be used to predict steady state stream depletion which accounts for the effects of nonlinear variation of captured wetland ET.

1.1.2. Scope

This study is carried out in three phases. In the first phase of the study, two analytical models are developed for stream depletion rate and volume produced by a pumping well. The first model describes the development of the analytical solution for stream depletion produced by nonuniform cyclic pumping from a deep semi-infinite phreatic aquifer. The solutions are obtained by the application of the superposition principle to Jenkins' solution for stream depletion produced by steady continuous pumping of a well (Jenkins, 1968). The second model describes the development of the analytical solution for stream depletion and captured wetland ET caused by continuous pumping of a well located in a shallow semi-infinite phreatic aquifer. The effects of ET are incorporated into the solutions as a linear function of water table depth.

The second phase of the research consists of two stages. The first stage is to develop a method that could describe the nonlinear behavior of wetland ET accurately. Anat et al.'s (1965) method to predict the steady state ET from the water table is used to develop this method. The dimensional analysis technique is used to combine this method with Hantush's equation for stream depletion so that the scaled parameters that influence the stream depletion and captured wetland ET could be determined. Dimensional analysis showed that the scaled steady state stream depletion depends on three independently scaled parameters: the pumping distance, the hydraulic conductivity, and the initial depth to water table.

The second stage of the phase is a numerical study of steady state stream depletion in a hypothetical stream-aquifer system by using the two dimensional finite element model. The numerical model is modified to incorporate the nonlinear variation of wetland ET as a function of water table depth. Anat et al.'s method is used to calculate ET losses in the model. The results of the numerical simulations are evaluated by the scaled parameters developed in the first stage. Three families of dimensionless graphs are developed that can be used to predict steady state stream depletion rates for a wide range of aquifer properties. These graphs are valuable tools that eliminate the necessity of the numerical model.

In the third phase, the study is summarized and the conclusions are presented.

CHAPTER II

LITERATURE REVIEW

2.1. Introduction

The objective of this study is to gain an improved understanding of the transient and steady state behavior of stream depletion and/or captured wetland ET caused by a pumping well located in a shallow water table aquifer. A review of the literature for stream depletion and evaporation (or ET) from the water table was necessary to meet this objective. This section is devoted to a review of the previous research in these areas. This review will be divided into two sections. The first section summarizes the studies related to stream depletion produced by continuous pumping wells. The second section reviews models that predict evaporation or ET as a function of the depth to the water table and unsaturated soil properties.

2.2. Stream Depletion by Pumping Wells

The study of the interactions between surface water features and aquifers started in the early 1940's. Theis

(1941) was the first investigator to derive an analytical expression that determines the percentage of the pumped water being diverted from the stream by a pumping well, provided there is a hydraulic connection between the aquifer and the stream. Later, Theis and Conover (1963) developed the first dimensionless graph for calculating the percentage of stream depletion during steady continuous pumping of a well.

Glover (1960) developed charts based on the theoretical equations of Glover and Balmer (1954) to determine the capture from the river which was computed in terms of the distance of the well from the river, the properties of the aquifer (storativity and transmissivity), and time.

Hantush (1955, 1964a, 1964b) derived the rate and volume of stream depletion for a leaky water table aquifer hydraulically connected to a straight stream. He developed the stream depletion rate and volume in terms of the complementary error function of the dimensionless pumping time and dimensionless leakage coefficient. He developed these equations by combining the drawdown equation for a leaky water table aquifer (Hantush and Jacob, 1955) with the generalized form of Darcy's equation.

Hantush (1965) also developed an analytical equation for depletion rate and volume from streams with semipervious beds. He replaced the resistance to flow due to the semiperviousness of the stream bed which is determined by use of a pumping test technique (Kazmann, 1948; Rorabaugh, 1956; and Hantush, 1959) by an equivalent resistance. This resistance is caused by a

horizontal flow through a semipervious layer of insignificant storage capacity which is lying between the aquifer and the streambed. He introduced this resistance in his previous analytical solutions as an additional length between the pumping well and the stream. Hantush (1967) made further refinements to his analysis and eliminated the assumption of a straight river of infinite length. He developed an analytical solution for stream depletion by pumping wells that are located near streams that border a quadrant aquifer.

Jenkins (1968) defined a "lumped" parameter known as the "sdf" which is a time scale that uniquely characterizes the aquifer response curve. The "sdf" is based on the aquifer parameters (transmissivity and specific yield) and the perpendicular distance from the stream to the well. He developed dimensionless plots of rate and volume of stream depletion based on the equations developed by Glover and Balmer (1954), and Hantush (1964a, 1965) so that calculation of the stream depletion rate and volume as a function of sdf and time would be easier for practical purposes. Furthermore, Jenkins (1968) described the residual impacts after pumping stopped and briefly discussed cyclic pumping. Jenkins (1968b) and Moulder and Jenkins (1969) also modeled a non-straight river of infinite length to determine stream depletion by using electric-analog and digital computer.

Recently, Burns (1983) used Jenkins' method to describe how to develop discrete unit response functions for unit periods of stress and showed how the shape of the response

function depended on the value of sdf. He used the unit response function and time series of aquifer stresses with a discretized version of the convolution equation to compute the time series of stream depletion.

None of the theoretical studies reviewed above indicate that the effect of a discharging well on a nearby stream is independent of the length of the reach of a stream-aquifer system. Taylor (1971) confirmed this by using a digital computer model of short and long reaches of a stream-aquifer system. From the results of digital computations, he concluded that short reaches of stream-aquifer systems gave comparable results to long reaches with considerably less effort and expense.

All of the analytical models briefly reviewed above rely on the linearity of the governing flow equation of the unconfined aquifer. The basic assumption required to have a linear aquifer system is that the drawdowns are small compared to the thickness of the aquifers. These models and the analytical solutions developed in the present study considered an average hydraulic conductivity and specific yield for the entire aquifer. They did not consider how sensitive the stream depletion was to stochastic variations of hydraulic conductivity and specific yield of the aquifer.

In a recent study, Hantush and Marino (1989) developed a stochastic water management model for the stream-aquifer system. The model can be used to optimize pumping patterns from the aquifer while minimizing the stream depletion rate

under specified system performance probability requirements. The model considers the distribution of the hydraulic conductivity and the specific yield of the aquifer. These parameters were assumed to be log-normally distributed. The stream depletion rate was introduced into the model as a function of random aquifer parameters with a known probability distribution. Hantush and Marino (1989) applied their model to a hypothetical situation so that they could examine the sensitivity of the pumping patterns and stream depletion by varying the statistical properties of the aquifer parameters. They concluded that the results obtained from the model indicated that the stream depletion rate was insensitive to the coefficient of variation of the log-specific yield and slightly sensitive to the probability levels, whereas, the depletion rate was highly sensitive to the hydraulic conductivity statistics.

Analytical solutions that are briefly reviewed above for computing streamflow depletion rates neglect conditions that exist in typical stream aquifer systems. Some of these conditions are (1) partial penetration of the stream to the aquifer, (2) the presence of the semipermeable layer which covers the streambed, (3) aquifer storage available to the pumping well from areas beyond the stream and (4) hydraulic disconnection between the stream and the aquifer. Recently, Spalding and Khaleel (1991) analyzed these conditions by using the 2-D finite element model, AQUIFEM-1, (Townley and Wilson, 1980). From the results of numerical experiments they

concluded that the analytical solutions can be in error by 20 percent for neglecting the partial penetration of the stream, by 45 percent for neglecting the existence of a semipermeable layer between the stream and the aquifer, and by 21 percent for neglecting the storage available in areas beyond the stream. They also found that neglecting hydraulic disconnection had only a minor effect. They indicated that the combined effects of these errors can be as high as 85 percent.

2.3. Steady State Evaporation From the Water Table

The steady state upward flow of water from the water table through the soil profile for evaporation from the soil surface was first studied by Moore (1939). He introduced water tables at the bottom of soil columns and allowed the soil to absorb water. The soil surface was subjected to evaporation and tensiometers were placed along the length of the column. By using these tensiometers, he observed the relationship between water pressure, moisture content, and rate of water loss from the water table. As a result of his experiments, he concluded that the finer soils supplied higher evaporation rates even at the greater depths to the water table.

Theoretical solutions of the flow equations for evaporation processes from the water table were given by several investigators, including Philip (1957), Gardner (1958), Staley (1957), Anat et al. (1965), Ripple et al.

(1972) and Warrick (1988).

Gardner (1958) analyzed upward flow rates with the water table at any particular depth and any suction head at the soil surface. For homogeneous soils, he started with the "diffusivity equation" that describes unsteady flow in partially saturated porous media. He solved this equation for the special case of steady one dimensional flow in a vertical (upward) direction.

$$z = \int_0^S \frac{dS}{1+\frac{q}{K_c}} \qquad (2.1)$$

Here z is the depth to water table, S is the suction head, q is the steady state evaporation flux, and K_C is the unsaturated hydraulic conductivity (it is sometimes called "capillary conductivity"). He defined an empirical equation for the unsaturated hydraulic conductivity as:

$$K_c = \frac{a_s}{b_s+S^n} \qquad (2.2)$$

Where a_s, b_s, and n are constants for particular soils. He substituted Equation 2.2 into Equation 2.1 and obtained analytical expressions for the steady state evaporation flux when n = 1, 3/2, 2, 3, and 4. Gardner also showed maximum values of evaporation as an inverse function of the depth to the water table when the suction head approaches infinity.

Gardner and Fireman (1958) conducted laboratory studies of evaporation from soil columns. The columns were saturated

and drained a few times in order to develop or simulate a structure of the soil in the columns as close as possible to soils in the field. The water was supplied from a reservoir through porous cups at the lower end of the column. They simulated different ranges of water table depths by varying the vertical position of the inflow reservoir. In addition they measured evaporation fluxes for two soils: Chino clay and Pachappa sandy loam. They found agreement between the theory and the experiment.

Staley (1957) conducted wind tunnel experiments to determine how the evaporation rate from a fine sand column was affected by the wind velocity and the depth of the water table. He also derived functional relationships between the evaporation rates under specific ambient conditions and the depth of the water table. Staley's approach was different from that employed by Gardner. He employed Darcy's law for the case of one dimensional flow in the vertical direction and rearranged this equation to give an explicit expression describing the rate of change of capillary pressure with the depth to the water table as a function of evaporation flux and capillary conductivity. He solved this expression for z which is identical in form to Gardner's equation (Equation 2.1).

Schleusener and Corey (1959) studied the role of hysteresis in reducing evaporation from the soils in the presence of a water table. They concluded that the analysis of upward movement of water from a water table in the absence of hysteresis effects does not provide a satisfactory

explanation for the inverse relation that Gardner (1958) found.

Anat et al., (1965) modified Duke's (1965) equation for maximum rate of upward flow for evaporation from the water table. They expanded the term in the infinite integral of Duke's equation into a convergent series and integrated it term by term. They obtained the first dimensionless explicit equation for maximum upward flux from the water table in terms of depth to water table, and the hydraulic properties of soil.

Ripple et al. (1972) also developed a set of dimensionless equations and graphs that can be used to estimate maximum steady state evaporation from the water table. Their treatment of evaporation was more flexible than previous investigators, because they considered the role of meteorological conditions. Their procedure makes it possible to estimate the steady state evaporation from soils including layered soils, with a high water table. The field data required include soil-moisture characteristic curves, water table depth, and a record of air temperature, air humidity, and wind velocity at one elevation (Hillel, 1980; Ripple et al., 1972).

Recently, Warrick (1988) developed additional analytical solutions for steady state evaporation from a shallow water table. He incorporated Gardner's unsaturated conductivity equation (Equation 2.2) into Richard's equation for steady state upward flow. His solution is valid for all $n > 1$, including fractional values and $b_s = 0$, therefore is more

general than Gardner's solution. However, Warrick's equation is an implicit equation and requires iteration to determine the value of steady state evaporation.

2.4. Summary

The literature review in the preceding sections shows that analytical solutions used to predict stream depletion in the case of nonuniform cyclic pumping are limited. It also showed that there is no analytical solution available for stream depletion which includes the effects of captured wetland ET.

The present study will go beyond these studies in several aspects. For example, in the first phase of the research, the first analytical model will focus on stream depletion caused by nonuniform cyclic pumping during the period when flow in the aquifer establishes a condition of dynamic equilibrium. It will show the magnitude of the error in depletion rates estimated by assuming steady-continuous pumping at the cycle-average rate. The second analytical model will focus on stream depletion and/or linear variation of captured wetland ET caused by the continuous pumping of a well from a shallow water table aquifer.

The literature review in this chapter showed that ET from the ground surface varies as a nonlinear function of the position of the water table. This indicates that the second analytical solution for stream depletion and captured wetland

ET has limitations. Therefore, the accuracy of the linear variation of captured wetland ET will be investigated.

In order to obtain a more accurate solution for stream depletion and captured wetland ET, numerical simulations will be carried out by using a 2-D finite element model. The model will be modified to incorporate the nonlinear variation of wetland ET as a function of the position of the water table. The numerical model will be applied to a hypothetical situation to simulate steady state stream depletion and captured wetland ET for a large range of aquifer parameters. The present study will also make use of the dimensional analysis technique to determine the scaled aquifer parameters. The result of the numerical simulations will be plotted in dimensionless graphs for a wide range of the scaled aquifer parameters. These dimensionless graphs will be useful tools for determining steady state stream depletion rates and nonlinear captured wetland ET rates without employing the numerical model.

CHAPTER III

STREAM DEPLETION BY CYCLIC PUMPING OF WELLS

3.1. Introduction

Groundwater withdrawals for irrigation have been increasing over the past two decades in humid regions of the U.S. These withdrawals occur primarily during summer months and impact wetlands, streams, and lakes. For example, a portion of the discharge from a pumping well located in an aquifer that is hydraulically connected to a stream consists of water captured from that stream (Figure 3.1). The groundwater withdrawal reduces the streamflow. This can occur as a reduction of groundwater flow to the stream or an increased flow from the stream to the aquifer. Besides reducing the streamflow, secondary effects include the possible reduction in quality of instream flow or the need to improve the quality of point discharges in an attempt to maintain instream water quality. This could be especially pronounced during drought periods. Assuming that the demand for consumptive water use will increase,it is important to continue improving the methods available for estimating the impacts of future groundwater use.

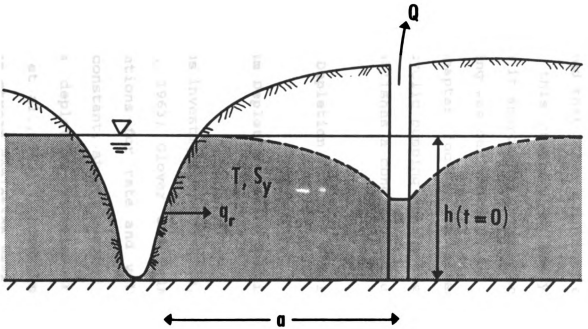

Figure 3.1. Cross section of the aquifer described by analytical method.

Previous works lead to analytical solutions describing the depletion of stream flow during a period of constant pumping. Superposition was used to obtain similar solutions for the period following a single episode of pumping and it was recognized that other solutions could be obtained by this method. In this chapter, an analytical method for stream depletion as it approaches dynamic equilibrium in response to cyclic pumping was derived.

This chapter focuses on stream depletion caused by nonuniform cyclic pumping during the period when flow in the aquifer establishes a condition of dynamic equilibrium.

3.2. Stream Depletion During a Single Pumping Cycle

3.2.1. Stream Depletion During Pumping

Previous investigators (Jenkins, 1968; Theis, 1941; Theis and Conover, 1963; Glover and Balmer,1954; Hantush,1964a) derived equations for rate and volume of stream depletion caused by a constant, steady pumping of water from an aquifer. This stream depletion is also referred to as capture (Bredehoeft et al.,1982). According to Jenkins (1968) the dimensionless stream depletion rate at time t is

$$\frac{q_r}{Q} = erfc\left(\sqrt{\frac{t_a}{4t}}\right) \quad 0 \le t \le \infty \tag{3.1}$$

and the dimensionless volume removed from the stream in time t is

$$\frac{V_r}{Qt} = \left(\frac{t_a}{2t}+1\right)\frac{q}{Q} - \sqrt{\frac{t_a}{4t}}\frac{2}{\sqrt{\pi}}e^{-\left(\frac{t_a}{4t}\right)} \quad 0 \le t \le \infty \tag{3.2}$$

In Equations 3.1 and 3.2

$$t_a = \frac{a^2 S_y}{T} \tag{3.3}$$

The term t_a is the response time of the aquifer which is used in this study in preference to Jenkins' (1968) stream depletion factor. In this stream depletion problem, t_a is a measure of the time required for the aquifer to reach a new equilibrium after a pumping stress Q is first introduced at the well located a distance "a" away from the stream boundary where water is captured.

To develop Equations 3.1 and 3.2, the following assumptions are required for the aquifer properties: (1) T is constant with time and space, therefore, drawdown is negligible compared to the thickness of the phreatic aquifer; (2) there is no recharge to the aquifer under natural conditions, so that the water-table is initially horizontal; (3) the aquifer is isotropic, homogeneous and semi-infinite in areal extent; (4) the stream that forms the boundary is straight and fully penetrates the aquifer; (5) water is instantaneously released from aquifer storage; the well fully penetrates the aquifer; (6) the pumping rate is steady during any period of pumping; (7) the temperature of the water in the stream is constant and is the same as the temperature of the water in the aquifer.

Equation 3.1 is plotted in Figure 3.2 where the solid line shows the stream depletion rate as it approaches the pumping rate which is shown by the broken line. As time goes to infinity the depletion rate approaches the pumping rate. The area under the q curve between zero and t gives the accumulated volume of stream depletion (v_r) at time t and the area between the solid line and the broken line in the same period is the accumulated volume of water mined from aquifer storage.

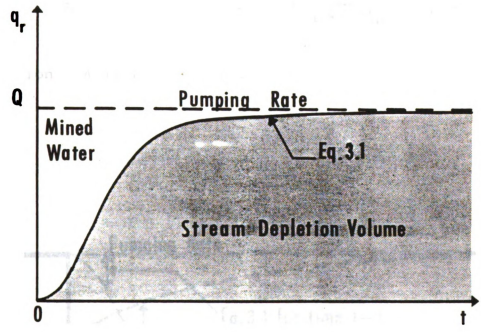

Figure 3.2 Stream depletion during constant-steady pumping.

3.2.2. Stream Depletion After Pumping Stops

Stream depletion continues after pumping stops (Jenkins, 1968). If t_p is the time the pump was on and t is the time

when conditions are assessed, the volume of water pumped from the well during this time is Qt_p. Assuming $t \geq t_p$, then as t approaches infinity, the volume of stream depletion v_r approaches Qt_p, if the stream is the only source of captured water. The rate and volume of stream depletion at any time after pumping ends can be computed using Equations 3.1 and 3.2 and the method of superposition. According to Jenkins (1968), the equation for rate of stream depletion after pumping ends is

$$q_r = Q\left(1-erf\sqrt{\frac{t_a}{4t}}\right)-Q\left(1-erf\sqrt{\frac{t_a}{4(t-t_p)}}\right) \quad t_p \leq t \leq \infty \qquad (3.4)$$

Equation 3.4 is plotted in Figure 3.3.

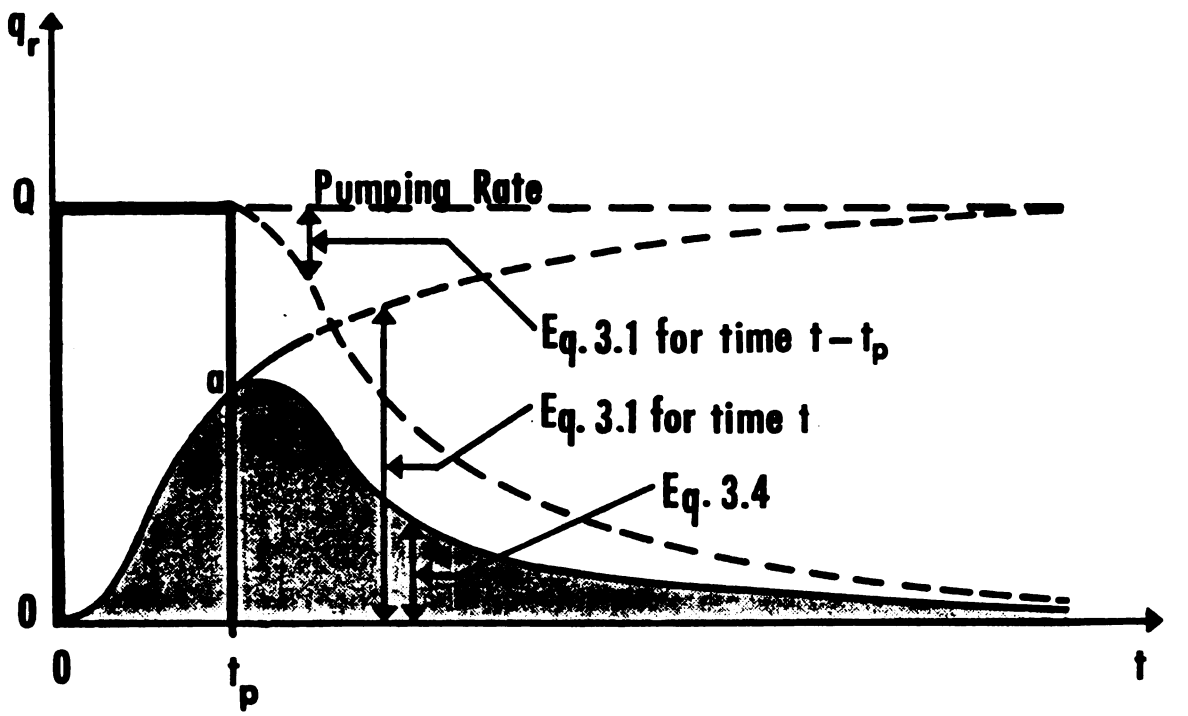

Figure 3.3. Stream depletion during and after pumping

3.3. Rate of Stream Depletion During Cyclic Pumping

3.3.1. Conceptual Description

The rate of stream depletion during cyclic pumping can be calculated using the principle of superposition and Equation 3.4. A detailed example is given below. Suppose t_p is the length of the pumping period as shown in Figure 3.4. Furthermore, suppose, this pattern repeats itself at intervals t_d as shown in Figure 3.4. The final stream depletion rate is obtained by adding the stream depletion rate produced by each individual pumping period. In the following section, an equation is derived to calculate the rate of stream depletion at any time after pumping starts.

3.3.2. Analytical Solution for Stream Depletion

An analytical expression for the rate of stream depletion during cyclic pumping can be written for the conceptual problem stated above. For constant t_d and t_p, if t_{0i}, t_{ni}, U_{0i} and U_{ni} are defined as follows:

$$t_{0i}=t-t_d i \tag{3.5a}$$

$$U_{0i}=\sqrt{\frac{t_a}{4t_{0i}}} \tag{3.5b}$$

$$t_{ni}=t-t_p-t_d i \tag{3.5c}$$

$$U_{ni}=\sqrt{\frac{t_a}{4t_{ni}}} \tag{3.5d}$$

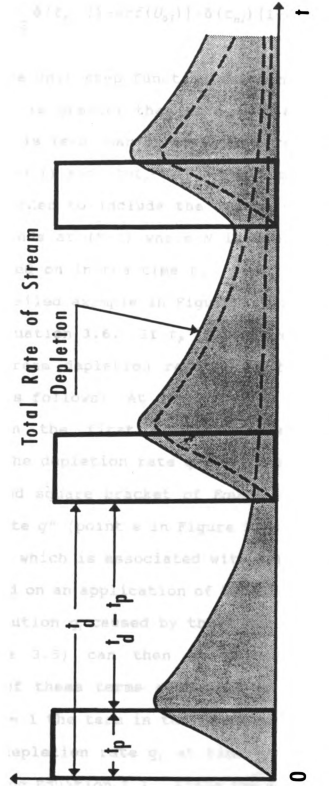

Figure 3.4. Construction of total stream depletion with the method of superposition for series of cyclic pumping.

and the rate of stream depletion is

$$q_r = Q\sum_{i=0}^{N-1} \delta(t_{0i})\,[1-erf(U_{0i})] - \delta(t_{ni})\,[1-erf(U_{ni})] \quad 0 \le t \le \infty \quad (3.6)$$

Here δ is the unit step function which has a value of 1 when its argument is greater than zero, and a value of zero when its argument is less than or equal to zero. The arguments are the terms $(t-t_d i)$ and $(t-t_p-t_d i)$. The summation over i starts at zero in order to include the impact of the first pumping cycle, and ends at $(N-1)$ where N is the number of times the pump is turned on in the time t.

The detailed example in Figure 3.5 is useful to show the nature of Equation 3.6. If t_p is 90 days and t_d is 360 days, then the stream depletion rate q_r at t = 450 days can be calculated as follows: At t = 450 days, $N-1$ = 1. When i = 0, the term in the first square bracket of Equation 3.6 calculates the depletion rate q_i' at t'= 450 days and the term in the second square bracket of Equation 3.6 calculates the depletion rate q'' (point e in Figure 3.5) at time t''= 360 days (t''= 450-90) which is associated with the recharge well; each term is based on an application of Equation 3.1. The depletion rate contribution q_i caused by the first pumping cycle (point f in Figure 3.5) can then be calculated by taking the difference of these terms according to Equation 3.6 ($q_0=q_0'-q_0''$). For i = 1 the term in the first bracket of Equation 3.6 calculates depletion rate q_1' at time t'= 90 days ($t'=t-t_d i$ = 450-360) using Equation 3.1. Since the argument $(t-t_p-t_d i)=0$,

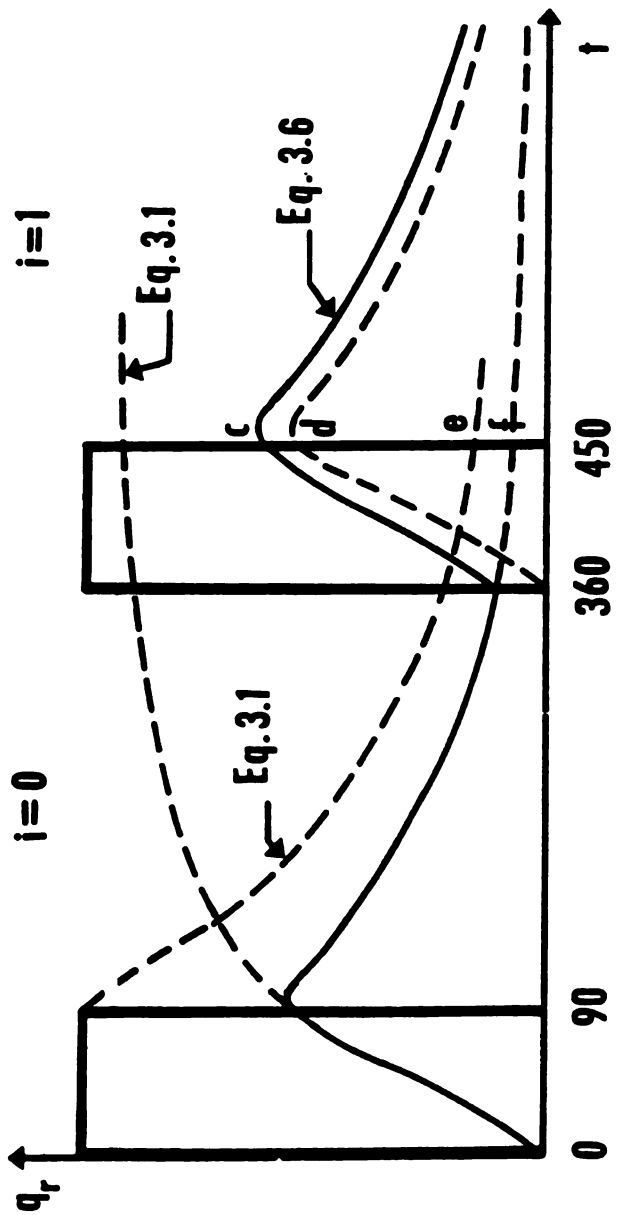

Figure 3.5. Example calculation of the rate of stream depletion by Equation 3.6 at t = 450 days.

the unit step function of the second term has a value of zero. Therefore, the second term in Equation 3.6 is $q_1''=0$. Thus, the depletion rate contribution q_1 of the second pumping cycle (point d in Figure 3.5) is according to Equation 3.6 $q_1=q_1'-q_1''$. The total impact rate q_r (point c in Figure 3.5) is calculated by summing q_0 and q_1 according to Equation 3.6.

3.4. Volumetric Stream Depletion During One Cycle of Pumping

3.4.1. Graphical Interpretation

Figure 3.6, a simplified version of Figure 3.4, shows the total stream depletion during one cycle produced by a series of pumping cycles. The total volume of stream depletion between the time t, which need not be a time of maximum q_r, and $t-t_d$ is the area under the curve *ab* in Figure 3.6b. This volume is the same as the summation of the areas below the individual curves *cd*, *ef*, and *gh* in Figure 3.6b. For the example shown in Figure 3.6 where $N=3$, *ef* is the recession limb from the first pumping cycle, *cd* is the recession limb from the second pumping cycle, and *gh* is the rising limb of the third pumping cycle. Since t_p, Q, and t_d are constant, the area under curve *cd* is the same as the area under curve *c'e*; also, the area under curve *gh* is the same as the area under curve *0c'*. Therefore, the total volume of stream depletion between the time $t-t_d$ and t is the same as the volume of

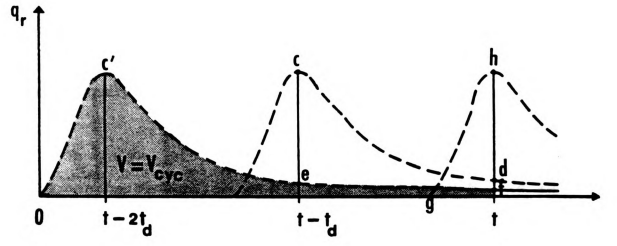

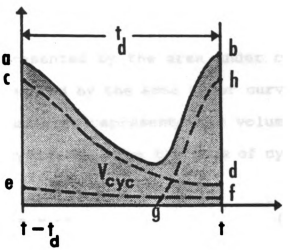

Figure 3.6. (a) Construction of total stream depletion for cyclic pumping when t_p and t_d are constant and (b) detail of Figure 3.6a between t - t_d and t.

stream depletion produced between zero and t by a single period of pumping. Recognizing this fact reduces a potentially complex mathematical problem to a very simple one, and an analytical expression for volumetric stream depletion over one cycle can easily be derived.

3.4.2. Analytical Solution

On the basis of the above explanation, Figures 3.7a and 3.7b can be plotted. The shaded area in Figure 3.7a is the same as the shaded area in Figure 3.7b. Each gives the total volume of stream depletion between time $t-t_d$, and t discussed in relation to Figure 3.6. This volume can be calculated using Equation 3.2.

If v_1 is the volume represented by the area under curve I and v_2 is the volume represented by the area under curve II (Figure 3.7b), then the shaded area represents the volume of stream depletion during one cycle, v_{cyc}, for the case of cyclic pumping. Here

$$v_{cyc} = v_1 - v_2 \tag{3.7}$$

where application of Equation 3.2 gives

$$v_1 = Qt\left(\left(\frac{t_d}{2t}+1\right) erfc\left(\sqrt{\frac{t_d}{4t}}\right) - \sqrt{\frac{t_d}{4t}}\frac{2}{\sqrt{\pi}}e^{-\frac{t_d}{4t}}\right) \tag{3.8a}$$

$$v_2 = Qt'\left(\left(\frac{t_d}{t'}+1\right) erfc\left(\sqrt{\frac{t_d}{4t'}}\right) - \sqrt{\frac{t_d}{4t'}}\frac{2}{\sqrt{\pi}}e^{-\frac{t_d}{4t'}}\right) \tag{3.8b}$$

where, $t' = t - t_p$

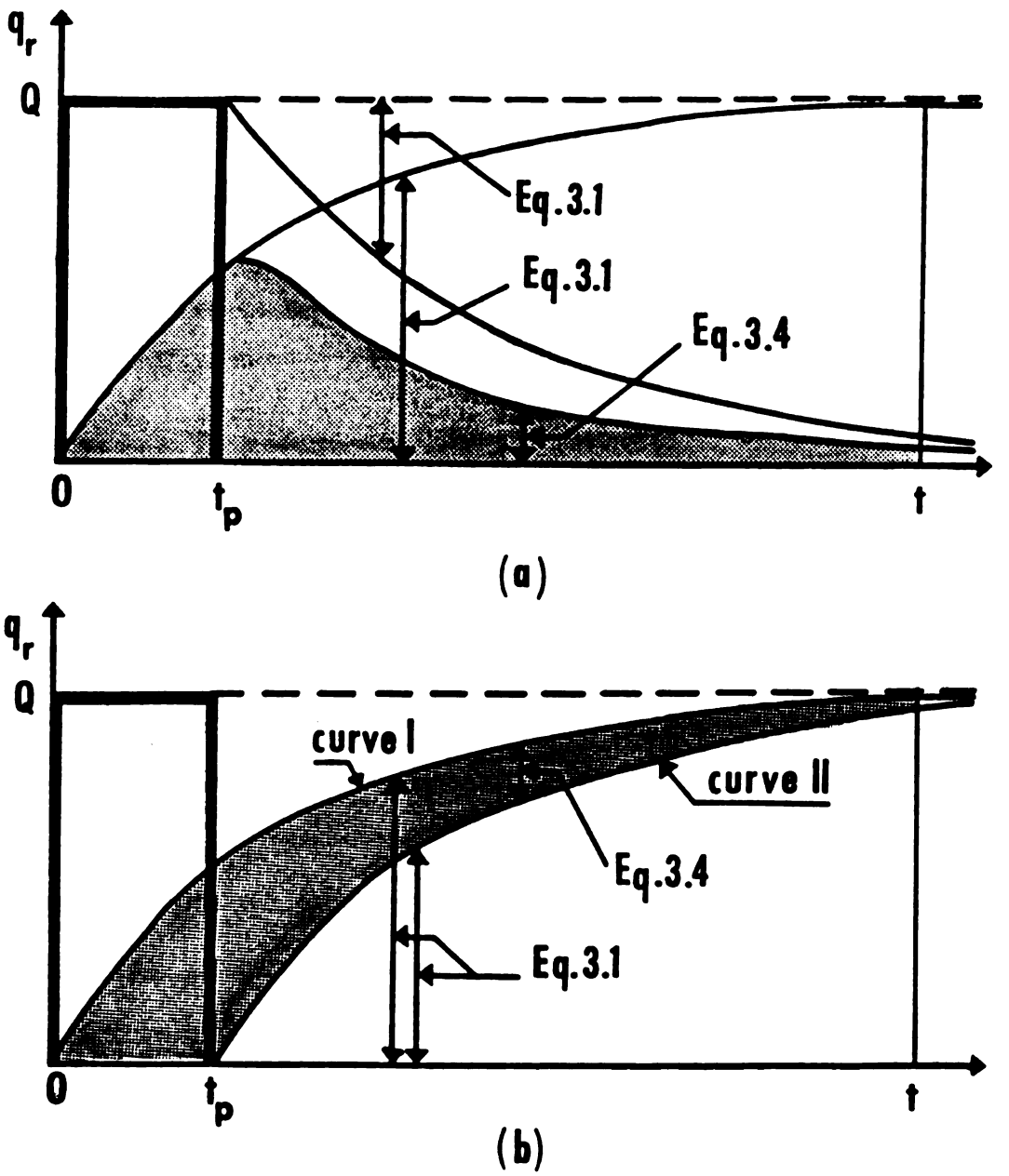

Figure 3.7. (a) Total stream depletion during the cycle ending at t and (b) alternate representation of Figure 3.7a

3.5. The Approach to and the Conditions at Dynamic Equilibrium

3.5.1. Conceptual Description

Dynamic equilibrium occurs when, during one cycle, the volume of stream depletion v_{CYC} (Equation 3.7) is equal to the volume of water pumped from the well. Let τ be the ratio of v_{CYC} to the volume of water pumped during one cycle,

$$\tau = \frac{v_{cyc}}{Qt_p} \tag{3.9}$$

Dynamic equilibrium occurs when $\tau = 1$. According to Equation 3.7, $v_{CYC} \rightarrow Qt_p$ only as $t \rightarrow \infty$. Thus, dynamic equilibrium occurs at $t = \infty$. For practical purposes, dynamic equilibrium occurs at a finite time if it is defined as occurring when $\tau = \tau^*$. In this study the value of τ^* was taken as 0.95. This practical state of dynamic equilibrium occurs at $t = t_e$.

3.5.2. Dependence of τ on the Pumping Cycle Characteristics, Aquifer Response Time, and Time

Substituting Equations 3.8a and 3.8b into Equation 3.9 and simplifying produces the following equation for τ:

$$\tau=\eta\left((2\zeta+1)\,erfc\sqrt{\zeta}-\frac{2}{\sqrt{\pi}}\sqrt{\zeta}e^{-\zeta}\right)-(\eta-1)\left((2\xi+1)\,erfc\sqrt{\xi}-\frac{2}{\sqrt{\pi}}\sqrt{\xi}e^{-\xi}\right) \tag{3.10}$$

where,

$$\eta = \alpha/\gamma$$

$$\zeta = 1/4\alpha$$

$$\xi = 1/[4(\alpha-\gamma)] \qquad (3.10a)$$

$$\alpha = t/t_a$$

$$\gamma = t_p/t_d$$

Equation 3.10 is plotted in Figure 3.8 for a range of dimensionless times α and γ. Table 3.1 contains data for the plot. Note that τ is independent of t_d/t_a even though the stream depletion rate q_r (Equation 3.6) shows such a dependence. The range of values of dimensionless time used in the figure were selected on the basis of the range of values of hydraulic conductivity, specific yield, and aquifer thicknesses given by Freeze and Cherry (1979) and summarized in Table 3.2. A typical value for t_p was taken as 90 days. The range of values for the distance from the pumping well to the river was 30 to 6,000 meters.

Figure 3.8 shows that lines of τ versus α collapse onto a single line as $\tau \rightarrow \tau^*$. This feature reveals a significant aspect of the time required for the aquifer-stream system to reach dynamic equilibrium. This may be seen most easily by using Figure 3.8 to determine the time required to reach equilibrium as the length of the pumping period decreases. That is, fix t_a, let τ= 0.95, and use Figure 3.8 to determine how long it takes, in each situation, for the aquifer stream system to come into equilibrium. Table 3.3 shows the

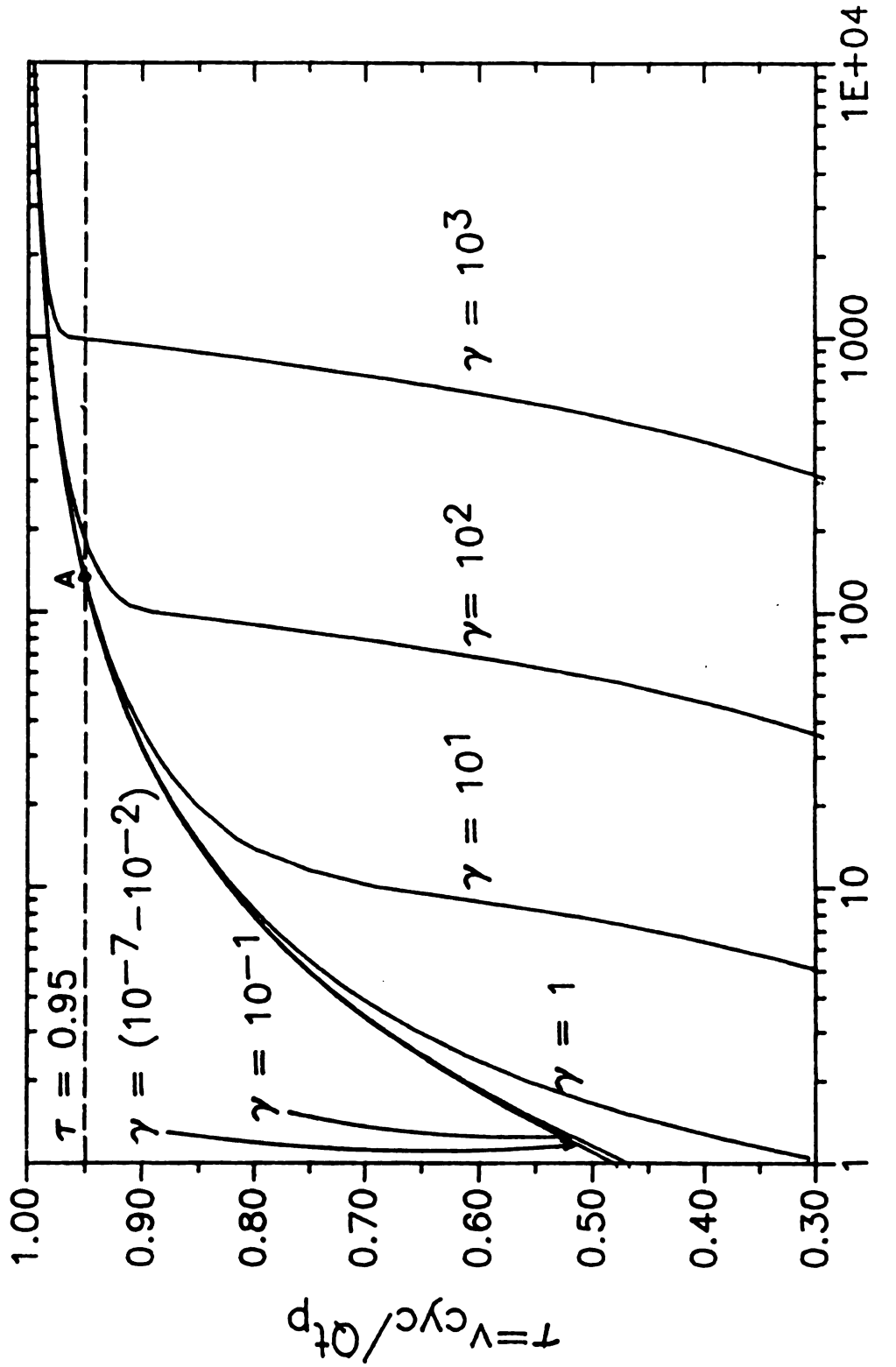

Figure 3.8. The dependence of τ, the dimensionless volume of stream depletion during one cycle on the scaled times α and γ.

Table 3.1 Data for dimensionless volume of stream depletion τ, corresponding to selected values of α and γ.

γ	10^{-7}	10^{-1}	1	10^{1}	10^{2}	10^{3}
α	Dimensionless volume of stream depletion (τ)					
1.000	0.4795	0.4680	0.3068			
1.500	0.5644	0.5570	0.4671			
2.000	0.6171	0.6125	0.5586			
2.500	0.6545	0.6514	0.6144			
3.000	0.6828	0.6805	0.6531			
3.500	0.7052	0.7034	0.6820			
4.000	0.7235	0.7219	0.7047			
4.500	0.7387	0.7374	0.7231			
5.000	0.7518	0.7506	0.7385			
5.100	0.7523	0.7510	0.7406	0.3018		
6.000	0.7727	0.7719	0.7627	0.3685		
7.000	0.7891	0.7885	0.7813	0.4436		
8.000	0.8025	0.8019	0.7961	0.5250		
9.000	0.8136	0.8131	0.8082	0.6034		
10.000	0.8230	0.8226	0.8184	0.6902		
15.000	0.8551	0.8548	0.8526	0.8170		
20.000	0.8743	0.8742	0.8727	0.8530		
25.000	0.8875	0.8874	0.8863	0.8733		
30.000	0.8972	0.8971	0.8964	0.8869		

Table 3.1 (cont'd.)

35.540	0.9055	0.9055	0.9047	0.8985	0.2931	
44.430	0.9155	0.9155	0.9150	0.9101	0.3740	
50.000	0.9203	0.9203	0.9199	0.9159	0.4298	
66.660	0.9307	0.9307	0.9307	0.9281	0.5794	
77.770	0.9358	0.9358	0.9358	0.9339	0.6831	
88.880	0.9400	0.9400	0.9400	0.9384	0.7874	
100.00	0.9434	0.9434	0.9434	0.9421	0.8920	
105.50	0.9449	0.9449	0.9449	0.9437	0.9109	
111.10	0.9463	0.9463	0.9463	0.9452	0.9188	
122.20	0.9488	0.9488	0.9488	0.9479	0.9285	
133.30	0.9510	0.9510	0.9510	0.9497	0.9349	
166.60	0.9562	0.9562	0.9562	0.9556	0.9465	
200.00	0.9600	0.9600	0.9600	0.9596	0.9532	
300.00	0.9674	0.9674	0.9674	0.9671	0.9639	
311.10	0.9685	0.9685	0.9685	0.9784	0.9649	0.2917
388.80	0.9713	0.9713	0.9713	0.9712	0.9692	0.3671
444.40	0.9732	0.9732	0.9732	0.9731	0.9715	0.4211
500.00	0.9747	0.9747	0.9747	0.9746	0.9733	0.4752
555.50	0.9760	0.9760	0.9760	0.9759	0.9748	0.5294
611.10	0.9771	0.9771	0.9771	0.9771	0.9761	0.5837
666.60	0.9781	0.9781	0.9781	0.9781	0.9772	0.6380
777.70	0.9797	0.9797	0.9797	0.9797	0.9790	0.7468
888.80	0.9810	0.9810	0.9810	0.9810	0.9805	0.8557
1000.00	0.9821	0.9821	0.9821	0.9821	0.9816	0.9648
1111.10	0.9830	0.9830	0.9830	0.9830	0.9826	0.9742
1222.20	0.9838	0.9838	0.9838	0.9838	0.9835	0.9773

Table 3.1 (cont'd.)

1666.60	0.9861	0.9861	0.9861	0.9861	0.9859	0.9830
2222.20	0.9880	0.9880	0.9880	0.9880	0.9878	0.9862
3333.30	0.9902	0.9902	0.9902	0.9902	0.9901	0.9893
4000.00	0.9910	0.9910	0.9910	0.9910	0.9910	0.9904
5000.00	0.9920	0.9920	0.9920	0.9920	0.9920	0.9919

Table 3.2 Range of Values of Hydraulic Conductivity, Specific Yield, Aquifer Thickness, Transmissivity and γ

Parameter	Range
Hydraulic Conductivity, K_s (m/day)	0.009 - 8550
Specific Yield, S_y	0.01 - 0.3
Aquifer Thickness, b (m)	6 - 100
Transmissivity, $T=K_s*b$ (m^2/day)	0.06 - $8.5(10)^5$
γ	10^{-7} - 10^6

results of these calculations. It can be seen from Table 3.3 that for small values of γ in the range $10^{-7} \leq \gamma \leq 10^{1}$, the time to equilibrium is constant multiple of t_a. This is revealed at point A in Figure 3.8 which shows that $\tau = 0.95$ for values of γ in the range $10^{-7} \leq \gamma \leq 10^{1}$ when the dimensionless time $\alpha = 1.27(10)^2$. Within this large range of α, t_e depends on t_a only! The details of the dependence are given by the value of α at point A which produces a simple expression for determining time to equilibrium

$$t_e = 127\, t_a \quad for \quad 10^{-7} \leq \gamma \leq 10^{1} \qquad (3.11)$$

On the other hand, large values of γ imply situations where the aquifer response time is small compared to the length of one pumping period i.e. $t_p >> t_a$. In this situation wells are close to the stream and stream depletion rates are approximately the same as the pumping rate. Figure 3.9 shows how the stream depletion rate (Equation 3.6) varies with time when γ is large. Here $\gamma = 900$, $t_a = 0.1$ days and the well is pumped at a rate of 300 m^3/day for 90 days of each year.

For large γ the rate of stream depletion should not be approximated by assuming pumping occurs at the equivalent cycle-average rate. Figure 3.9 shows how poorly the capture rate produced by pumping the same volume at the equivalent cycle average rate approximates the capture produced by cyclic pumping. Here $t_d = 360$ days so, $Q_{ld} = 300*90/360 = 75$ m^3/day.

Table 3.3. Values of time to practical state of dynamic equilibrium t_e at $\tau = 0.95$ for corresponding values of γ

γ	t_e
10^3	$9.80(10)^2\ t_a$
10^2	$1.85(10)^2\ t_a$
10^1	$1.27(10)^2\ t_a$
10^0	$1.27(10)^2\ t_a$
10^{-1}	$1.27(10)^2\ t_a$
10^{-2}	$1.27(10)^2\ t_a$
10^{-3}	$1.27(10)^2\ t_a$
10^{-4}	$1.27(10)^2\ t_a$
10^{-5}	$1.27(10)^2\ t_a$
10^{-6}	$1.27(10)^2\ t_a$
10^{-7}	$1.27(10)^2\ t_a$

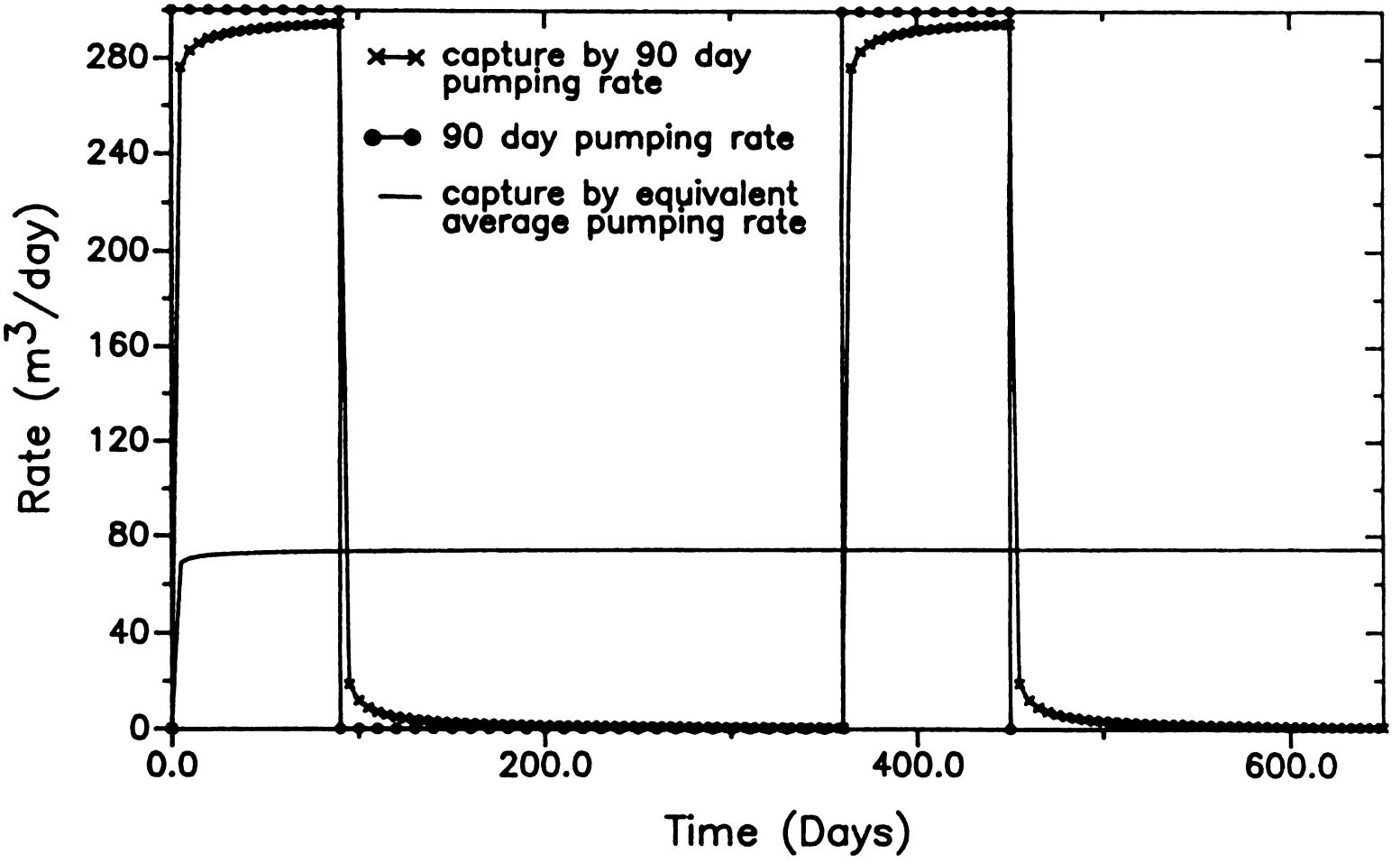

Figure 3.9. Comparison of stream depletion rate caused by cyclic pumping and the equivalent cycle-average rate of steady-continuous pumping when $\gamma = 900$.

3.5.3. Accuracy of Stream Depletion Rates Calculated with the Cycle-Average Pumping Rate

The previous example illustrates two rather obvious points: First, the stream depletion rate is essentially the pumping rate for wells located close to the stream. Second and more important, some measure is needed to characterize the error in a stream depletion rate calculated by assuming pumping at the cycle-average rate when infact the pumping is nonuniform and cyclic. Let the error criterion be defined by the equation

$$\beta = 1 - \frac{q_c}{q_{max}} \qquad (3.12)$$

Here β is the error caused by approximating the effects of cyclic pumping by assuming continuous, steady pumping at the equivalent cycle-average rate; q_c is the rate of stream depletion caused by continuous, steady pumping; and q_{max} is the maximum rate of stream depletion caused by cyclic pumping. Values of β have been determined at time t_e when dynamic equilibrium is first established. Table 3.4 shows the data developed to define the variation in β; time to dynamic equilibrium was calculated implicitly using Equation 3.10 for $\tau = 0.95$ for a range of values of γ. This calculated value of t_e was used in Equation 3.1 to calculate q_c, assuming pumping at the equivalent cycle-average rate, Q_w. The maximum rate of stream depletion at dynamic equilibrium, q_{max}, was determined

Table 3.4. Values of β corresponding to selected values of λ and γ.

λ	2	4	8	12
γ		β		
1000.	0.5000	0.7500	0.8750	0.9167
100.	0.4921	0.7460	0.8730	0.9154
33.3	0.4792	0.7360	0.8680	0.9120
10.0	0.4528	0.7164	0.8562	0.9039
5.00	0.4237	0.6938	0.8434	0.8950
3.33	0.3998	0.6744	0.8319	0.8871
2.00	0.3644	0.6433	0.8130	0.8739
1.33	0.3266	0.6073	0.7903	0.8578
1.00	0.2943	0.5740	0.7684	0.8420
0.700	0.2465	0.5213	0.7318	0.8154
0.500	0.1989	0.4596	0.6852	0.7805
0.333	0.1420	0.3699	0.6085	0.7206
0.200	0.0777	0.2459	0.4778	0.6095
0.133	0.0419	0.1569	0.3574	0.4942
0.100	0.0247	0.1062	0.2732	0.4037
0.075	0.0135	0.0678	0.1978	0.3140
0.050	0.0049	0.0324	0.1143	0.2012
0.033	0.0014	0.0134	0.0589	0.1156
0.020	0.0002	0.0034	0.0216	0.0493
0.014	0.0000	0.0011	0.0093	0.0242
0.010	0.0000	0.0003	0.0037	0.0112

by a search procedure using Equation 3.6 between the time t_e-t_d to t_e. Value of β were then calculated using Equation 3.12 and are shown in Figure 3.10 as a function of the independent variables γ and $\lambda = t_d/t_p$.

Figure 3.10 can be used to determine β. For example, assume a well located 1272.8 meters away from the stream, pumping 90 days in one year at the rate 300 m^3/day. If the aquifer transmissivity is 900 m^2/day, and the specific yield is 0.1, then the aquifer response time t_a = 180 days, the dimensionless pumping period γ = 0.5 and the dimensionless cycle length λ = 4. With these parameters, the error $\beta \approx 0.46$ can be found from Figure 3.10. Figure 3.11 shows stream depletion rates during one complete cycle at the equilibrium time of 22933 days for the above conditions. This figure illustrates how inadequate the cycle-average approximation q_C is, especially if the maximum rate of stream depletion q_{max} occurs during a critical time of the year.

The listing of the computer program that calculates τ, q_{max}, and β given in the Appendix B.

3.6. Summary and Conclusions

Stream depletion produced by nonuniform, cyclic pumping from a well located in a hydraulically connected aquifer was studied. The mathematical treatment required standard use of superposition theory and the existing analytical solutions for

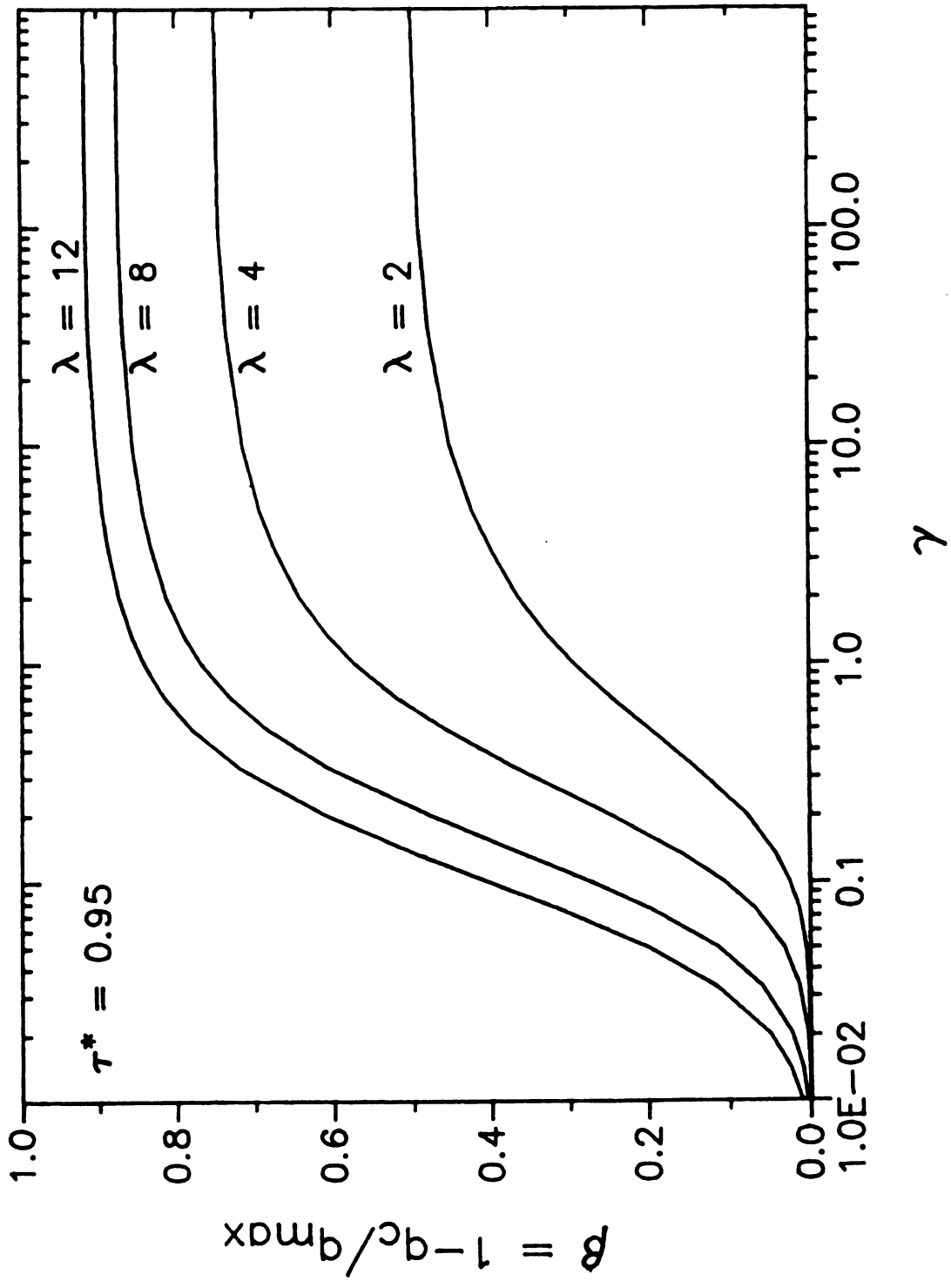

Figure 3.10. The accuracy of stream depletion rates calculated with the cycle-average pumping rate.

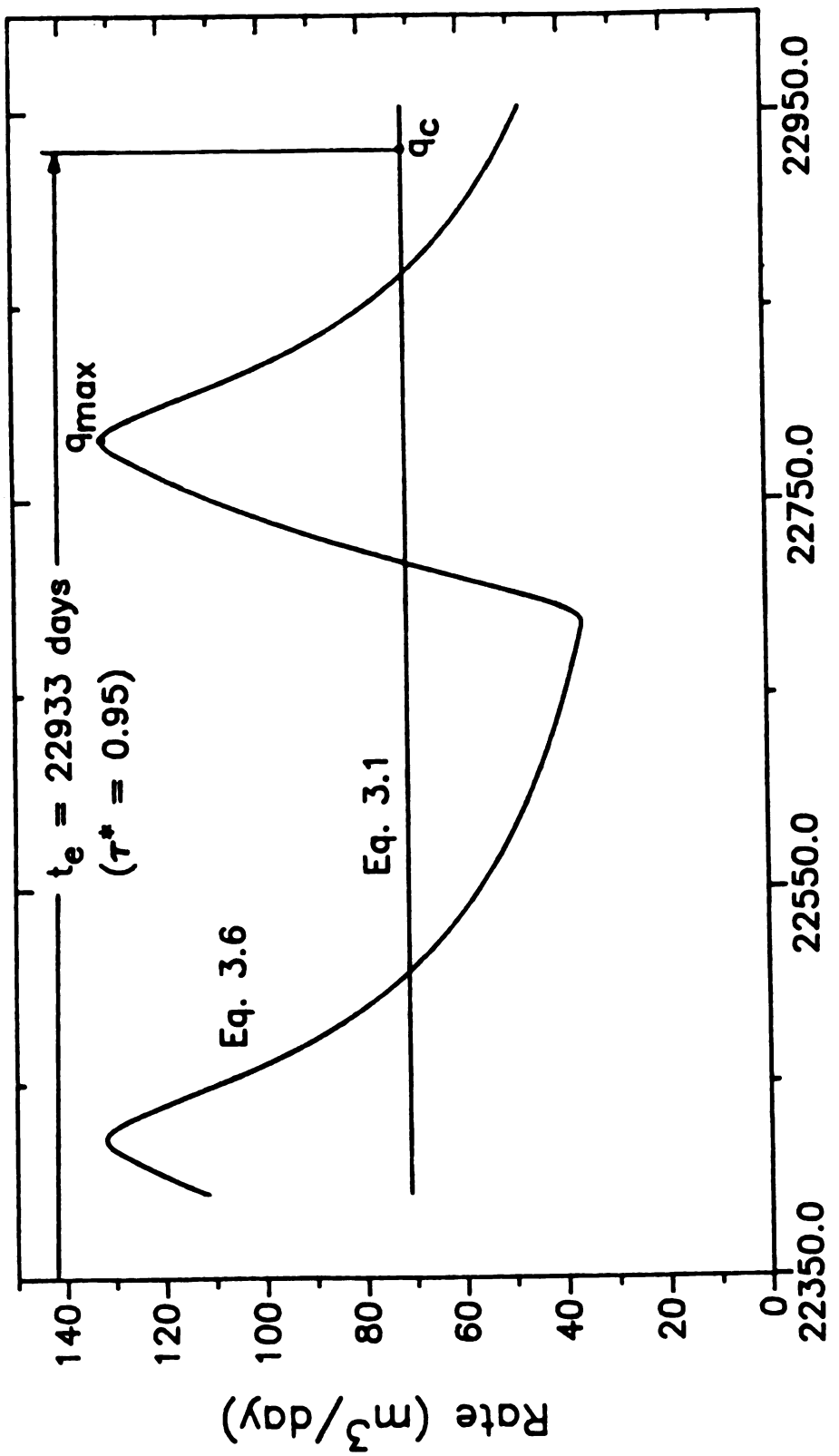

Figure 3.11. Comparison of stream depletion rate caused by cyclic pumping and the equivalent cycle-average rate of steady-continuous pumping when γ = 0.5 and τ = 0.95.

steady, continuous pumping. The solutions obtained are appropriate only when the actual field conditions approach the assumed conditions. Study focused on the approach to and conditions at dynamic equilibrium.

The τ criterion was developed for determining the time required to achieve a practical state of dynamic equilibrium. An analytical expression for τ was obtained (Equation 3.10) and plotted (Figure 3.8) for a practical range of the independent variables. Equation 3.10 was obtained by recognizing that the volume of stream depletion over one cycle, from $t-t_d$ to t, is the same as the volume of stream depletion between the start of pumping and the time t by a single period of pumping (Figure 3.6). Equation 3.8 shows that τ depends on the values of α and γ but that it is independent of the value of t_d/t_a even though the stream depletion rate shows such a dependence (Equation 3.6). Analysis of the τ relationship produced Equation 3.11 which shows that time to equilibrium depends on t_a alone for small values of γ. Inspection of conditions when γ is large lead to the recognition that such wells are close enough to the stream to reach equilibrium within the first pumping period so that the nonuniform pumping pattern is an accurate representation of the stream depletion pattern.

Having obtained a consistent basis for determining the occurrence of dynamic equilibrium permitted study of stream depletion rates at dynamic equilibrium. The β criterion

(Figure 3.10) was developed to characterize the error in depletion rates estimated by assuming steady, continuous pumping at the cycle-average rate. Figure 3.10 showed that under some circumstances, the cycle-average approximation is not an adequate representation of the pumping pattern.

CHAPTER IV

STREAM DEPLETION BY A PUMPING WELL INCLUDING THE EFFECTS OF LINEAR VARIATION OF CAPTURED WETLAND EVAPOTRANSPIRATION

4.1. Introduction

A pumping well located in a wetland-stream aquifer system, where the water table is close to the ground surface, captures some of the well discharge from wetland evapotranspiration (ET) and the rest from the bounding stream (Figure 4.1). Pumping lowers the water table in the wetland so that water is captured by reducing ET losses. The water captured from ET will not be captured from streamflow. Therefore, estimates of streamflow reduction based on methods that do not account for captured evapotranspiration are conservative and over estimate the reduction in streamflow. On the other hand, neglecting the fact that a lowered water table in the wetland may reduce the flux of groundwater up to the wetland surface may result in a failure to identify circumstances that can threaten survival of wetland biology.

Analytical solutions describing the stream depletion rates and volume during periods of steady continuous pumping were summarized in the previous chapter. In addition to these

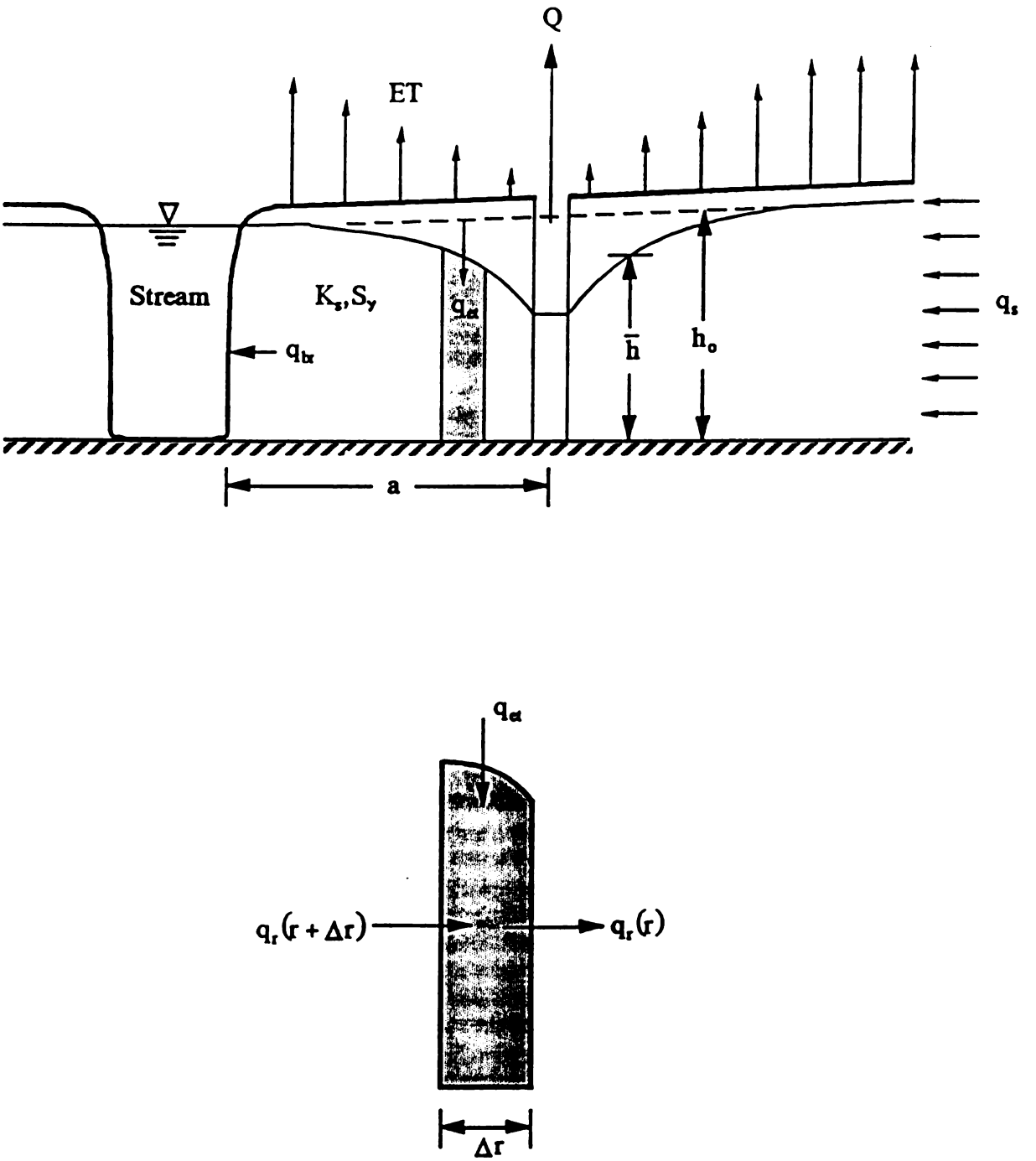

Figure 4.1. Cross section of the semi-infinite stream-wetland aquifer system during pumping.

studies, Hantush (1955, 1964a) developed analytical expressions for stream depletion, for induced leakage from the lower confined aquifer and for mined water from the aquifer storage by continuous pumping wells from a leaky water table aquifer. He also developed solutions to estimate stream depletion, induced leakage from the lower aquifer, and mined water from the aquifer storage by gravity wells in sloping leaky water table aquifers (Hantush, 1964b).

This chapter focuses on the development of analytical solutions that predict captured wetland evapotranspiration and stream depletion in a semi-infinite wetland area where water is continuously pumped from a shallow phreatic aquifer that is bounded by a stream. The model developed in this chapter is based on the Hantush's solutions for pumping from a leaky water table aquifer which is hydraulically connected to a bounding stream.

4.2. Analytical Model Development

4.2.1. Model Assumptions

In addition to the assumptions stated in the third chapter, the following two groups of assumptions are required in order to obtain the analytical model developed in this chapter. The first group of assumptions for the aquifer properties is: (1) there is no recharge to the aquifer from the aquifer surface; however, there is a constant horizontal

boundary flux to the aquifer and this flux supplies the groundwater for evapotranspiration and groundwater discharged to the stream (see Figure 4.1); (2) the boundary flux is not influenced by pumping; (3) water in the unsaturated zone, except for the region close to the well, is always drained to an equilibrium condition; that is, whenever drawdown occurs, soil water in the unsaturated zone is redistributed instantaneously. This assumption was justified by Skaggs and Tang (1976, 1978) and Skaggs (1978) for shallow water table aquifers with high hydraulic conductivity soils.

The second group of assumptions for wetland ET is as follows: (1) Initially the water table is at the ground surface, so that evapotranspiration from the wetland is at the potential rate before pumping; (2) the ground surface is shifted to the bottom of the root zone so that steady state evaporation flux from the water table can be replaced by steady state ET flux from the water table. This assumption was also used by Skaggs (1978) to account for ET from a shallow water table aquifer; (3) evapotranspiration captured at the wetland surface varies linearly with water table depth for drawdown $s \leq d_0$. Here d_0 is the depth at which the evapotranspiration flux becomes zero.

One of the assumptions in the previous chapter is that the specific yield does not vary with the position of the water table and time. This is a valid assumption for deep water table aquifers. Duke (1972) and Gillham (1984) showed

that for shallow water table aquifers with fine textured soils, the specific yield depend on the position of the water table and time. Duke (1972) showed that for Touchet silt loam the relative specific yield changes greatly for depths between 0 meter to 8 meter below the ground surface. This indicates that the unsteady stream depletion and/or captured wetland ET obtained from the analytical solution developed later in this chapter (Equations 4.15 to 4.21) might be in error especially when the value of hydraulic conductivity is low. Duke also showed that for fine sand the relative specific yield values are the same for two different water table depths when the bubbling pressure head is 105 cm. This indicates that, as the values of hydraulic conductivity of soil increases, the bubbling pressure head decreases; in addition a small drawdown in the water table will result in a maximum yield. Therefore, specific yield can be assumed constant for high conductivity soils. This assumption was also used by Skaggs (1975, 1978), and Bredeoheft et al. (1982).

4.2.2. Flow Equation

The governing equation for flow in the control volume, shown as a shaded area in Figure 4.1, can be described approximately by the following differential equation (Hantush, 1964a):

$$\frac{\partial^2 \bar{h}^2}{\partial x^2} + \frac{\partial^2 \bar{h}^2}{\partial y^2} + \frac{2 q_{et}}{K_s} = \left(\frac{S_y}{T}\right) \frac{\partial \bar{h}^2}{\partial t} \qquad (4.1)$$

Here, T is the transmissivity, S_y the specific yield, K_s the saturated hydraulic conductivity, q_{et} the captured evapotranspiration flux, and $\bar{h}(x,y,t)$ the depth of water in the observation well screened throughout the aquifer during pumping. This depth is the average hydraulic head that is intercepted by the observation well and approximately equal to both, $h(x,y,t)$, the depth of water above the base of the aquifer during pumping and $h_b(x,y,t)$, the depth of water in a piezometer that is open at the base of the aquifer (Hantush, 1963, 1964a).

As stated above, the captured evapotranspiration flux is assumed to be a linear function of the water table depth in the aquifer. Although Gardner (1958), Anat et al. (1965), Ripple et al. (1972) and Warrick (1988) showed that evapotranspiration is a highly nonlinear function of water table depth, it was necessary to make this assumption for the following reasons: (1) to obtain a partial differential equation that would yield an analytical solution, (2) to gain a better understanding of the general behavior of the system for a wide range of aquifer parameters during pumping. It is recognized that the linear variation of ET assumption in the analytical solution might produce results that are in error. However, the magnitude of the error is not known a priori. Therefore, it is valuable to develop an analytical solution so

that the magnitude of error in the results caused by this assumption could be investigated. The analytical solution can also be used as a qualitative tool to show the behavior of the system. Prickett and Lonnquist (1971), Trescott et al. (1976), Bredeoheft et al. (1982), and McDonald and Harbaugh (1988) also used this assumption in a hypothetical situation to show how phreatophyte evapotranspiration was captured by steady continuous pumping. With this assumption, captured ET can be written as

$$q_{et} = \frac{PET(h_i - \bar{h})}{d_0} \quad for \quad (h_i - \bar{h}) \leq d_0 \qquad (4.2)$$

Here, *PET* is the potential evapotranspiration rate, h_i is the elevation of the piezometric surface required in order for the groundwater flux that supplies evapotranspiration to be equal to the potential ET rate and d_0 is the depth where q_{et} is equal to the potential ET rate. Substitution of Equation 4.2 into Equation 4.1 gives the following:

$$\frac{\partial^2 \bar{h}^2}{\partial x^2} + \frac{\partial^2 \bar{h}^2}{\partial y^2} + \frac{2PET(h_i - \bar{h})}{d_0 K_s} = \left(\frac{S_y}{T}\right)\frac{\partial \bar{h}^2}{\partial t} \qquad (4.3)$$

Equation 4.3 is the approximate partial differential equation for groundwater flow in the system shown in Figure 4.1. This equation is identical in form to Hantush's (1964a) equation for flow to a well in a horizontal, leaky water table aquifer (Figure 4.2). Thus, his procedure can be followed to

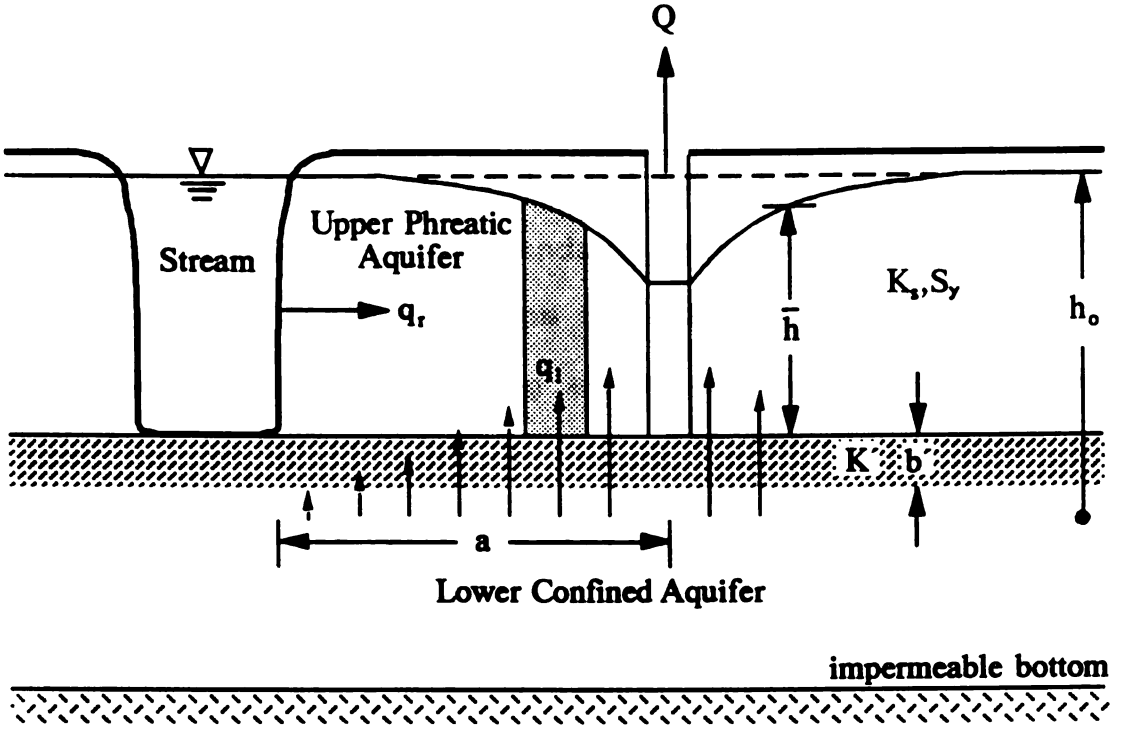

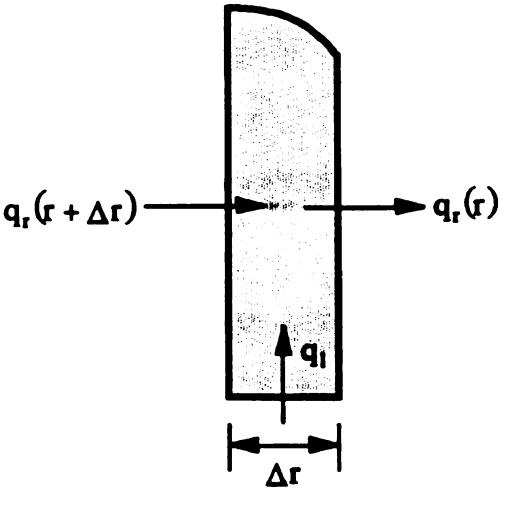

Figure 4.2. Cross section of the leaky water table aquifer during pumping (After Hantush, 1964a).

solve Equation 4.3. This leads to analytical solutions that predict captured wetland ET and captured streamflow.

Following Hantush (1964a), suppose $h_o(x,y,t_o)$ is the distribution of water table depth that would have prevailed in the flow system if the well had not been pumped. That is, h_o is the solution to the boundary value problem shown in Figure 4.3 when the discharge from the pumping well is equal to zero at $t = t_o$. The governing equation for flow in this system then can be written by replacing h with h_o in Equation 4.3:

$$\frac{\partial^2 h_o^2}{\partial x^2} + \frac{\partial^2 h_o^2}{\partial y^2} + \frac{2PET(h_1 - h_o)}{d_o K_s} = \left(\frac{S_y}{T}\right)\frac{\partial h_o^2}{\partial t} \qquad (4.4)$$

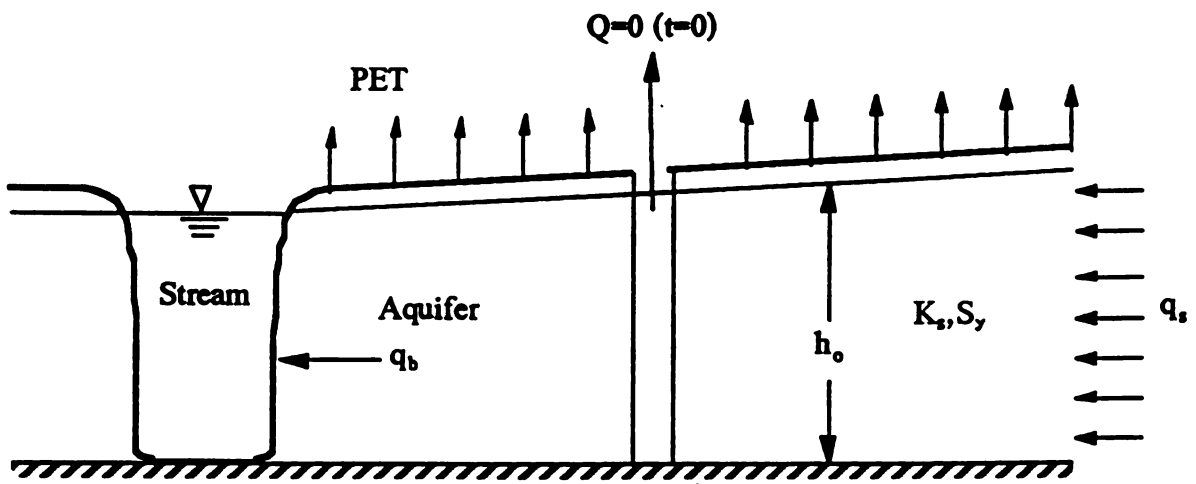

Figure 4.3. Cross section of the semi-infinite stream-wetland aquifer system before pumping.

The superposition principle may be used to combine Equations 4.3, and 4.4. This gives the following differential equation for determining drawdown from the initial condition

in the aquifer

$$\frac{\partial^2(h_0^2-\bar{h}^2)}{\partial x^2}+\frac{\partial^2(h_0^2-\bar{h}^2)}{\partial y^2}-\frac{2PET(h_0-\bar{h})}{d_0K_s}=\left(\frac{S_y}{T}\right)\frac{\partial(h_0^2-\bar{h}^2)}{\partial t} \qquad (4.5)$$

Equation 4.5 is a nonlinear partial differential equation which Hantush (1964) linearized by assuming $(h_0-\bar{h})<h_0$; that is, drawdown is negligible compared to the saturated thickness. Then, if the variables Z and $\bar{b}$ are defined as follows:

$$Z = h_0^2-\bar{h}^2 \qquad (4.6)$$

$$\bar{b} = 0.5(h_0+\bar{h}) \qquad (4.7)$$

Equations 4.6 and 4.7 may be substituted into Equation 4.5 and the resultant differential equation manipulated to give

$$\frac{\partial^2 Z}{\partial x^2}+\frac{\partial^2 Z}{\partial y^2}-\frac{Z}{B}=\left(\frac{S_y}{T}\right)\frac{\partial Z}{\partial t} \qquad (4.8)$$

Here,

$$B = \sqrt{\frac{Td_o}{PET}} \qquad (4.9)$$

and the initial and boundary conditions are:

$$\begin{aligned} Z(x,y,0) &= 0 \\ Z(\infty,y,t) &= 0 \\ Z(0,y,t) &= 0 \\ Z(x,\pm\infty,t) &= 0 \end{aligned} \qquad (4.10)$$

The point sink that represents the pumping well requires that

$$\lim_{r \to 0} \left(r \frac{\partial Z}{\partial r} \right) = -\frac{Q}{\pi K_s}$$

where, $r = [(x-a)^2+y^2]^{1/2}$. Equation 4.8 and its solution are valid as long as the drawdown $(h_i-\bar{h})$ in the aquifer is less than or equal to d_0. Here B is an "ET capture coefficient" that serves the role of Hantush's "leakage coefficient". The linear dependence of q_s on drawdown $(h_i-\bar{h})$ results in a constant B as in the leakage problem.

4.2.3. The relationship between d_0, PET, and soil properties

To obtain an analytical solution to Equation 4.8, d_0 in Equation 4.9 must be determined in terms of *PET* and the unsaturated soil hydraulic properties. Warrick's equation was linearized to obtain a relationship between d_0, *PET*, and the unsaturated soil hydraulic properties. According to Warrick (1988) the steady state ET flux, q_e, is related to the depth to the water table, d, and the unsaturated soil properties by the following equation:

$$d = h_d \left(\left(\frac{K_s A_n}{q_e} \right)^{1/n} - \left(\frac{q_e K_s}{(K_s+q_e)^2} \right) \sum_{j=0}^{\infty} a_j \right) \qquad (4.11)$$

Here h_d is the displacement head during imbibition cycle, n is the pore-size distribution parameter ($n > 1$) and

$$A_n = \left(\left(\frac{\pi}{n}\right) \operatorname{cosec}\left(\frac{\pi}{n}\right)\right)^n \qquad (4.12a)$$

$$a_0 = \frac{n}{n+1} \qquad (4.12b)$$

$$a_{j+1} = \frac{(j+1)\left(\frac{q_e}{K_s+q_e}\right) a_j}{1+j+(1/n)} \qquad for \quad j \geq 0 \qquad (4.12c)$$

Equation 4.11 is an implicit nonlinear relationship between depth to water table and the ET flux. The general nature of this equation is shown in Figure 4.4 for the situation where K_S= 3000 cm/day and *PET* = 0.5 cm/day. This figure shows that the ET flux is constant and equal to *PET* when d is less than or equal to d_C. Here d_C is the critical depth where the ET flux is equal to *PET*. As the water table drops below d_C, the ET rate decreases rapidly at first but goes to zero only as the depth to water table approaches ∞. If the position of the water table is above d_C, the soil is capable of transmitting higher flux than *PET*. Since the upper limit of q_e is limited by atmospheric conditions, then q_e= *PET* when $d \leq d_C$. If the position of the water table is below d_C, then the ET flux is limited by the flux that can be transmitted by the soil profile. The value of d_C can be determined from the intersection of these two curves as shown in Figure 4.4. Here d_C= 21.2 cm was obtained for K_S=3000 cm/day and *PET*=0.5 cm/day.

To find a relationship between d_0, *PET* and the soil properties, q_e in Equation 4.11 is assumed to vary linearly

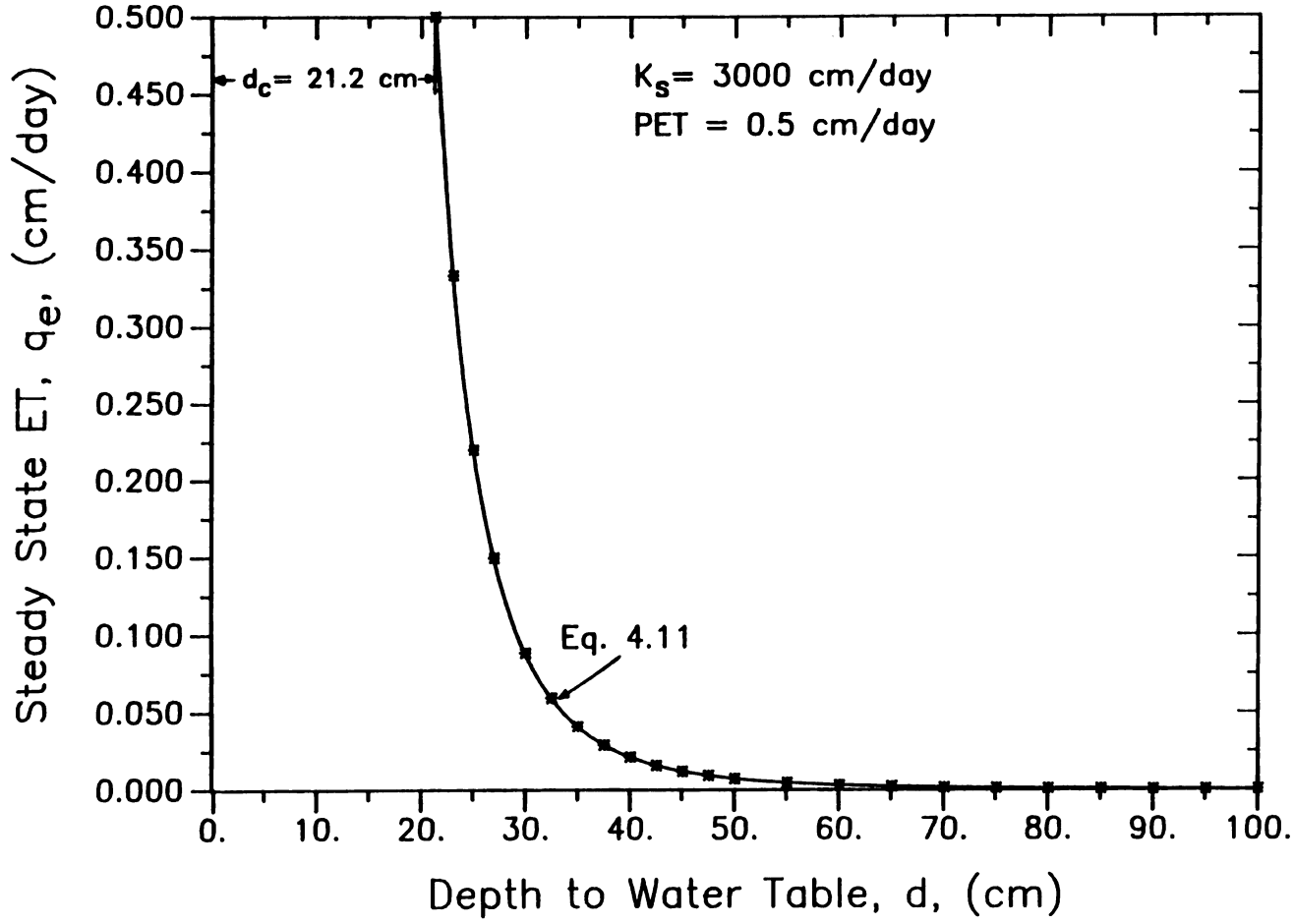

Figure 4.4. Dependence of evapotranspiration on depth to water table when K_s = 3000 cm/day.

between *PET* and zero as the position of the water table varies between the ground surface and d_0.

$$q_e = PET\left(1-\frac{d}{d_0}\right) \quad for \quad d < d_0 \tag{4.13a}$$

$$q_e = C*PET \quad for \quad d = d_0 \tag{4.13b}$$

The depth d_0 is calculated by substituting Equation 4.13b into Equation 4.11.

$$d_o = h_d\left(\left(\frac{K_s A_n}{C*PET}\right)^{1/n} - \left(\frac{C\ PET\ K_s}{(K_s+C*PET)^2}\right)\sum_{j=0}^{\infty} a_j\right) \tag{4.14}$$

$$a_{j+1} = \frac{(j+1)\left(\frac{C\ PET}{K_s+C\ PET}\right)a_j}{1+j+(1/n)} \quad for \quad j\geq 0 \tag{4.14a}$$

Here *C* is a fractional coefficient. For example, $C = 0.0001$ implies that the ET flux is assumed to be zero when q_e is *C*PET*. Conceptually Figure 4.5 shows how steady state captured ET flux varies linearly between zero and *(1-C)*PET* as the position of the water table varies between the ground surface and d_0.

In Equations 4.11 and 4.14, the displacement head and pore-size distribution parameter can be determined by empirical relationships given by Campbell (1985). However these relationships are not reliable for high conductivity soils. Therefore, the values of the displacement head and the pore-size distribution must be determined experimentally (Corey, 1990).

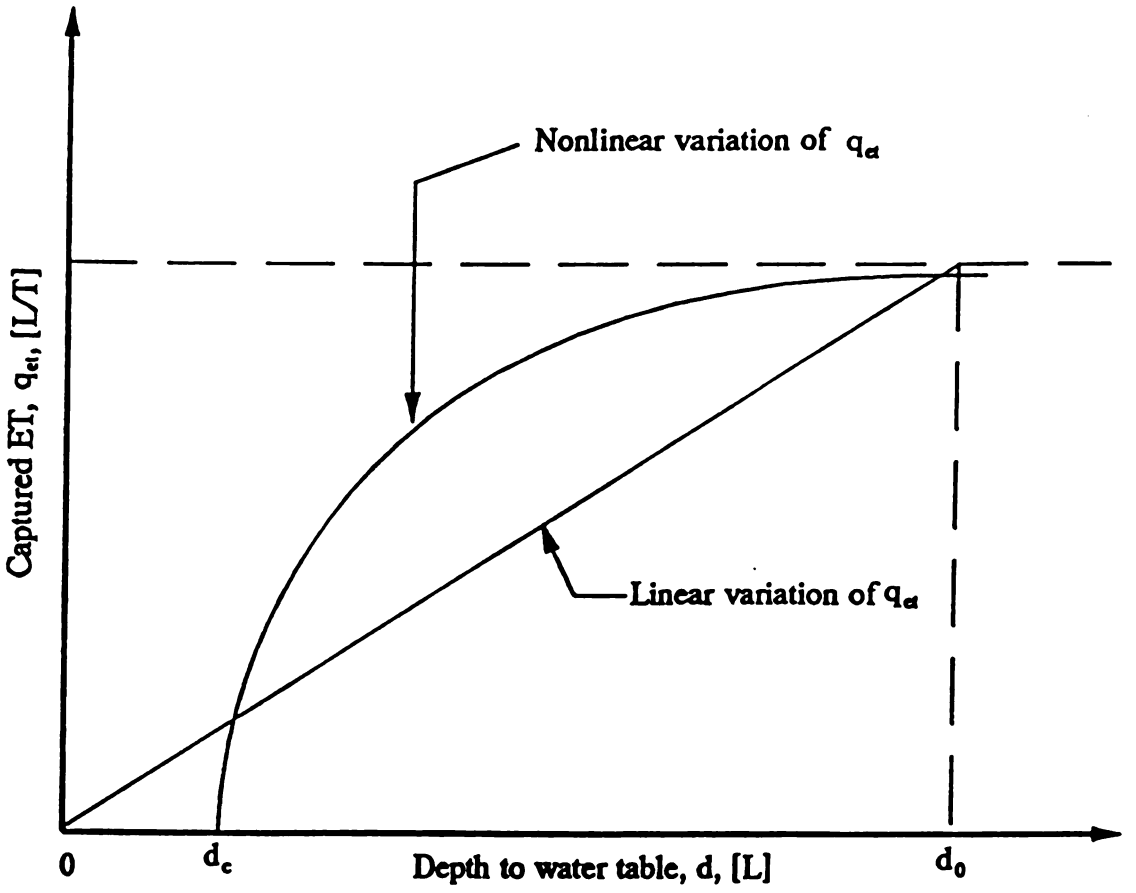

Figure 4.5. Linear and nonlinear dependence of captured ET, q_{et}, on the depth to water table.

4.2.4. Solutions for Drawdown, Stream Depletion, Mined Water, and Captured ET

According to Hantush (1964a), Equation 4.8 can be solved to determine the following relations (see Appendix A):

For drawdown,

$$s = \frac{Q}{4\pi T}\left(W(u, \frac{r}{B}) - W(u', \frac{r'}{B})\right) \qquad (4.15)$$

where,

$$u = r^2 S/4Tt$$

$$u'^2 = r'^2 S/4Tt$$

$$r'^2 = (x+a)^2 + y^2$$

For the rate of stream depletion,

$$q_r = 0.5Q(e^{-\epsilon}\ erfc(\beta_\epsilon) + e^{\epsilon}\ erfc(\eta_\epsilon)) \qquad (4.16)$$

where

$$\epsilon = a/B$$

$$\alpha = t/t_a$$

$$\beta_\epsilon = (0.5/\sqrt{\alpha}) - \epsilon\sqrt{\alpha}$$

$$\eta_\epsilon = (0.5/\sqrt{\alpha}) + \epsilon\sqrt{\alpha}$$

For the volume of stream depletion,

$$v_r = Qt\left(\frac{q_r}{Q} + \frac{1}{4\alpha\epsilon}(e^{\epsilon}\ erfc(\eta_\epsilon) + e^{-\epsilon}\ erfc(\beta_\epsilon))\right) \qquad (4.17)$$

For the rate that water is mined from aquifer storage,

$$q_m = Q\ e^{-(\epsilon\sqrt{\alpha})^2}\ erf(0.5/\sqrt{\alpha}) \tag{4.18}$$

and for the volume of mined water,

$$v_m = Qt\left(\frac{1-\frac{q_r+q_m}{Q}}{\alpha\epsilon^2}\right) \tag{4.19}$$

Then, following Hantush, the captured ET flux can be calculated as

$$q_{et} = Q - (q_r+q_m) \tag{4.20}$$

and the volume of captured ET,

$$v_{et} = Qt - (v_r+v_m) \tag{4.21}$$

During the steady state (as $t \rightarrow \infty$) equations for the rate and volume of stream depletion can be simplified as:

$$q_r = Q\ e^{-\epsilon} \tag{4.22}$$

$$v_r = Q\ e^{-\epsilon}\left(t-\frac{a\ B\ S}{2T}\right) \tag{4.23}$$

At steady state, Equations 4.18 and 4.19 reduce to;

$$q_m = 0 \tag{4.24}$$

$$v_m = \frac{B^2\ S\ Q}{T}\ (1-e^{-\epsilon}) \tag{4.25}$$

and equations for the rate and volume of captured ET become:

$$q_{et} = Q\,(1-e^{-\epsilon}) \tag{4.26}$$

$$v_{et} = Q\left(t-e^{-\epsilon}\left(t-\frac{S\,B}{T}\left(\frac{a}{2}+B\right)\right)+\frac{B^2S}{T}\right) \tag{4.27}$$

In Equation 4.15, $W(u,r/B)$ is a leaky aquifer well function which is available in tabular form in many references (Hantush, 1956; Walton, 1962; and Hantush, 1964a). The variable B in Equations 4.15 to 4.27 must be defined by Equation 4.9 in order to account for captured ET as linear function of water table depth.

Equations 4.16 to 4.27 are valid for $s<d_o$. According to Equation 4.2, the maximum possible ET capture at a point is PET. Thus, the solution for the case where $q_a = 0$ can be obtained by taking $PET = 0$ in Equation 4.9. Then $\epsilon = 0$ and Equations 4.16 and 4.17 reduce to Glover and Balmer's (1954) and Jenkins's (1968) equations for a nonleaky water table aquifer where evapotranspiration processes are neglected. Note that q_a in Equations 4.20 and 4.26 is the total captured ET flux i.e. the captured flux integrated over the entire surface area effected.

Figure 4.6 shows conceptually how stream depletion and captured ET rates vary with time if the pumping rate Q is continuous. The dashed line in this figure shows the stream depletion when the effects of ET are neglected. The lower solid curve shows the stream depletion rate when the effects of ET capture are included, and the upper solid curve which starts from the pumping rate at $t = 0$ and approaches the

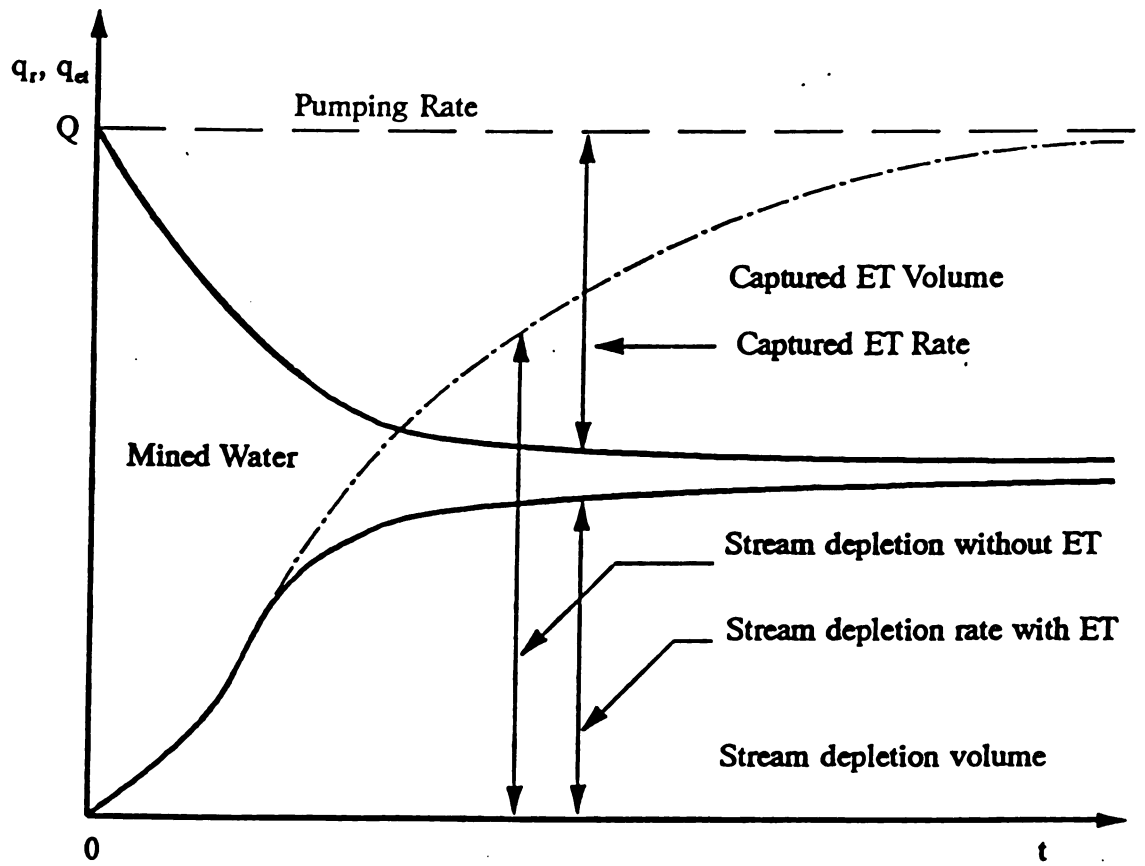

Figure 4.6. Transient behaviour of stream depletion and captured ET rates when pumping is continuous.

stream depletion rate as time increases, shows the captured ET. The area under the lower solid curve (q_r curve) between zero and time t gives the accumulated volume of stream depletion (v_r) at time t. The area between the upper solid curve (captured ET curve) and the dashed horizontal line (pumping rate) in the same period is the accumulated volume of captured ET. The area between the two solid curves in the same period is the accumulated volume of water mined from aquifer storage.

The temporal response of the system exhibits the following characteristics that can be seen in Figure 4.6. Pumping causes a drawdown cone to develop in the aquifer. Initially, most of the water removed is mined from aquifer storage. As pumping continues, the drawdown cone enlarges. This generates a horizontal flow to the well by reducing the groundwater flow to the stream as well as reducing the vertical flux from the water table that supplies ET at the ground surface. The system reaches steady state when mining ends at which time the discharge from the well must equal the total rate of capture from the stream and ET boundaries.

Equations 4.16 and 4.18 can be written in dimensionless form as:

$$\tau_{dr} = f(\epsilon, \alpha) \qquad (4.28a)$$

$$\tau_{dm} = f(\epsilon, \alpha) \qquad (4.28b)$$

and Equation 4.22 can be written in dimensionless form as:

$$\tau_{er} = f(\epsilon) \qquad (4.29)$$

where,

$\tau_{er} = q_r/Q$,

$\tau_{em} = q_m/Q$.

Calculation of stream depletion rate and water removed from the aquifer storage by Equations 4.16 and 4.18 require evaluation of the complementary error function and the error function. These equations were evaluated numerically (see the listing of the computer program in Appendix B) and plotted in Figure 4.7 in terms of the dimensionless parameters suggested by Equations 4.28a and 4.28b.

In Figure 4.7, for the solid lines that increase as the dimensionless time, α; increases represent dimensionless stream depletion, τ_{er}; and the dashed lines that decrease with increasing α represent dimensionless water mined, τ_{em}, from aquifer storage. This figure can be used to determine the rates of stream depletion, mined water, and ET capture at any desired time for the range of values of the dimensionless pumping distance, ϵ, shown in the figure. In order to make the value of $\epsilon = 0$ in Figure 4.7, either *'a'* or *PET* has to be zero. The *'a'* = 0 case indicates that the well is in the stream. The *PET* = 0 case indicates that the ET prior to pumping is zero so there is no ET to capture. Figure 4.7 shows that as the dimensionless pumping distance increases,

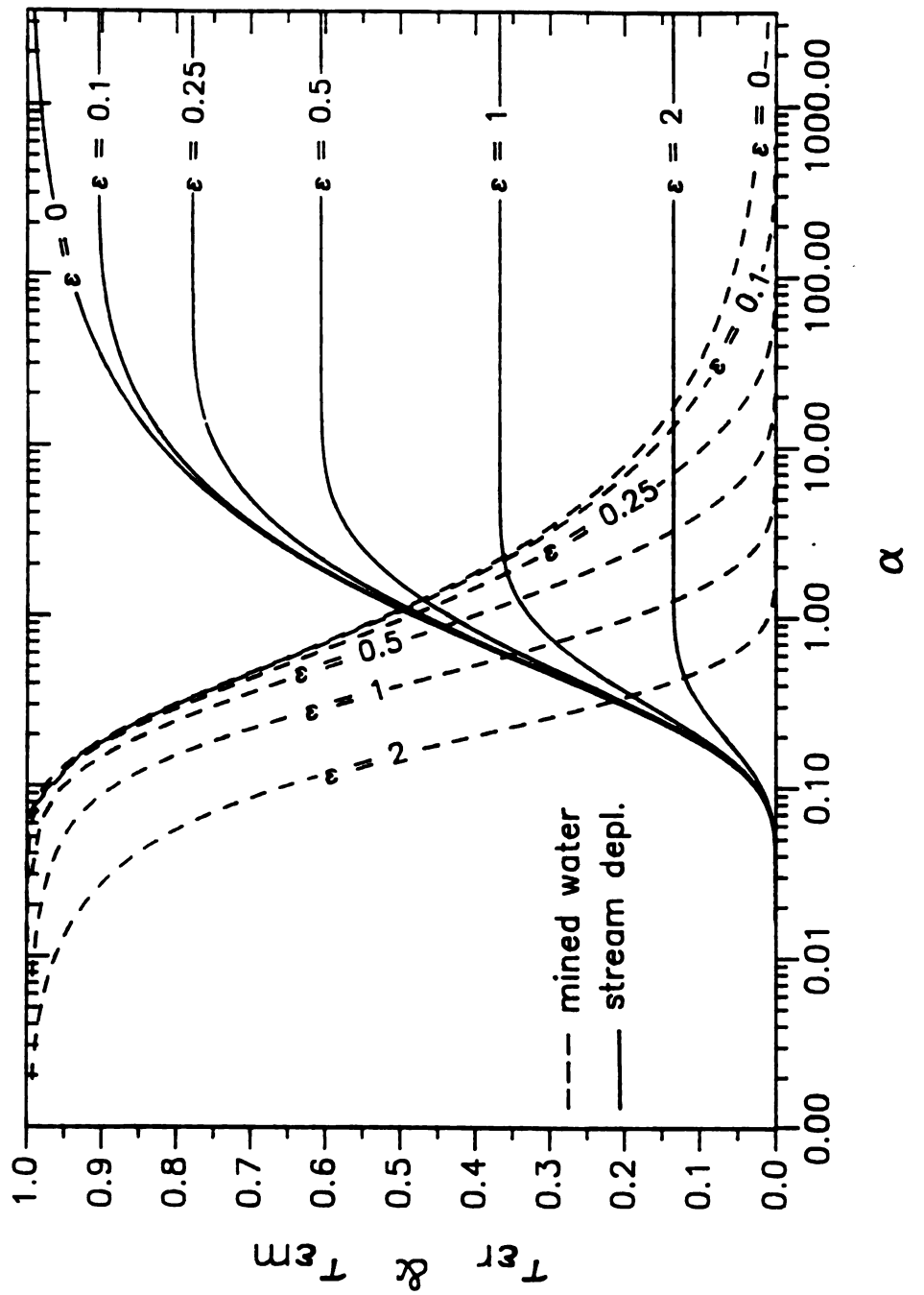

Figure 4.7. The dependence of τ_{df}, and τ_{dm} on the scaled time, α, and the scaled pumping distance, ϵ, during continuous pumping.

the portion of the well discharge captured from the stream decreases; whereas, the portion of the well discharge captured from the wetland ET increases. Furthermore, when the distance between the pumping well and the stream increases, the aquifer response time, t_a, increases (Jenkins, 1968; Burns, 1983). Burns (1983) showed that as t_a increases, the response of the recharge boundary (stream) to the pumping is slowed which results in less stream depletion at any instant of time. Moreover, as the distance between the pumping well and the stream increases, the area from which ET may be captured increases. This results in a larger rate of ET captured from the wetland and a smaller rate of stream depletion.

Figure 4.7 can be used to determine the time when the practical steady state condition is reached. Theoretically, steady state is reached when mining stops, that is, $q_m = 0$. According to Equation 4.18, $q_m \rightarrow 0$ in two cases. The first case is $\epsilon \rightarrow \infty$ and the second case is $\alpha \rightarrow \infty$. In the first case, ϵ can approach infinity either as $a \rightarrow \infty$ or as $B \rightarrow 0$. For a given stream-wetland-aquifer system the value of B is constant, thus ϵ can approach infinity only as $a \rightarrow \infty$. This situation can be seen in Figure 4.7; as ϵ increases, the time to steady state decreases. As explained above, as 'a' increases, the value of t_a increases. This indicates that the major portion of the pumped water is being captured from the wetland ET long before the effects of the drawdown reached the stream. In the second case, α can approach infinity either as $t \rightarrow \infty$ or as $t_a \rightarrow 0$. If

'a' is fixed, then α can approach infinity only as $t \rightarrow \infty$. For practical purposes, steady state is reached at a finite time if it is defined as occurring when $\tau_{cm}=\tau^{*}_{cm}$. In this study the value of τ^{*}_{cm} was taken as 0.01. This practical steady state is reached at $t = t_e$. Substituting the value of τ^{*}_{cm} and t_e into Equation 4.18 and solving for t_e results in the following:

$$t_e = -\frac{t_a}{\epsilon^2}\left(-4.605-\ln\left(erf\sqrt{\frac{t_a}{4t_e}}\right)\right) \qquad (4.30)$$

Equation 4.30 is an implicit equation for t_e which can be solved by trial and error methods. The dimensionless form of Equation 4.30 could have been plotted for determining the value of t_e. This would have eliminates the need to solve Equation 4.30.

The dimensionless rate of stream depletion at steady state is plotted in Figure 4.8 in terms of the dimensionless pumping distance suggested by Equation 4.29. This figure shows that for a fixed value of 'B' the rate of stream depletion decreases as 'a' increases. This figure also shows that at steady state, as 'a' increases, captured ET increases too, since q_m= 0 at steady state. From this analysis, it can be deduced that the coefficient B is the radius of the characteristic area required to capture Q from the wetland area where ET is at the potential rate.

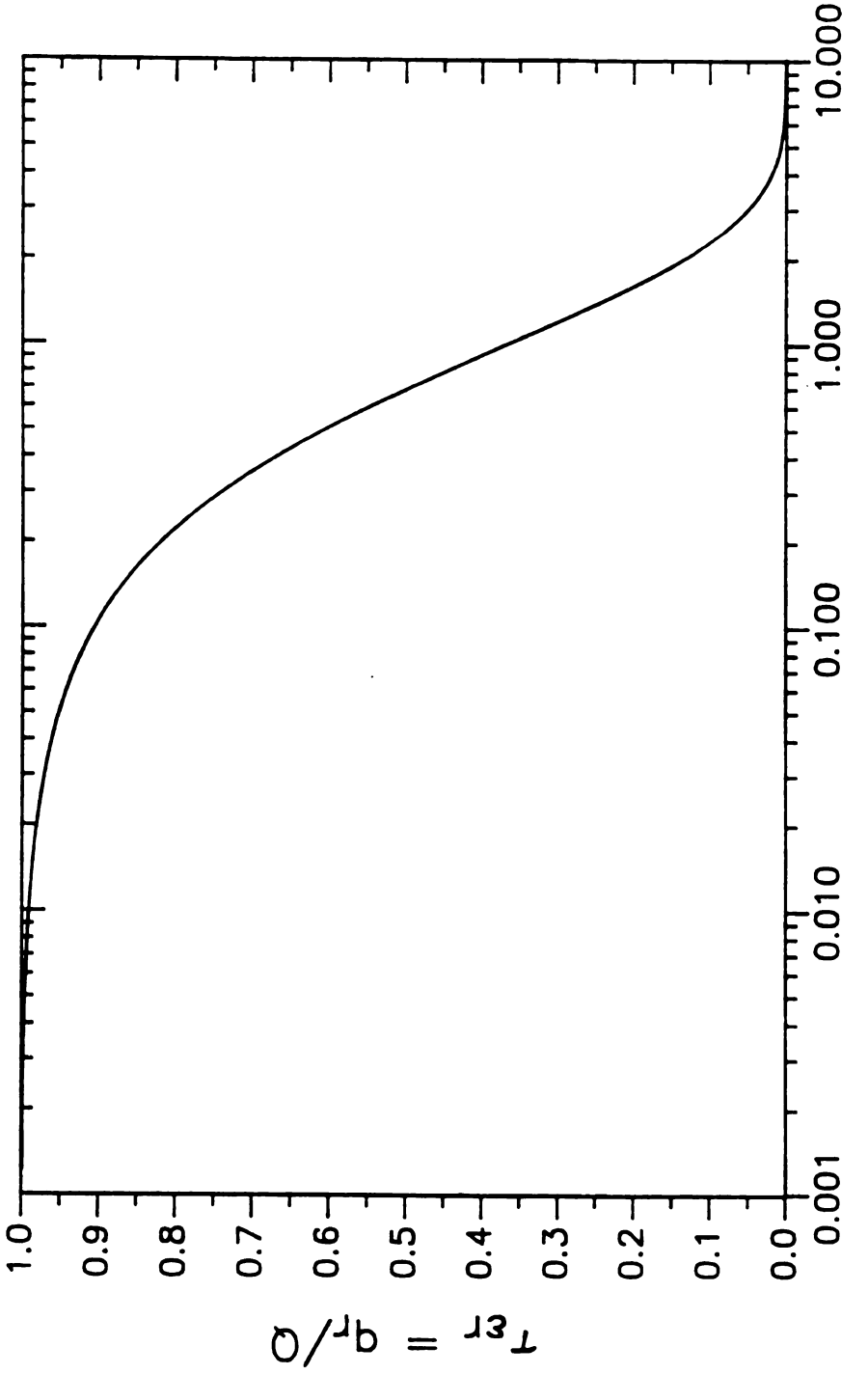

Figure 4.8. Dependence of τ_{ET}, the scaled steady state stream depletion on the scaled pumping distance, ε, when ET varies as a linear function of water table depth.

4.2.5. Discussion of the Solution

The results of the analytical model developed in this chapter are valid when the actual field conditions approach the assumed conditions. The actual field conditions can be described as a stream-wetland-aquifer system where the water table is shallow. In this system, Duke (1972) and Gillham, (1984) have shown that the specific yield depends on the position of the water table and time. The variable specific yield assumption is discussed in section 4.2.1 in detail, thus, it will not be discussed in this section again. Furthermore, Gardner (1958), Anat et al., (1965), Ripple et al., (1972), and Warrick (1988) have shown that ET from the wetland surface varies as a nonlinear function of the position of the water table depth and the unsaturated soil hydraulic properties. The effects of a linear variation of ET assumption on the accuracy of results obtained from the analytical model is investigated in this section.

The analytical model results at steady state might therefore deviate from the results obtained from a model that describes the actual system in more detail. As explained in section 4.2.4 that as long as *'d'* is less than d_c, there is no reduction in wetland ET and as *'d'* drops below d_c, the ET rate decreases as a nonlinear function of *'d'*. Contrary to the assumption of a nonlinear variation of ET, Figure 4.5 shows that even small change in *'d'* produces a reduction in the

wetland ET rate in the case of a linear ET assumption. Therefore, a linear dependence of captured ET on the depth to water table can produce a substantial amount of error in predicting the rate of stream depletion and capture wetland ET at steady state. Figure 4.9 shows the magnitude of error in steady state stream depletion rates obtained from the analytical model as compared to results obtained from a model that employes the nonlinear dependence of ET on the depth to water table. The latter results are obtained with a numerical solution to the nonlinear form of Equation 4.1 (Equation 5.1). Figure 4.9 shows the results of the numerical model and the analytical model at steady state for pumping distance varying from 0 m to 1600 m. This figure shows the comparison for K_s=43.2 m/day. The comparison is also made for the lower range of values of K_s and presented in the next chapter.

Figure 4.9 also shows the steady state stream depletion rates obtained from the analytical model for three different values of d_0. These values of d_0 are computed with Equation 4.14 by adjusting the value of C. It is apparent from the figure that when the value of d_0 is small, the results obtained from the analytical model are in substantial error. The amount of error could be decreased if the value of C in Equation 4.14 could be altered in order to increase the value of d_0. It was deduced from this analysis that a theoretical basis is needed to justify the above method that determines the value of d_0 that reduces the error. However, it is not

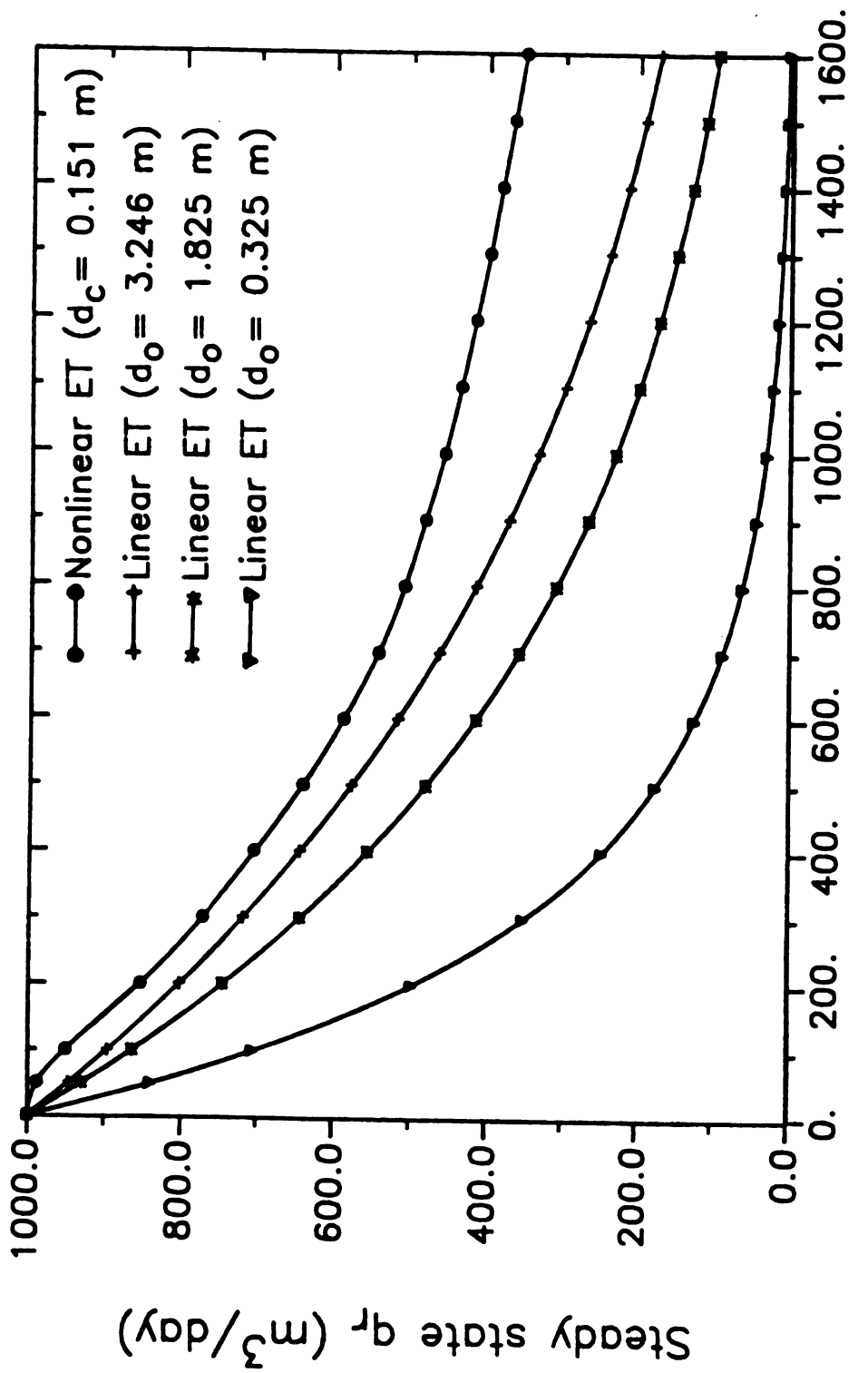

Figure 4.9. Comparison of steady state stream depletion rates obtained from the nonlinear ET model (AQUIFEM) when d_c=0.151 m, with the depletion rates obtained from the linear ET model for different values of d_o (Analytical model).

possible to define such a method at this stage of the study. Therefore, the analytical model developed in this chapter is restricted significantly as a quantitative tool, but it is still valuable as a qualitative tool.

4.3. Solution of Partial Differential Equation Using A 2-D Finite Element Model

A 2-D horizontal finite element model, AQUIFEM-1 (Townley and Wilson, 1980), was modified to incorporate linear and nonlinear variation of ET as a function of water table depth. The objectives of this modification were (1) to compare the analytical model results with a numerical solution of the equation and (2) to prepare the numerical model for further investigations. The governing flow equation of the numerical model is a second order nonlinear parabolic partial differential equation and it is solved iteratively by employing the finite element method, based on the Galerkin technique with linear finite elements (Townley and Wilson, 1980).

4.3.1. Formulation and Description of the Hypothetical Aquifer for 2-D Finite Element Model Application

In order to compare the finite element results with the analytical solution, the aquifer is located adjacent to a

flowing surface water feature (Figure 4.10a). The aquifer is 4400 meters wide and 6300 meters long. Initially, the water table in the aquifer is horizontal and very close to the soil surface so that ET is at the potential rate. The aquifer is bounded by a fully-penetrating stream on the southern side and bounded by no-flow boundaries on the other sides. The well is located 800 meters away from the stream as shown in Figure 4.10a and pumps water from the aquifer at a constant rate of 3000 m^3/day. Table 4.1 shows the characteristics of the hypothetical aquifer. The aquifer domain shown in Figure 4.10a is divided into triangular finite elements for the application of the numerical model. Three grid configurations were designed in order to determine the effects of spatial discretization of the aquifer domain on the accuracy of the numerical model results. Table 4.2 shows the total number of elements, the total number of nodes and the dimensions of the grid in the vicinity of the well and the stream in each configuration.

The finite element and analytical models were applied to the aquifer described above to predict the stream depletion and captured wetland ET. Figure 4.11 shows the results of the simulation from both models for comparison.

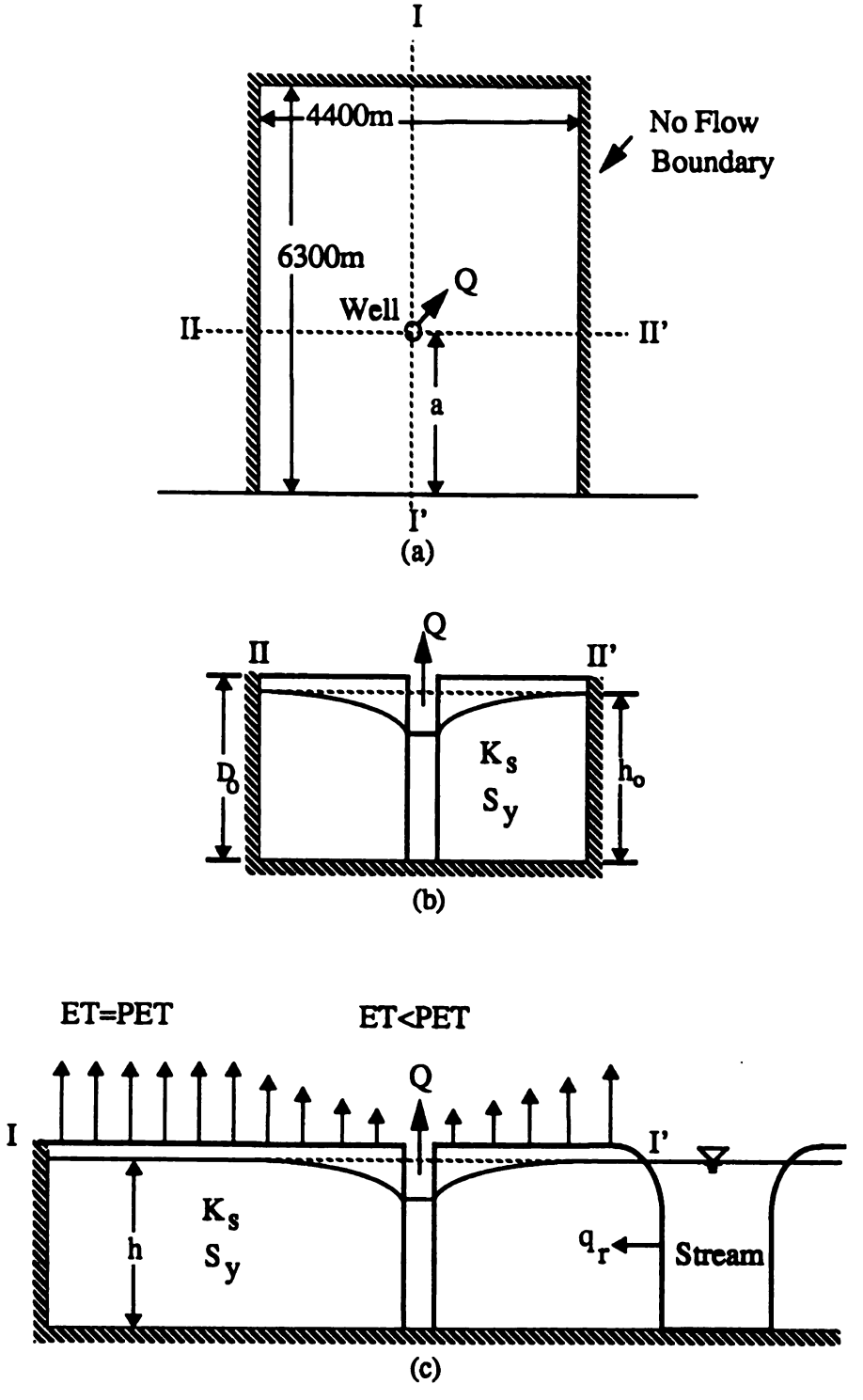

Figure 4.10. (a) Plan view of the hypothetical aquifer, (b) cross section II-II', (c) cross section I-I'.

Table 4.2. Characteristics of the hypothetical aquifer

(1)	(2)
Aquifer thickness, D_0 (meter)	30.01
Initial saturated thickness, h_0 (meter)	30.00
Saturated hydraulic conductivity, K_s (meter/day)	30.00
Specific yield, S_y	0.10
Maximum ET depth, d_0 (meter)	0.70
Potential ET rate, (meter/day)	0.005

Table 4.2. Characteristics of the grid configurations used in the finite element model

	Total number of nodes	Total number of elements	Dimensions of the the smallest elem. (Base width X height)
Configuration 1	416	744	200 X 200
Configuration 2	1081	2024	100 X 100
Configuration 3	2808	5396	50 X 50

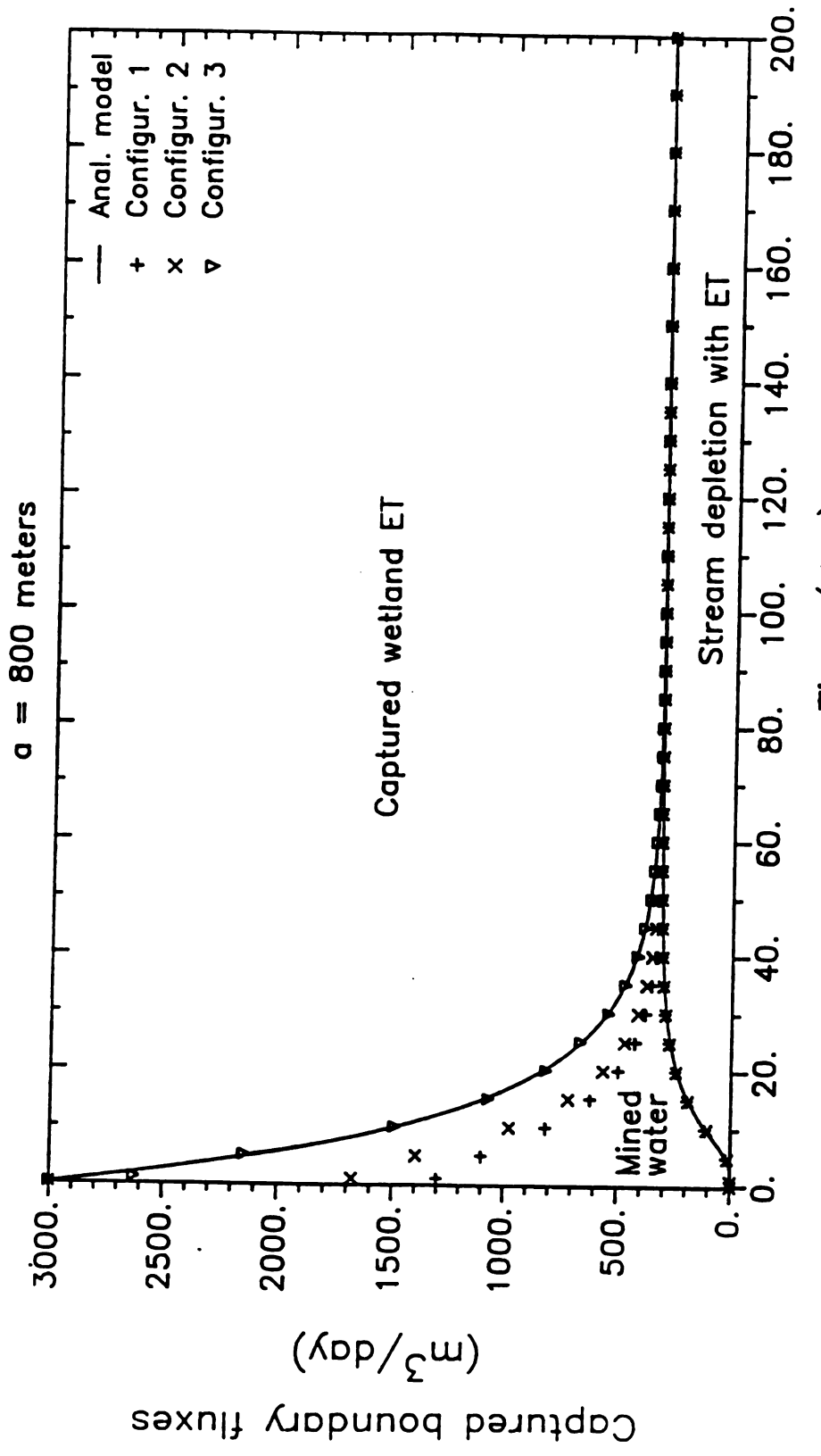

Figure 4.11. Comparison of the boundary fluxes produced by the analytical model and by the 2-D finite element model.

4.3.2. Comparison of the Analytical Model and 2-D Finite Element Model Results

Figure 4.11 shows stream depletion rates and captured ET rates obtained from both models using 1 day time increments for the computations during continuous pumping. This figure shows that stream depletion rates obtained from both models agreed well throughout the simulation for each configuration. table 4.1 and table 4.2. Stream depletion rates obtained from the finite element model are observed to converge to the rates obtained from the analytical model as $\Delta t \rightarrow 0$.

Stream depletion rates agreed well for all the configurations described in Table 4.2. However, the captured ET rates obtained from the finite element model are considerably different from those obtained with the analytical model during early pumping for configurations 1 and 2. These results agreed well throughout the simulation for configuration 3. Figure 4.11 shows the simulation results for the three configurations. This clearly indicates that as spatial discretization of the aquifer domain gets smaller in the vicinity of the well and the stream, captured ET rates obtained from the numerical model converge to rates obtained from the analytical model. At late time, when steady flow is established, the two models converge for all configurations.

As stated earlier, the analytical model describes the behavior of a semi-infinite aquifer while the numerical model

was applied to the finite aquifer domain shown in Figure 4.10. It is apparent that there is no influence of the no-flow boundaries in the results obtained with the analytical model, whereas, the results produced by the numerical model could be influenced if the drawdown cone reached the no-flow boundaries of the aquifer. Figure 4.12 and Figure 4.13 show that the water table is unaffected at the no-flow boundaries. Figure 4.12 shows the water table elevations at cross section II-II′ when a steady state condition is obtained. The well is located 2200 meters from both the eastern and western no-flow boundaries. The piezometric head at the boundary computed by the finite element model is 30.0 meters which is the same as the initial piezometric head and the drawdown at the well is approximately equal to 1.6 meters. This amount of drawdown at the well indicates that the analytical solution is in error in the vicinity of the well since drawdown at the well is greater than d_0 = 0.7 meter. Figure 4.13 shows the water table elevations at cross section I - I′ at steady state. The water table profile between the well and the northern no-flow boundary of the aquifer indicates that this boundary of the aquifer did not influence the results either.

4.4. Summary and Conclusions

An analytical model was developed that predicts the stream depletion by a steady continuous pumping well where the

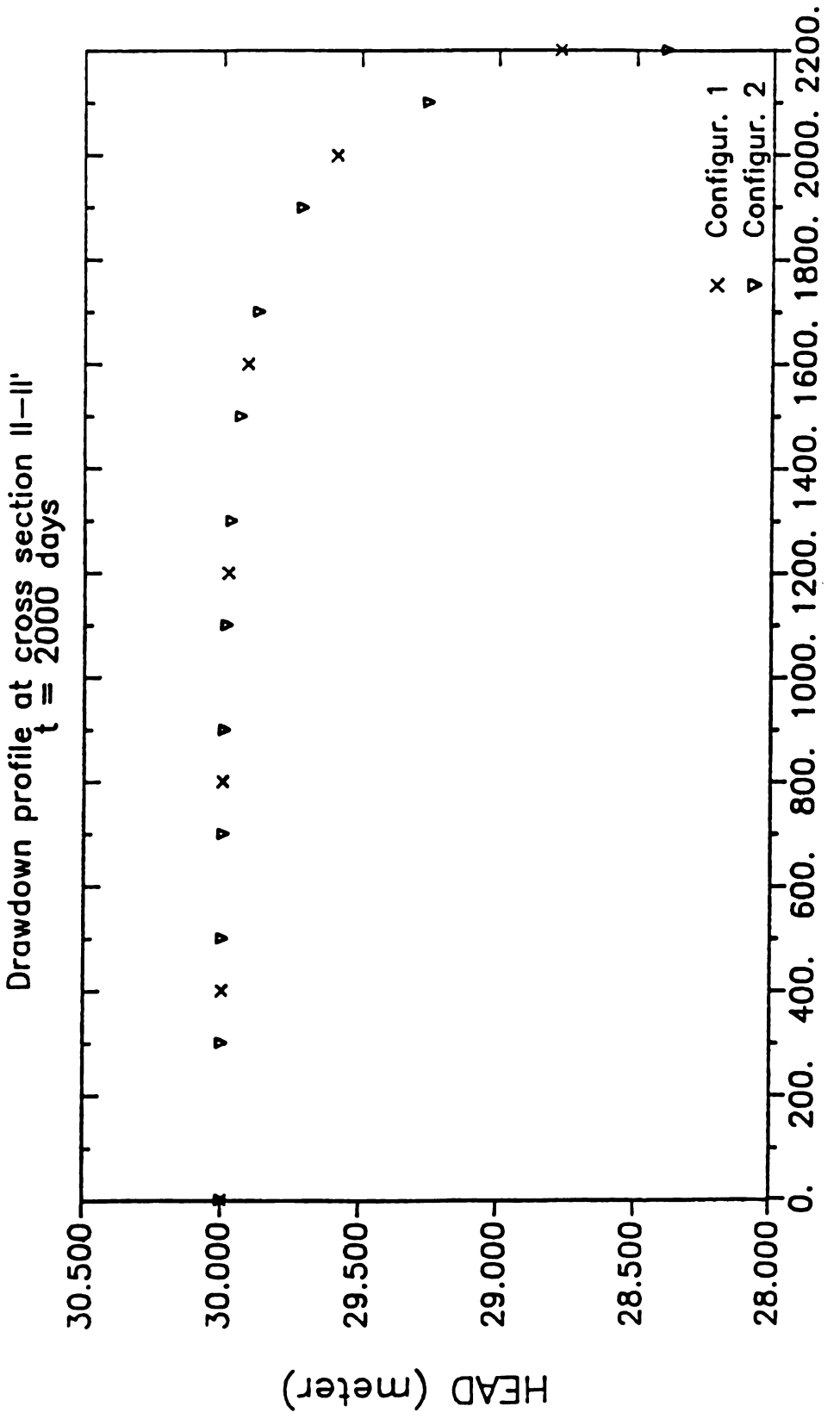

Figure 4.12. Water table profile computed by the 2-D finite element model along the cross section II - II′ at t = 2000 days.

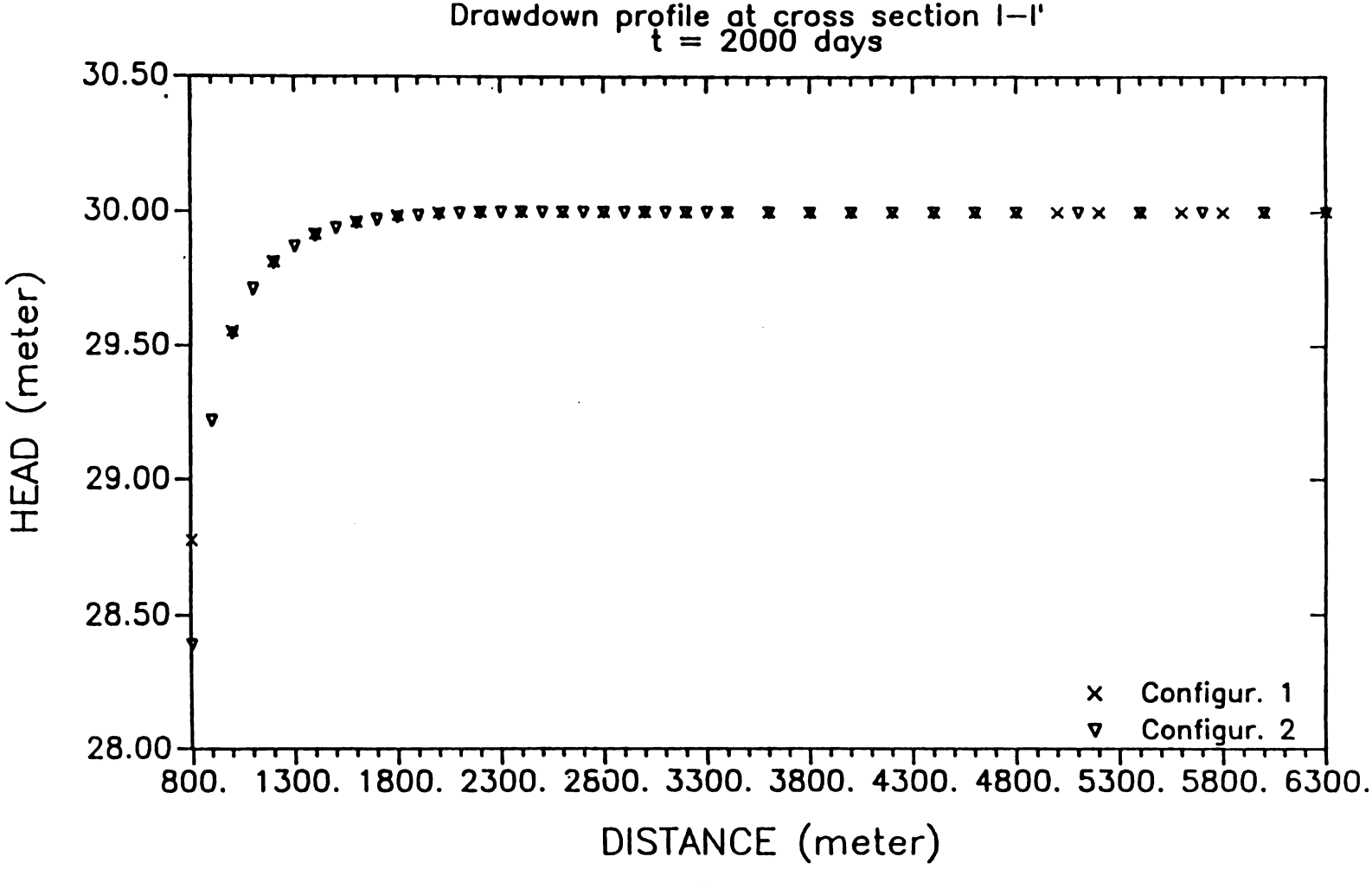

Figure 4.13. Water table profile computed by the 2-D finite element model along the cross section I - I'at t = 2000 days.

effects of captured ET are taken into account. The analytical model is based on Hantush's solution for pumping from a leaky phreatic aquifer connected to a bounding fully penetrating stream. Hantush's leakage from the lower confined aquifer was interpreted to describe a reduction in wetland ET resulting from the drawdown of the water table in a shallow phreatic aquifer. It was assumed that ET varies as a linear function of the drawdown in the phreatic aquifer so that ET is at the potential rate with zero drawdown and zero at a depth d_0. An explicit relationship was derived that shows how potential ET and d_0 are related to Hantush's leakage coefficient. Properties of unsaturated soils were incorporated into the solution by using Warrick's relationship between ET flux and depth to water table to determine d_0.

Application of the analytical model showed that as the dimensionless distance between the well and the stream increases (increasing ϵ), the portion of the pumping well discharge captured from wetland ET increases; whereas, the portion captured from the stream decreases. This resulted from increased aquifer response time and increased area from which ET could be captured. A dimensionless graph (Figure 4.7) was developed that shows the relationship between stream depletion, water mined from aquifer storage, captured wetland ET, and time. The analysis indicated that Figure 4.7 can be used to determine the time, t_e, when the system reaches practical steady state. Analysis of Figure 4.7 also showed

that as scaled pumping distance (ϵ) increases, the system reaches steady state faster than the case where the effects of captured ET was neglected.

A dimensionless graph (Figure 4.8) for the rate of stream depletion at steady state was also developed as a function of the scaled pumping distance. This graph could easily be used to determine the stream depletion rate and captured ET rate at steady state for known value of the scaled pumping distance.

The solutions obtained in this study are appropriate only when the actual field conditions approach the assumed conditions. The accuracy of the steady state stream depletion, based on the assumption that captured ET rate linearly depends on the position of the water table, was investigated. The analysis indicated that this assumption could result in substantial error in stream depletion rate when d_0 was small. The analysis also indicated that the magnitude of this error could be decreased as the value of d_0 was increased. However, there was no theoretical procedure to determine the value of d_0 which could minimize the error.

Additional error could be expected from the analytical model results during the transient period. This error would be produced as a result of the constant specific yield assumption for soils that have low hydraulic conductivity values. It was concluded from the above analysis that the analytical model is restricted significantly as a quantitative tool, but it is still valuable as a qualitative tool.

It was determined that the analytical model is also a valuable tool for determining the optimum finite element grid density which produces accurate stream depletion rates and captured wetland ET rates during the transient period.

CHAPTER V

STREAM DEPLETION BY A PUMPING WELL INCLUDING THE EFFECTS OF NONLINEAR VARIATION OF CAPTURED WETLAND EVAPOTRANSPIRATION

5.1. Introduction

In the previous chapter, an analytical solution for stream depletion and captured wetland ET produced by a continuous pumping well from a shallow water table aquifer is derived. A linear variation of captured wetland ET is incorporated into the flow equation in order to obtain the analytical solution. The assumption of linear variation of wetland ET as a function of water table depth is found to overestimate the captured wetland ET and underestimate the stream depletion for the values of d_0 defined by Equation 4.14. When pumping starts and the drawdown cone develops and propagates in the aquifer, reduction in wetland ET starts immediately with the assumption of the previous chapter. Contrary to the assumption of a linear variation of ET, it is shown in previous chapter (section 4.2.3) and by Ripple et al., (1972) that there is no change in ET until the depth to the water table is equal to the critical depth, d_c. When the depth to the water table exceeds d_c, ET is reduced according

to Warrick's relationship (Equation 4.11) given in chapter 4.

The objective of this chapter is to develop a method that can be used to predict the steady state stream depletion rate produced by a pumping well which includes the effects of captured wetland ET. For this method a nonlinear variation of wetland ET as a function of the water table depth and the soil properties is incorporated into the flow equation. Because of the nonlinear behavior of ET, the governing flow equation becomes nonlinear, as shown in section 5.2.2. Thus, there is no known analytical solution. To solve the flow equation for stream depletion a 2-D finite element model (Townley and Wilson, 1980) is employed for a hypothetical situation. To generalize the numerical results for stream depletion, dimensional analysis is employed to find the functional relationship between the stream depletion rate, the aquifer properties, and the pumping characteristics. As a result of dimensional analysis, the scaled steady state stream depletion will be shown to depend on five independent scaled variables in the case where ET varied as a nonlinear function of the water table depth. Therefore, it is not practical to generalize the simulation results in this case. In order to reduce the number of scaled independent parameters, the nonlinear variation of ET is approximated by a step variation of ET as a function of water table depth. This assumption reduced the number of scaled independent parameters to three; thus, it is practical to present the numerical results graphically. The scaling of the flow equation in the case of

the nonlinear variation of ET as well as the step variation of ET is explained in detail in section 5.2.4.

The accuracy of stream depletion rates obtained from the numerical model by incorporating the step ET assumption is determined by comparing stream depletion rates resulting from the nonlinear ET assumption. The comparison is made during the transient period because the numerical model results oscillate in the step ET case. The oscillation is caused by the spatial discretization of the aquifer domain and the insufficiently small time intervals that are practical for the transient computations. The accuracy analysis of the depletion rates is presented in section 5.3.2. Excellent agreement is found between stream depletion rates that were obtained from the numerical models. This indicated that steady state stream depletion rates can be obtained numerically by employing the nonlinear variation of ET and that such results can be presented in the dimensionless form developed by employing the step assumption.

From the results of the computer simulations, families of dimensionless graphs were developed for a wide range of soil hydraulic properties and pumping distances. Provided the basic assumptions of the model are satisfied, these graphs provide a means for easily determining the steady state stream depletion and captured wetland ET rates if the following parameters are known: the transmissivity of the aquifer, the displacement head, the pore size distribution parameter (Anat et al., 1965), the initial position of the water table, the

perpendicular distance between the river and the well, the pumping rate, and the annual average *PET* rate.

5.2. Model Development

5.2.1. Model Assumptions

In addition to the assumptions for the aquifer properties stated in chapters 3 and 4, the following assumptions are required for wetland ET. These assumptions are necessary to make use of the advantage of dimensional analysis technique and to develop the families of dimensionless graphs from the results of numerical simulations: (1) the ground surface is located from the bottom of the root zone. With this assumption, the steady state evaporation rate from the water table can be replaced by the steady state ET rate from the water table. This assumption was also used by Skaggs (1978) to determine the reduction in steady state ET rate from a shallow water table aquifer. Skaggs also incorporated the effects of the storage in the root zone into his water management model. However, the effects of the storage in the root zone will not be included in this study in order to limit the number of dimensionless parameters; (2) the rate of evapotranspiration captured at the wetland surface is zero when the depth to the water table is less than or equal to the average critical depth, $\bar{d}_c$, and occurs at the potential rate when the position of the water table exceeds $\bar{d}_c$ (see Figure

5.1). The concept of $\bar{d}_c$ as it relates to captured wetland ET will be explained in more detail in section 5.2.4; (3) the initial depth to the water table, d_i, is constant and parallel to the ground surface; (4) the average critical depth is always greater than the initial depth to the water table so that the ET rate from the wetland surface is at the potential rate before pumping.

5.2.2. Flow Equation

The governing differential equation for two-dimensional, essentially horizontal, groundwater flow in a homogeneous isotropic aquifer is (see Figure 5.1):

$$\frac{\partial}{\partial x}\left(h\frac{\partial h}{\partial x}\right)+\frac{\partial}{\partial y}\left(h\frac{\partial h}{\partial y}\right)+\frac{F}{K_s}=\frac{S_y}{K_s}\frac{\partial h}{\partial t} \qquad (5.1)$$

In equation 5.1, K_s is the saturated hydraulic conductivity, S_y specific yield, F flux per unit area that leaves or enters the aquifer and, $h(x,y,t)$ is the piezometric head during pumping. If the bottom of the aquifer is coincident with the horizontal datum, then, $h(x,y,t)$ is the saturated aquifer thickness. Because of the product $(h\partial h/\partial x_i)$, Equation 5.1 is a nonlinear second order parabolic partial differential equation. This equation is solved for $h(x,y,t)$ by the 2-D finite element groundwater flow model and the values of $h(x,y,t)$ are used to calculate the stream depletion rates and

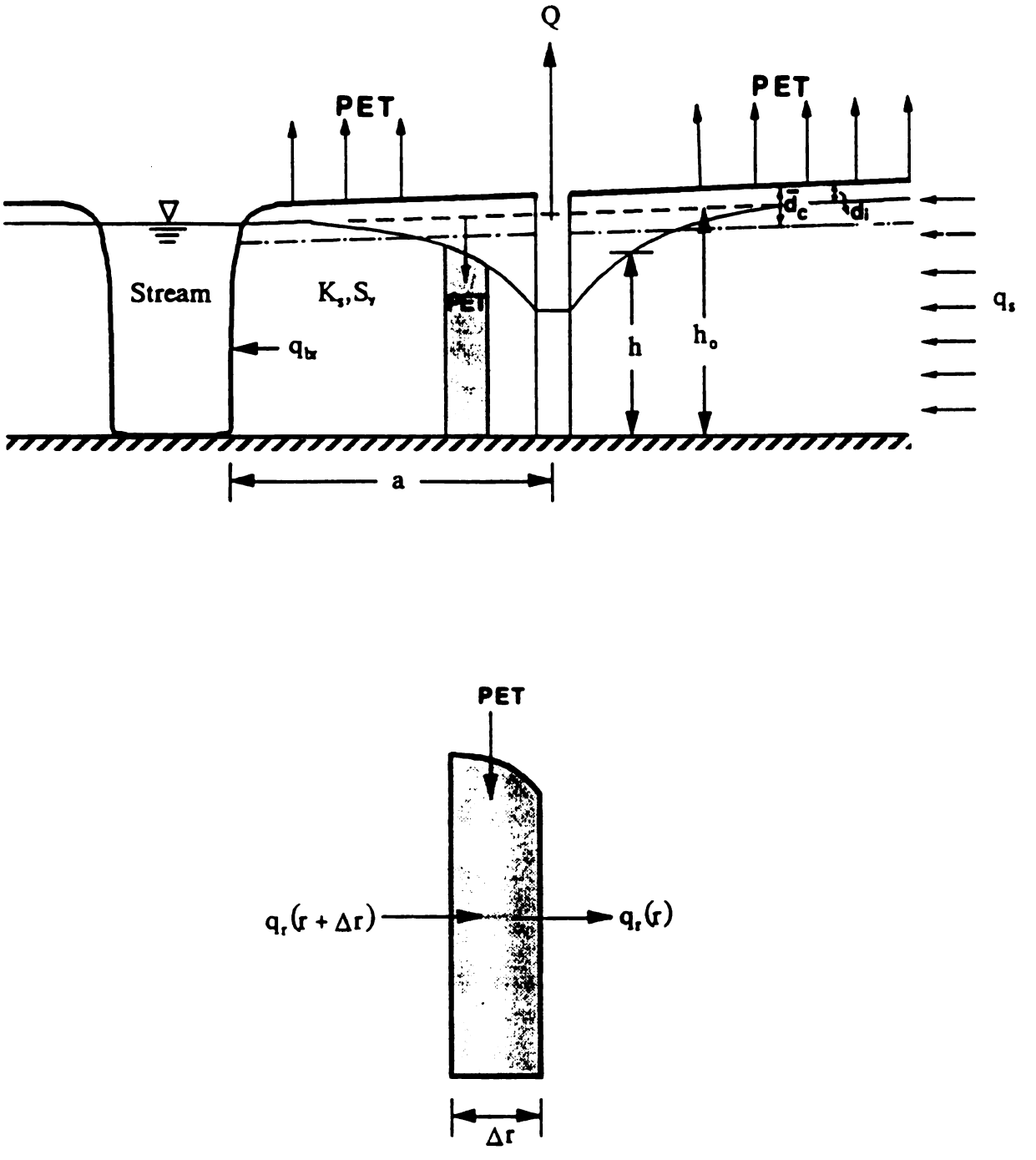

Figure 5.1. Cross section of the semi-infinite stream-wetland aquifer system described by Equation 5.1.

captured wetland ET rates as discussed in section 5.2.4.

To determine the most influential parameters on stream depletion and captured wetland ET rates, Equation 5.1 is manipulated as follows. The product $(h\partial h/\partial x_i)$ can be written as

$$h\frac{\partial h}{\partial x_i} = \frac{1}{2}\frac{\partial h^2}{\partial x_i} \qquad (5.2a)$$

and

$$\frac{S_y}{K_s}\frac{\partial h}{\partial t} = \frac{S_y}{2T}\frac{\partial h^2}{\partial t} \qquad (5.2b)$$

Substituting Equations 5.2a and 5.2b into Equation 5.1 and manipulating gives

$$\frac{\partial^2 h^2}{\partial x^2} + \frac{\partial^2 h^2}{\partial y^2} + \frac{2F}{K_s} = \frac{S_y}{T}\frac{\partial h^2}{\partial t} \qquad (5.3)$$

Equation 5.3 is the partial differential equation for groundwater flow in the system shown in Figure 5.1. This equation looks similar to Equation 4.3 except for the third term on the left hand side. This term represents the scaled flux per unit surface area that leaves or enters the aquifer and varies from PET/K_s to zero depending on the position of the water table.

Suppose $h_0(x,y,t_0)$ describes the position of the water table that would have prevailed in the flow system if the well had not been pumped. That is, h_0 is the solution to the boundary value problem shown in Figure 5.2, when the discharge from the well is equal to zero at $t = t_0$. The flow equation

for this undisturbed system can be written by replacing h with h_0 and $2F/K_s$ with $2PET/K_s$ in Equation 5.3.

$$\frac{\partial^2 h_0^2}{\partial x^2} + \frac{\partial^2 h_0^2}{\partial y^2} + \frac{2PET}{K_s} = \frac{S_y}{T}\frac{\partial h_0^2}{\partial t} \qquad (5.4)$$

Equation 5.4 is linear in h_0^2 since PET/K_s is constant.

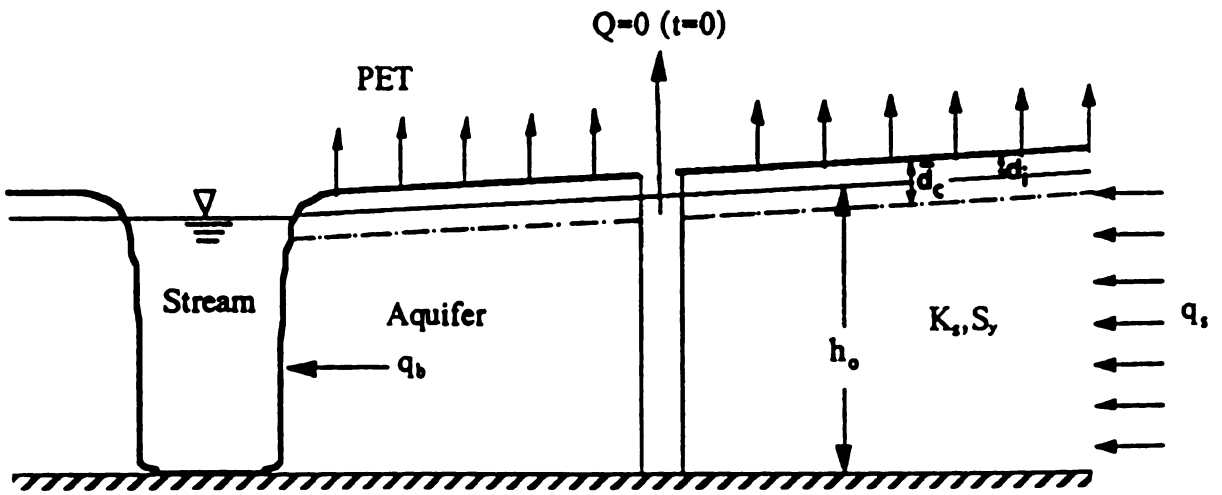

Figure 5.2. Cross section of the semi-infinite stream-wetland aquifer system prior to pumping.

Combining Equations 5.3 and 5.4 by the superposition principle yields

$$\frac{\partial^2 (h_0^2-h^2)}{\partial x^2} + \frac{\partial^2 (h_0^2-h^2)}{\partial y^2} + \frac{2q_e}{K_s} = \frac{S_y}{T}\frac{\partial (h_0^2-h^2)}{\partial t} \qquad (5.5)$$

In Equation 5.5 q_e/K_s is the scaled ET flux leaving the aquifer

surface. This term is variable according to Anat et al.'s (1965) equation that is presented in the next section. Therefore, Equation 5.5 is a nonlinear partial differential equation and no analytical solution is known. Although, Equation 5.5 is nonlinear, it can be manipulated so that the most influential parameters that affect the stream depletion and captured wetland ET could be obtained. If the parameter Z is defined as follows:

$$Z = h_0^2 - h^2 \tag{5.6}$$

Substituting Equation 5.6 into Equation 5.5 yields

$$\frac{\partial^2 Z}{\partial x^2} + \frac{\partial^2 Z}{\partial y^2} + \frac{2q_e}{K_s} = \frac{S_y}{T}\frac{\partial Z}{\partial t} \tag{5.7}$$

The initial and boundary conditions are:

$$\begin{aligned} Z(x,y,0) &= 0 \\ Z(\infty,y,t) &= 0 \\ Z(0,y,t) &= 0 \\ Z(x,\pm\infty,t) &= 0 \end{aligned} \tag{5.7a}$$

The point sink that represents the discharging well requires that

$$\lim_{r\to 0}\left(r\frac{\partial Z}{\partial r}\right) = -\frac{Q}{\pi K_s} \tag{5.7b}$$

where $r^2=(x-a)^2+y^2$. Equation 5.7 is still nonlinear because the third term on the left hand side did not change.

5.2.3. The Nonlinear Relationship for q_e as a Function of Water Table Depth

In the previous chapter, Warrick's (1988) equation was linearized to determine d_0 in term of *PET* and the unsaturated soil hydraulic properties. During the latter part of this study, it was found that an explicit relationship had been developed by Anat et al. (1965) for estimating the steady state ET flux in terms of the depth to the water table and the soil hydraulic properties. An investigation was conducted to determine if this relationship is as accurate as Warrick's relationship. According to Anat et al. (1965), the steady state ET flux is related to the depth to water table and the unsaturated soil hydraulic properties by the following equation:

$$q_e = \left(\left(\frac{h_d\, K_s^{1/n}}{d}\right)\left(1+\frac{1.886}{n^2+1}\right)\right)^n \qquad (5.8)$$

The ET flux in Equation 5.8 may be limited by either of two boundaries. The first is the atmospheric boundary at the soil surface where the upper limit of the ET flux is *PET*, and the second is the water table boundary where the ET flux is negligible when the position of the water table is below $\bar{d}_C$. Figure 5.3a shows how the steady state ET flux varies between the two boundaries and Figure 5.3b shows how the steady state captured ET flux varies. The dashed lines in Figure 5.3a and

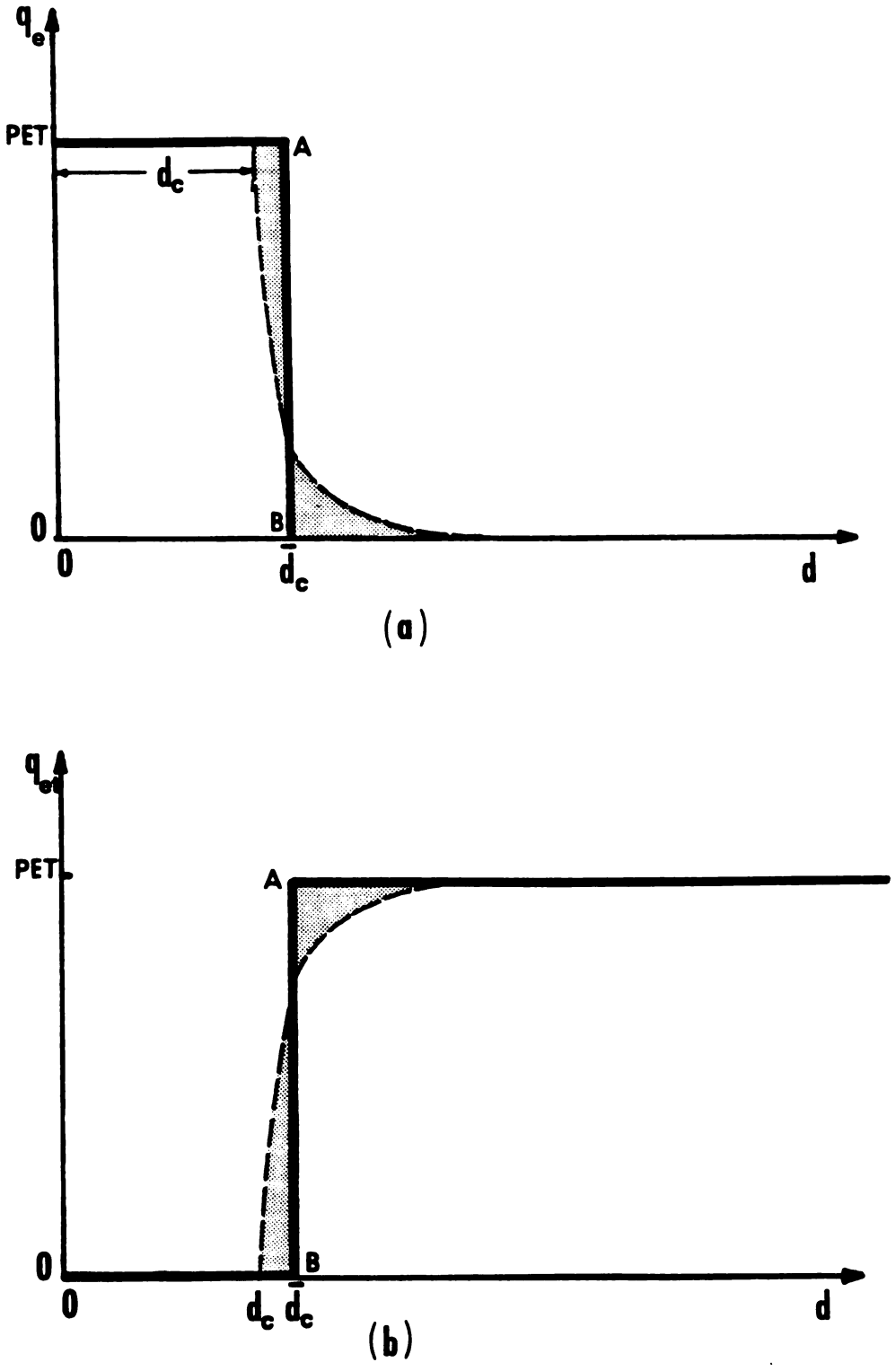

Figure 5.3. (a) Dependence of steady state ET flux on the depth to water table, (b) Dependence of steady state captured ET flux on the depth to water table.

Figure 5.3b depicts the nonlinear relation calculated by Equation 5.8. The dashed line in Figure 5.3a shows that the steady state ET flux is constant and equal to PET until the depth to water table reaches d_c. As the water table drops to a depth that is greater than d_c, the steady state ET flux starts to decline very rapidly, and theoretically, it becomes zero only at depth $d=\infty$.

The critical depth where the ET rate is equal to the *PET* rate can be found by replacing q_e with *PET* and d with d_c in Equation 5.8 and solving for d_c;, this yields,

$$d_c = h_d \left(\left(\frac{K_s}{PET} \right)^{1/n} \left(1 + \frac{1.886}{n^2+1} \right) \right) \qquad (5.9)$$

5.2.4. Scaling the Flow Equation

An analytical solution of Equation 5.7 with respect to given boundary conditions is not known. Therefore, a numerical method (finite element method) is used to obtain the solution.

The numerical model used in this study requires considerable time to operate and substantial expense for computer time. Consequently, it is an objective of this part of the study to obtain results in a form that may be applied to as wide a range of field conditions as practical. This is accomplished by expressing the governing equation and

its boundary conditions in terms of such dimensionless variables that the model produces similar results within the largest possible range of physical situations. This involves choosing the most appropriate set of variables to describe the physical system shown in Figure 5.1 and non-dimensionalizing the variables with appropriate scaling variables.

In order to include the effects of a nonlinear variation of q_e/K_s on stream depletion, it is necessary to express this term in terms of the most appropriate soil parameters suggested by Equation 5.8, the initial conditions, and the atmospheric boundary conditions. Equation 5.8 and the discussion that followed it in the previous section shows that,

$$\frac{q_e}{K_s} = f\left(\frac{d}{h_d}, n, \frac{d_i}{h_d}, \frac{PET}{K_s}, \frac{d_c}{h_d}\right) \qquad (5.10)$$

Here d/h_d is the scaled depth to water table, d_i/h_d is the scaled initial depth to water table, d_c/h_d is the scaled critical depth. In Equation 5.10, the first two terms on the right hand side are introduced by Equation 5.8, the third term is introduced by the initial condition, and the last two terms are introduced by the atmospheric boundary condition. In this equation d_i is the initial depth to water table, an important physical parameter that influences the rate of stream depletion and captured ET. For example, suppose $d_i = 0$, that is, the water table is at the ground surface before pumping.

In this case the water table has to be lowered more than d_c before any wetland ET is captured. If initially $d_i=d_c$, the reduction in wetland ET starts as soon as the water table drops and this could produce a higher ET capture rate and lower stream depletion rate.

As indicated above the objective of this section is to find the most appropriate scaled parameters that influence the magnitude of stream depletion. Therefore, dimensional analysis was used to find these scaled physical parameters. The mathematical relationship between the stream depletion rate and Equation 5.7 is given by Hantush (1964b).

$$q_r = \frac{1}{2} K_s \int_{-\infty}^{+\infty} \left(\frac{\partial Z}{\partial X}\right)_{x=0} dy \qquad (5.11)$$

According to Equation 5.11, the stream depletion rate can be determined if the gradient of Z in the vicinity of the stream can be integrated along the stream boundary. The functional relationship between the stream depletion rate and other parameters suggested by Equations 5.7 and 5.11 can be written as,

$$\frac{q_r}{K_s} = f\,(Z) \qquad (5.12)$$

where,

$$Z = \frac{Q}{K_s} . f\left(a, x, y, \frac{q_e}{K_s}, \frac{S_y}{Tt}\right) \qquad (5.13)$$

Equations 5.10 and 5.13 can be substituted into Equation 5.12. The resulting equation can be manipulated by employing the dimensional analysis technique, incorporating boundary conditions of $x=0$ and integrating from $y=-\infty$ to $y=\infty$ as suggested by Equation 5.11. This yields

$$\frac{q_r}{Q} = f\left(\frac{a}{h_d}, n, \frac{d_i}{d_c}, \frac{a}{d_c}, \frac{K_s}{PET}, \frac{Tt}{a^2 S_y}\right) \qquad (5.14)$$

Equation 5.14 shows that the scaled stream depletion during a transient period depends on six scaled independent parameters when q_s varies as a nonlinear function of the depth to the water table. The reason that the parameter d does not show up in Equation 5.14 is because the parameter Z is related to the drawdown produced by the pumping well. In other words, the solution of Equation 5.7 for Z is equivalent to solving for drawdown in the aquifer. Since d is the combination of the drawdown and d_i, it is redundant to include d in Equations 5.13 and 5.14. As $t\to\infty$, the system approaches steady state. Thus, the scaled time can be eliminated from Equation 5.14.

$$\frac{q_r}{Q} = f\left(\frac{a}{h_d}, n, \frac{d_i}{d_c}, \frac{a}{d_c}, \frac{K_s}{PET}\right) \qquad (5.15)$$

Equation 5.15 shows that even at steady state, the scaled stream depletion depends on five independent scaled parameters in the case of a nonlinear variation of wetland ET. Although, the dimensional analysis technique revealed the appropriate

dimensionless parameters that influence the steady state depletion rate, it is impractical to develop useful results in this case. The impracticality stems from the extremely large number of computer solutions that would be required and the difficulty of using the information if obtained.

To reduce the number of scaled parameters introduced by the assumption of a nonlinear variation of wetland ET and to take advantage of dimensional analysis, the step variation of ET assumption is adopted. With this assumption, q_e/K_s is either equal to PET/K_s or zero depending on whether the depth to the water table is greater than $\bar{d}_c$ (See Figures 5.3a and 5.3b). Moreover, Corey (1990) indicated that incorporation of the step variation of wetland ET into the numerical model would produce more accurate results than the linear variation of wetland ET.

As shown in Figures 5.3a and 5.3b, it is necessary to determine $\bar{d}_c$ so that the step variation of wetland ET can accurately approximate the nonlinear variation of wetland ET. The value of $\bar{d}_c$ shown in Figure 5.3 is determined by the following procedure: (1) Equation 5.8 is evaluated numerically for a wide range of soil types. (2) As a first guess, the vertical line AB in Figures 5.3a and 5.3b is located on d_c. (3) The shaded areas on the right and on the left side of AB are computed. (4) The position of AB is adjusted by locating it into a new position and then the shaded areas at the new position are computed. (5) The depth $\bar{d}_c$ defines the position of the vertical line AB so that the two areas are equal to

each other.

The procedure described above to find the value of $\bar{d}_c$ is applied to soil types varying from fine clean sand to silty sand. The soil types that are used to evaluate Equations 5.8 and 5.9 numerically are obtained from Anat et al.'s (1965) report (page 23-26). Thus, the soil parameters, K_s, h_d, and n are the same as theirs. The annual average *PET* rate used in Equation 5.9 is taken as 0.005 m/day for humid regions (Merva, 1990). The results of the numerical evaluations of Equations 5.8 and 5.9 show that the value of $\bar{d}_c$ is approximately 1.08 times the value of d_c for fine clean sand and 1.13 times for silty sand. In this study, $\bar{d}_c = 1.1 d_c$ is taken for practical purposes. Thus, the value of $\bar{d}_c$ can be written in terms of the displacement head, the saturated conductivity, the *PET* rate and the pore-size distribution parameter using Equation 5.9 as

$$\overline{d_c} = 1.1 h_d \left(\left(\frac{K_s}{PET} \right)^{1/n} \left(1 + \frac{1.886}{n^2+1} \right) \right) \qquad (5.16)$$

For $n \geq 6$, the second term on the right hand side of Equation 5.16 is approximately equal to 1, thus Equation 5.16 can be simplified further,

$$\overline{d_c} = 1.1 \left(h_d^n \frac{K_s}{PET} \right)^{\frac{1}{n}} \qquad (5.17)$$

The functional relationship between q_e/K_s, the soil

parameters, the atmospheric conditions and the initial conditions for the block ET case can be obtained with the aid of Equation 5.10 and the discussion that immediately follows. As indicated before, the first two terms on the right hand side of Equation 5.10 are introduced by Equation 5.8 which determines the dashed curves in Figures 5.3a and 5.3b. Since Equation 5.8 is not used to determine the ET flux as a function of the depth to water table in the step ET case, these two terms on the right hand side of Equation 5.10 can be eliminated and also d_c can be replaced by $\bar{d}_c$. Thus, Equation 5.10 in the step ET case simplifies to

$$\frac{q_e}{K_s} = f\left(\frac{d}{\bar{d}_c}, \frac{d_i}{\bar{d}_c}, \frac{PET}{K_s}\right) \qquad (5.18)$$

Equations 5.17 and 5.18 can be substituted into Equations 5.12 and 5.13. The resulting equation can be manipulated by dimensional analysis and by the boundary conditions of $x=0$ and by integrating from $y=-\infty$ to $y=\infty$ suggested by Equation 5.11.

$$\frac{q_r}{Q} = f\left(\frac{a}{h_d}, \left(\frac{d_i}{h_d}\right)^n, \frac{K_s}{PET}, \frac{Tt}{a^2 S_y}\right) \qquad (5.19)$$

Equation 5.19 indicates that, in the case of step ET variation, the solution of Equation 5.7 for the scaled stream depletion rate, q_r/Q, depends on four independent scaled variables. These variables are the scaled initial depth to water table, $(d_i/h_d)^n$; the scaled pumping distance, a/h_d; the

scaled saturated hydraulic conductivity, K_s/PET; and the scaled time, Tt/a^2S_y.

At steady state the scaled time in Equation 5.19 can be eliminated. Thus, Equation 5.19 becomes,

$$\frac{q_r}{Q} = f\left(\frac{a}{h_d}, \left(\frac{d_i}{h_d}\right)^n, \frac{K_s}{PET}\right) \qquad (5.20)$$

Since the number of independent scaled variables has been reduced to three, it is practical to represent the results of numerical simulations graphically.

5.3. Numerical Solution of Flow Equation for Hypothetical Situation

This section of the study is related to the development of dimensionless graphs that can be used to predict the scaled steady state stream depletion as expressed by Equation 5.20. In order to develop families of dimensionless curves for stream depletion rate, the 2-D finite element model Aquifem-1 (Townley and Wilson, 1980) is modified first to incorporate the nonlinear behavior of wetland ET as a function of water table depth and soil hydraulic properties, and second to incorporate the step variation of wetland ET as a function of the water table depth. For the remainder of this chapter, the first model will be referred to as the nonlinear ET model (NL-ET model) and the second model will be referred to as the

step ET model (ST-ET model). The governing flow equation of the numerical model is given by Equation 5.1 which is nonlinear and it is solved iteratively by employing the finite element method, based on the Galerkin technique with linear finite elements.

5.3.1. The Hypothetical Aquifer

The hypothetical aquifer used for the numerical simulations in this chapter is the same one (Figure 4.10) that is described in chapter 4. In order to account for the effects of scaled pumping distance, the well is located at the center line (I - I′ in Figure 4.10) and the position of the well varies from 100 meters to 2500 meters from the stream, and pumps water from the aquifer at a constant rate. Table 5.1 summarizes the range of values of the hypothetical aquifer properties. In this table, the range of values of the aquifer thickness and the range of values of the initial depth to water table are assumed. The range of the values of the annual average *PET* rate was suggested by Merva (1990) for humid regions. Also, the range of values of the saturated hydraulic conductivity, the displacement head and the pore-size distribution parameter are given by Brooks and Corey (1964), Anat et al (1965), and Freeze and Cherry (1979). These soil hydraulic properties are given for the upper range of silt loam soils and for the upper to lower range of clean sand. The range of the values of $\bar{d}_c$ is calculated according

to Equation 5.10.

The aquifer domain shown in Figure 4.10a is divided into triangular elements for the application of the numerical model. The two grid configurations used in this part of the study (configurations 2 and 3) are the same as those in chapter 4. Table 4.2 summarizes the total number of elements, the total number of nodes and the dimensions of the smallest elements in the vicinity of the pumping well in each configuration.

Table 5.1 Range of Values of the Aquifer Parameters

Parameter	Range
Hydraulic conductivity[1,2,3] (m/day)	0.85 - 50
Displacement head[1,2] (m)	.10 - .70
Pore-size distribution parameter [1,2], n	6 - 12
Average critical depth[4], $\bar{d}_c$=1.1 d_c (m)	.20 - 1.50
initial depth to water table[5], d_i (m)	0 - 1.20
Total aquifer thickness[5] (m)	30.00
Potential ET rate[6] (m/day)	0.005 - 0.009

(1) Brooks and Corey (1964)
(2) Anat et al. (1965)
(3) Freeze and Cherry (1979)
(4) Computed by Eq. 5.10
(5) Assumed
(6) Merva (1990)

5.3.2. Accuracy of the Solution

The finite element model is applied to the aquifer described above to predict the stream depletion produced by a pumping well. The results of the numerical simulations are used first to check the influence of the grid discretization on the accuracy of stream depletion rates and captured ET rates, and second to compare the accuracy of the depletion rates that are obtained from the ST-ET model with the true values of depletion rates. It is assumed that the true values of depletion rates are obtained from NL-ET model. This comparison is made within the range of aquifer parameters that are given in Table 5.1. Finally, having established a method for obtaining accurate solutions with reasonable computational effort, steady state simulations with the NL-ET model are used to develop dimensionless families of graphs for q_r for the range of aquifer parameters given in Table 5.1.

It is necessary to determine how configuration 3 influences the accuracy of stream depletion rates as well as captured ET rates that are obtained from the numerical model. This was done by comparing the numerical results with those for two analytical models presented in chapter 3 and chapter 4, for steady continuous pumping. The numerical model is applied to configuration 3 for two cases. In the first case, the transient stream depletion is determined by neglecting the effects of wetland ET. In the second case, transient stream depletion rates and captured wetland ET rates are determined

by assuming a linear variation of ET as a function of water table depth. The numerical model for each case is executed six times for the three different values of K_s given in Table 5.1, and the two different values of 'a'. K_s is chosen such that the lowest, the mid, and the highest values of the range are used. It is found that the depletion rates that are obtained from the numerical model and from the analytical models are in excellent agreement (the relative error < 1%) for configuration 3. This indicates that spatial discretization in configuration 3 is adequate.

It is concluded in section 5.2.4 that the depletion rates can be presented graphically by using the ST-ET parameters if the ST-ET model can accurately approximate the true values of stream depletion. Therefore, it is necessary to determine the accuracy of the depletion rates that are obtained from the ST-ET model. This is determined by comparing transient q_r results for ST-ET and NL-ET generated using configuration 3. The comparison of the results from both models is made for K_s=43.2 m/day, 8.64 m/day and 0.864 m/day when a=500 m and d_i=0.01 m and plotted in Figures 5.4, 5.5, and 5.6. Here the values of h_d and n are varied according to the values of K_s, since these parameters depend on each other (Brooks and Corey, 1964; Anat et al., 1965; Corey 1986). Figures 5.4, 5.5, and 5.6 indicate that as the values of hydraulic conductivity decrease the accuracy of the depletion rates obtained from the ST-ET model increases.

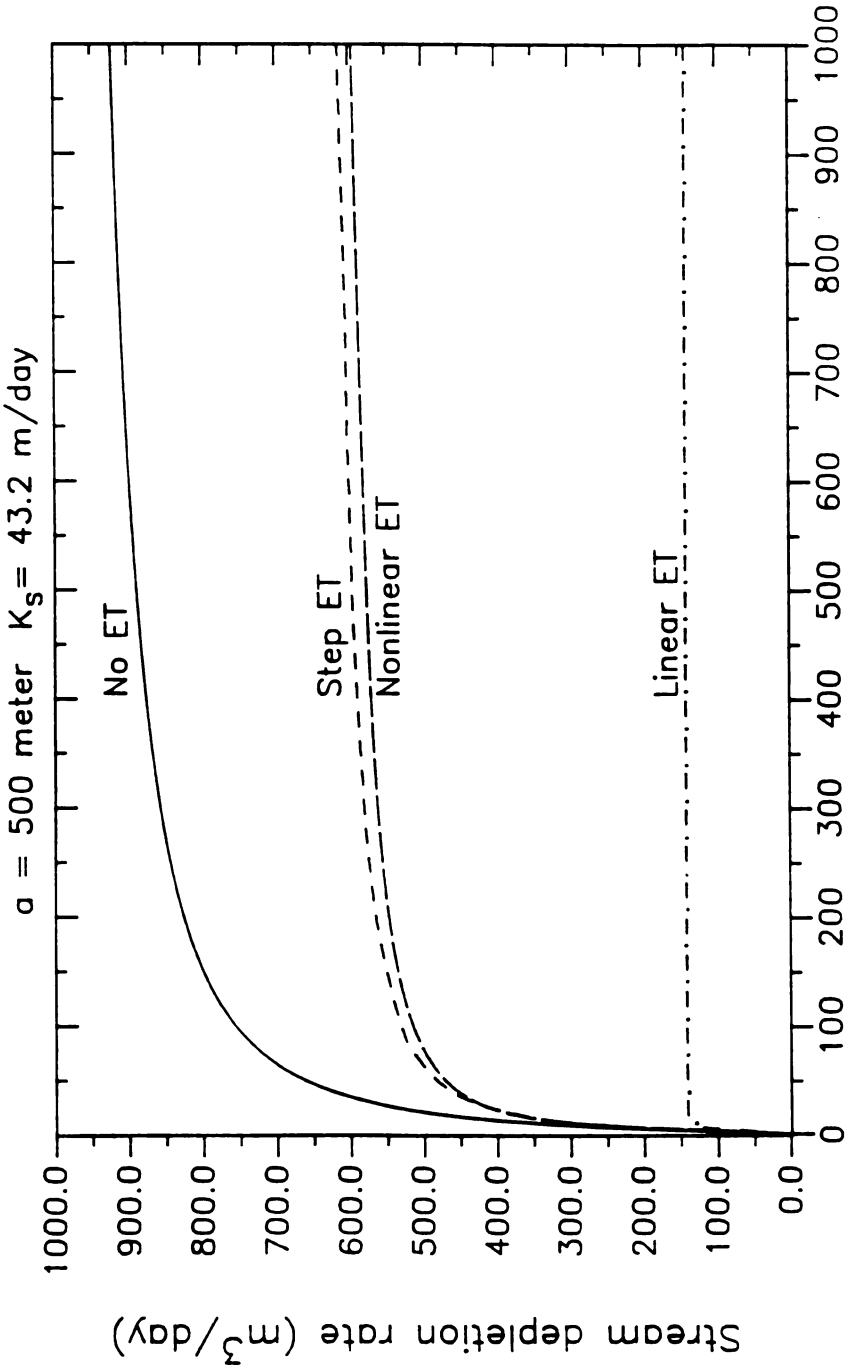

Figure 5.4. Comparison of the stream depletion rates obtained from the linear ET, the nonlinear ET, the step ET, and no ET models when a = 500 m, K_s=43.2 m/d, and d_i= 0.01 m.

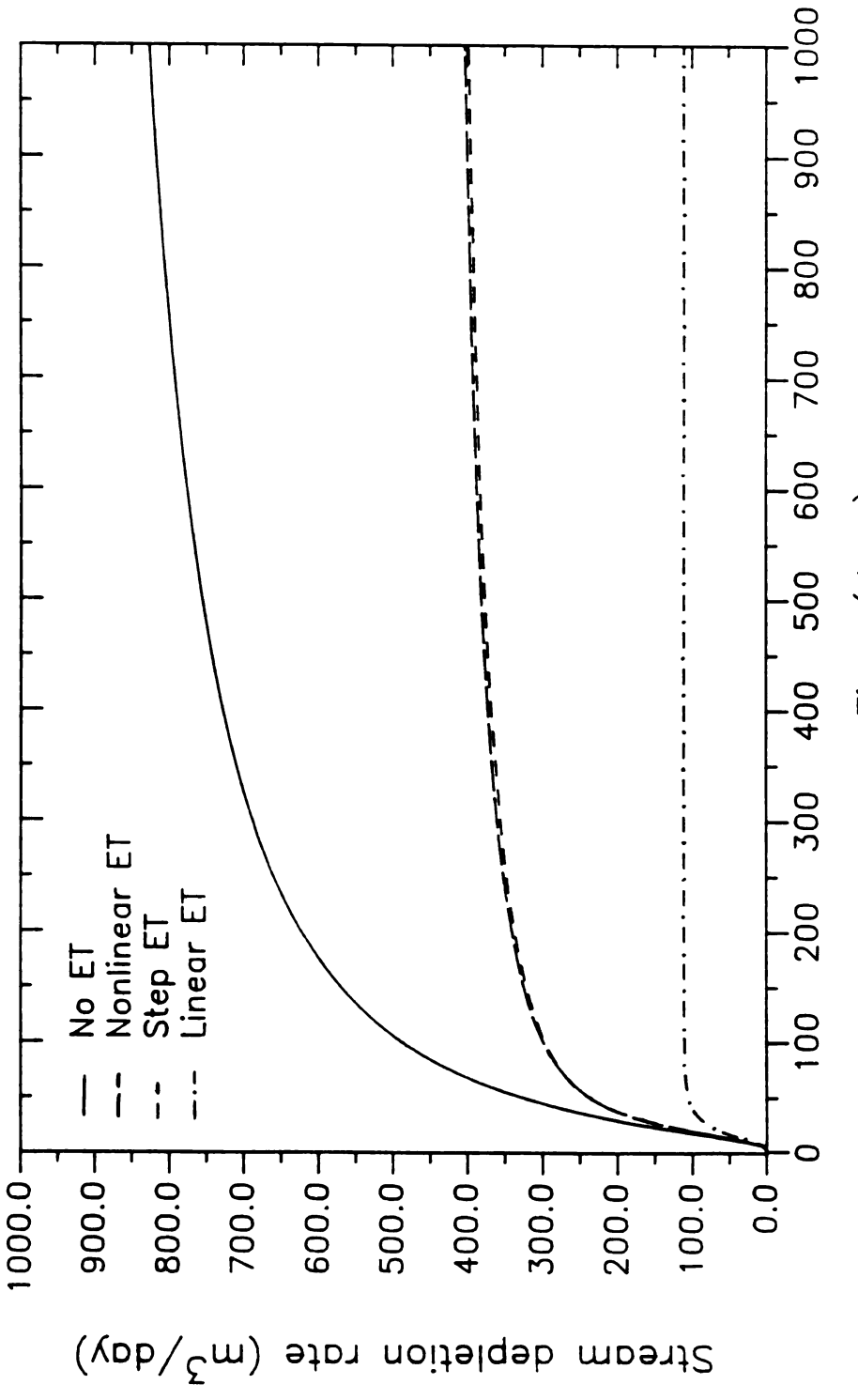

Figure 5.5. Comparison of the stream depletion rates obtained from the linear ET, the nonlinear ET, the step ET, and no ET models when a = 500 m, K_s=8.64 m/d, and d_i= 0.01 m.

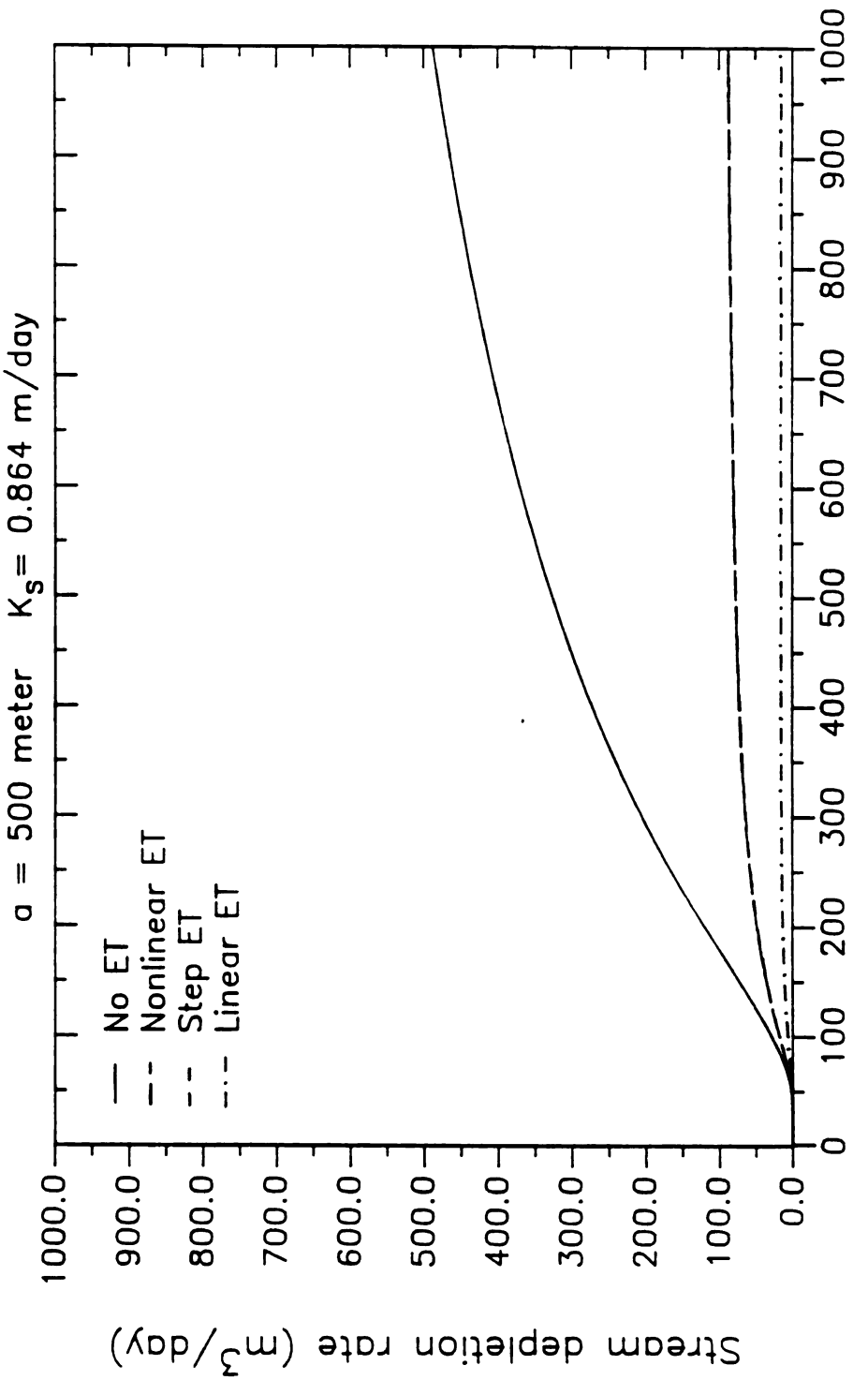

Figure 5.6. Comparison of the stream depletion rates obtained from the linear ET, the nonlinear ET, the step ET, and no ET models when a = 500 m, K_s=.864 m/d, and d_i= 0.01 m.

Figure 5.4 shows that the relative error is approximately 3 % between the depletion rates obtained from the ST-ET model and the NL-ET model when K_S=43.2 m/day and d_i=0.01 m. Since the maximum relative error occurs when K_S=43.2 m/day, it is necessary to investigate the accuracy of the ST-ET model results for K_S=43.2 m/day and for different range of values of d_i and *'a'*. The ST-ET model is run when K_S=43.2 m/day, d_i=d_C, *a*=200 m and *a*=1000 m. The maximum relative error in these cases is less than 6 %. This indicated that the ST-ET model results are accurate for practical purposes, thus, the ST-ET model parameterization (Equation 5.20) can be used to represent the NL-ET model results (Equation 5.15).

Stream depletion rates obtained by incorporating the linear variation of wetland ET and by neglecting the effects of captured wetland ET (No ET model) are also plotted in Figures 5.4, 5.5, and 5.6 for comparison. These figures clearly document that the depletion rates obtained by incorporating a step variation of wetland ET are very accurate compared to depletion rates obtained by incorporating a linear variation of wetland ET.

Although it is not readily apparent, Figure 5.4 shows that stream depletion rates are fluctuating in the case of a step variation of ET as the system approaches steady state. These fluctuations occur due to the spatial discretization of the aquifer domain and the insufficiently small time intervals that are practical for the transient computations. It is observed that these fluctuations could be eliminated if the

grid density were finer and time interval smaller. However, this would make the computational cost as well as execution time unfeasible.

In order to obtain the scaled steady state stream depletion suggested by Equation 5.20, the numerical model is forced to predict the final steady state solution by using the information at the final time step of the transient calculations. This indicates that the accuracy of the final steady state results depend on the accuracy of results obtained from the final time step of the transient computation. Because of the oscillations of q_r obtained by ST-ET model during the transient period, predictions of steady state q_r with this model are inaccurate. It is shown that during the transient period, stream depletion rates that are obtained from the ST-ET model do accurately approximate the depletion rates obtained from the NL-ET model. Therefore the NL-ET model is used to predict the final steady state stream depletion rate, and the results are presented by using the ST-ET model parameters.

As indicated above, the final steady state stream depletion is computed by using the results of the final time step of the transient computations. Numerical simulations for stream depletion in the case of nonlinear variation of ET showed that the system approaches the final steady state asymptotically. However, when the values of K_s are small and *'a'* is large, the system approaches the steady state much slower than in the case where K_s is large and *'a'* is small.

In these kinds of cases, the numerical model requires an unreasonably long time for transient computations so that it could predict the final steady state stream depletion rate. Thus, the CPU time required to run the model would not be practical. To reduce the CPU time and maintain the accuracy in these cases, the steady state depletion rate is predicted by extrapolating the lines for stream depletion and captured ET until they intersect (dashed lines in Figure 5.7). The error introduced by extrapolation is controlled by carrying out the transient computations for a period long enough that the rate that water is mined from aquifer storage (the rate shown as BC in Figure 5.7) is less than 10% of the stream depletion rate (rate AB shown in Figure 5.7). If the extrapolation had not been used, the error in depletion rate at this time would be 10 %. Thus, the error in steady state q_r is less than 10% after the extrapolation.

Figure 5.7 shows that for K_s= 8.64 m/day and a=1000 meters, both stream depletion rate and captured ET rate approach their steady state values very slowly as time increases. It is observed from the numerical simulations that this asymptotical approach to a steady state value is much slower for lower range of values of K_s and higher values of 'a' than shown in Figure 5.7. Therefore, a longer period of time is required to execute the numerical model for smaller values of K_s and larger values of 'a' for configuration 3 so that the above criteria for extrapolation is achieved. For example, it took 26 hours of CPU time to obtain the results at

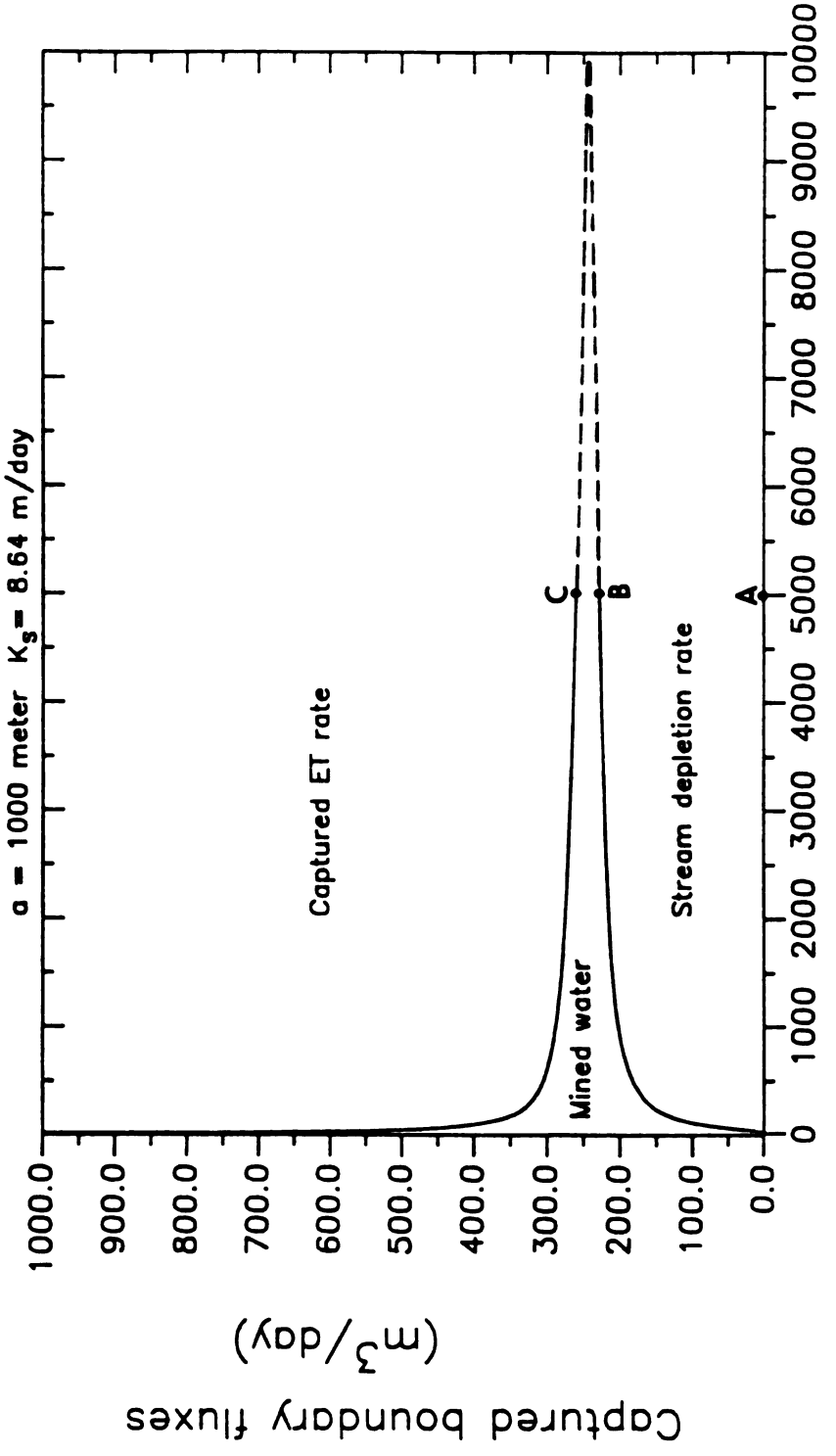

Figure 5.7. Variation of captured boundary fluxes obtained from the nonlinear ET model when a=1000 m, K_s=8.64 m/d, d_i=0.1 m.

time t=5000 days for K_s=8.64 m/day and a=1000 meter shown in Figure 5.7. In order to reduce this time and to control the relative error within 10 %, the numerical model is applied to configuration 2.

Since configuration 2 has coarser grid density than configuration 3, it is important to check the influence of configuration 2 on the accuracy of the depletion rate before the development of the families of dimensionless graphs. The scaled steady state stream depletion rates obtained by applying the numerical model to configuration 2 are compared with those obtained by applying the model to configuration 3 for three different values of K_s/PET and a/h_d. Table 5.2 shows these scaled depletion rates, the values of K_s/PET, a/h_d, and the relative error of configuration 2 depletion rates. The relative error is determined by comparing the results of configuration 2 with the results of configuration 3. Table 5.2 shows that the amount of relative error in q_r obtained by using configuration 2 increases as the value of a/h_d increased when $K_s/PET = 10^4$. In order to find the maximum amount of relative error in steady state q_r, the numerical model is executed for a/h_d = 20000 (a=2000 m) and $K_s/PET = 10^4$. The relative error in this case is also less than 10% (9.6%). This indicates that as the distance between the pumping well and the stream increases, the growth rate in relative error in steady state q_r decreases. Therefore, at steady state, configuration 2 produces approximately 90% accurate results. This amount of accuracy in this study is assumed to be

acceptable for practical purposes, since using this configuration reduced the CPU time about one order of magnitude.

Table 5.2 Comparison of the scaled steady state q_r obtained from configurations 2 and 3

K_s/PET	a/h_d	Config. 2 q_r/Q	Config. 3 q_r/Q	Relative err.(%)
10^4	2000	1.000	0.988	1
	6000	1.000	0.964	5
	10000	0.972	0.902	8
10^3	800	0.649	0.670	3
	2000	0.420	0.425	1
	4000	0.287	0.291	1
10^2	286	0.325	0.326	.3
	715	0.160	0.159	.6
	1430	0.107	0.106	.9

5.3.3. Discussion of Scaled Families of Curves for Stream Depletion

Dimensionless families of graphs that may be used to predict the steady state stream depletion rates and captured wetland ET rates are developed by using the results of

numerical simulations. Graphs (Figures 5.8, 5.9, and 5.10) are plotted for values of K_S/PET equal to 10^4, 10^3, and 10^2 and $(d_i/h_d)^n$ between 0 and 100. The symbols in Figures 5.8, 5.9, and 5.10 show the values of steady state stream depletion rates obtained from the numerical simulations. These data points are connected to each other by fitting the best curve. These figures provide a means for easily determining the steady state stream depletion rates for values of K_S/PET, $(d_i/h_d)^n$, and a/h_d within the range of values presented.

Figures 5.8, 5.9, and 5.10 show that the scaled steady state stream depletion, q_r/Q, approaches zero as a/h_d approaches infinity; whereas, q_r/Q approaches 1.0 as a/h_d approaches zero. This can be interpreted as follows: as the pumping distance increases, the aquifer response time increases and this produces a lower rate of stream depletion. An increase in the value of a/h_d also indicates that the area from which ET may be captured increases, thus, producing higher ET capture. This trend can be observed from these figures for all the range of values of K_S/PET and $(d_i/h_d)^n$.

Figure 5.8 shows that when the value of the scaled conductivity is high, the steady state stream depletion rate can not be neglected even for large values of a/h_d. This figure also confirms the importance of the initial depth to water table as explained in section 5.2.4. For instance, as the value of $(d_i/h_d)^n$ approaches zero, steady state stream depletion rates increase, and the major portion of the well discharge is captured from the stream, although the value of

a/h_d is large. As the value of d_i approaches zero, captured ET from the wetland decreases. This occurs because the sum (d_i+s) approaches the drawdown, s, and ET capture begins only when $s>\bar{d}_C$ instead of $(d_i+s)>\bar{d}_C$, and this causes a lower ET capture rate and a higher stream depletion rate.

In Figures 5.8, 5.9 and 5.10, the lowest curve for $(d_i/h_d)^n$ is the case where the product $d_i/\bar{d}_C \approx 1$. In this case, ET capture from the wetland starts immediately after the pumping starts, and as the value of a/h_d increases, the major portion of the well discharge is being captured from wetland ET. The upper horizontal line in Figures 5.8, 5.9, and 5.10 (q_r/Q = 1.0) is the case where $d_i > \bar{d}_C$. In this case, the ET rate from the wetland surface is zero, thus, all the pumped water is captured from the stream for all the values of a/h_d.

Figures 5.9 and 5.10 show the variation of the steady state stream depletion rates for lower values of K_S/PET. The curves in these figures are closer to each other than the curves in Figure 5.8 for the given range of $(d_i/h_d)^n$. This can be interpreted as follows: the effects of the initial position of the water table is a more influential parameter for determining steady state stream depletion rate when K_S is higher. Although d_i is more effective when K_S is higher, Figures 5.9 and 5.10 also show the effects of $(d_i/h_d)^n$ on the magnitude of q_r/Q distinctively. This indicates that the initial position of the water table can influence the stream depletion and/or captured ET rates even when the value of saturated hydraulic conductivity is low.

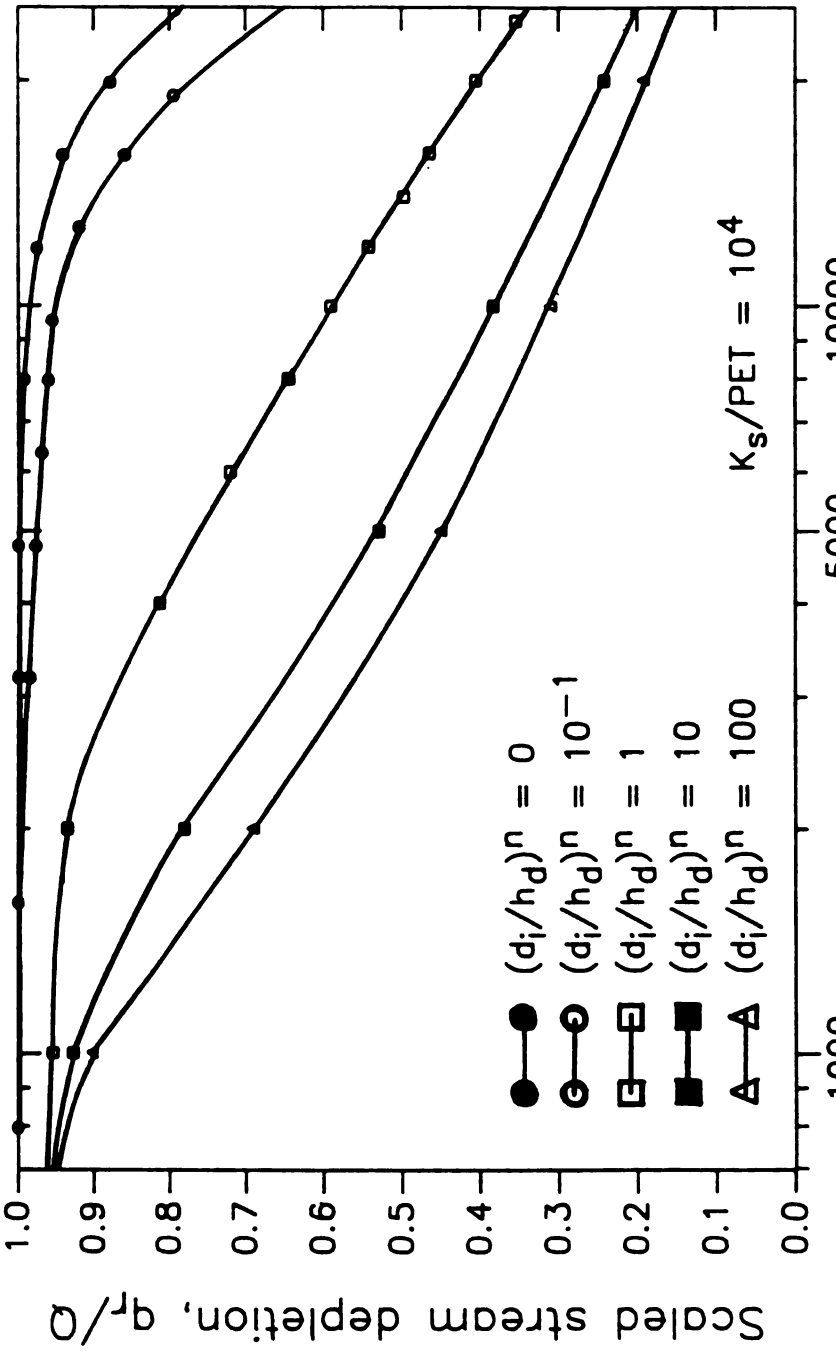

Figure 5.8. Dependence of the scaled steady state stream depletion on the scaled pumping distance and the scaled initial depth to water table when $K_s/PET = 10^4$.

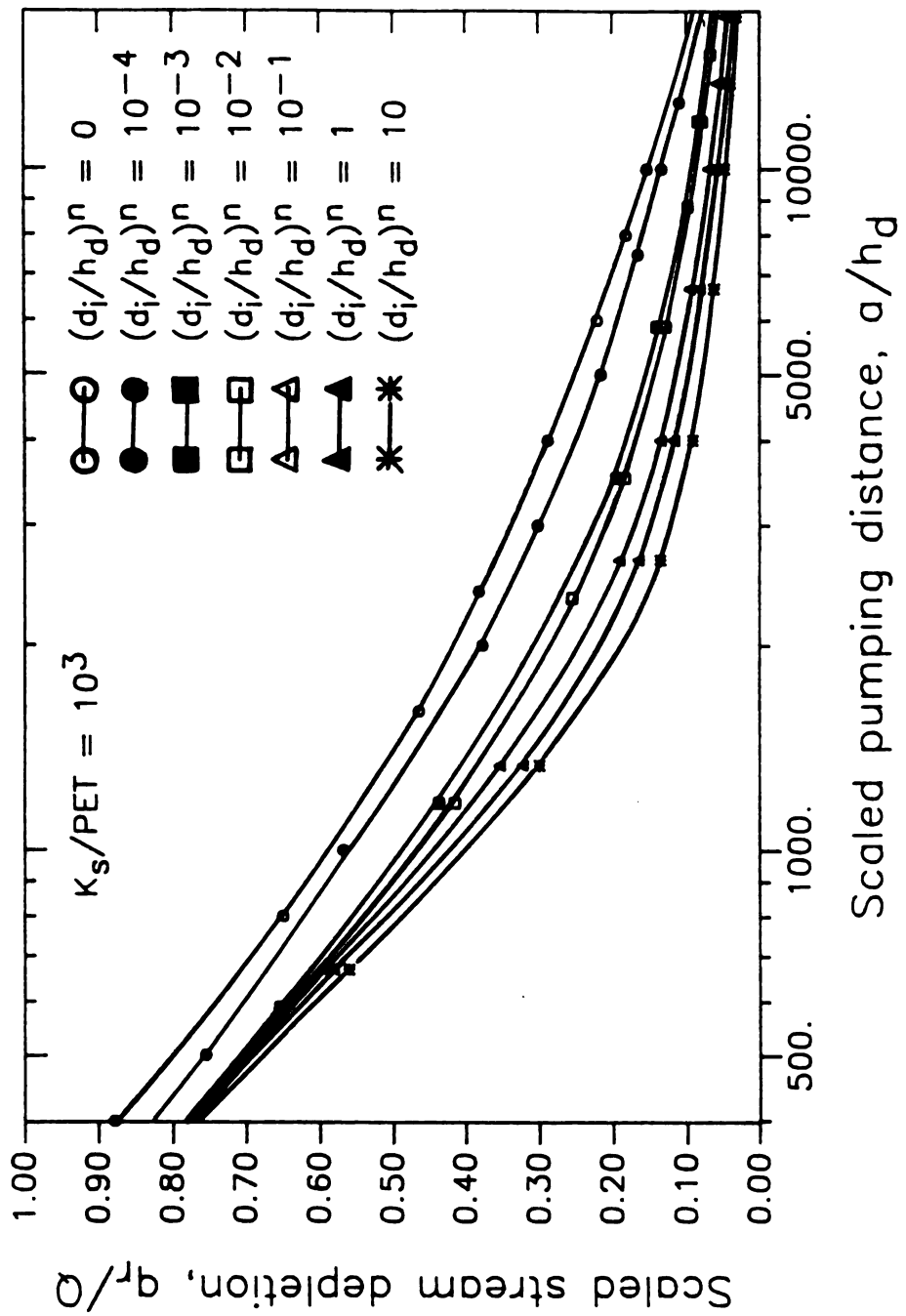

Figure 5.9. Dependence of the scaled steady state stream depletion on the scaled pumping distance and the scaled initial depth to water table when $K_s/PET = 10^3$.

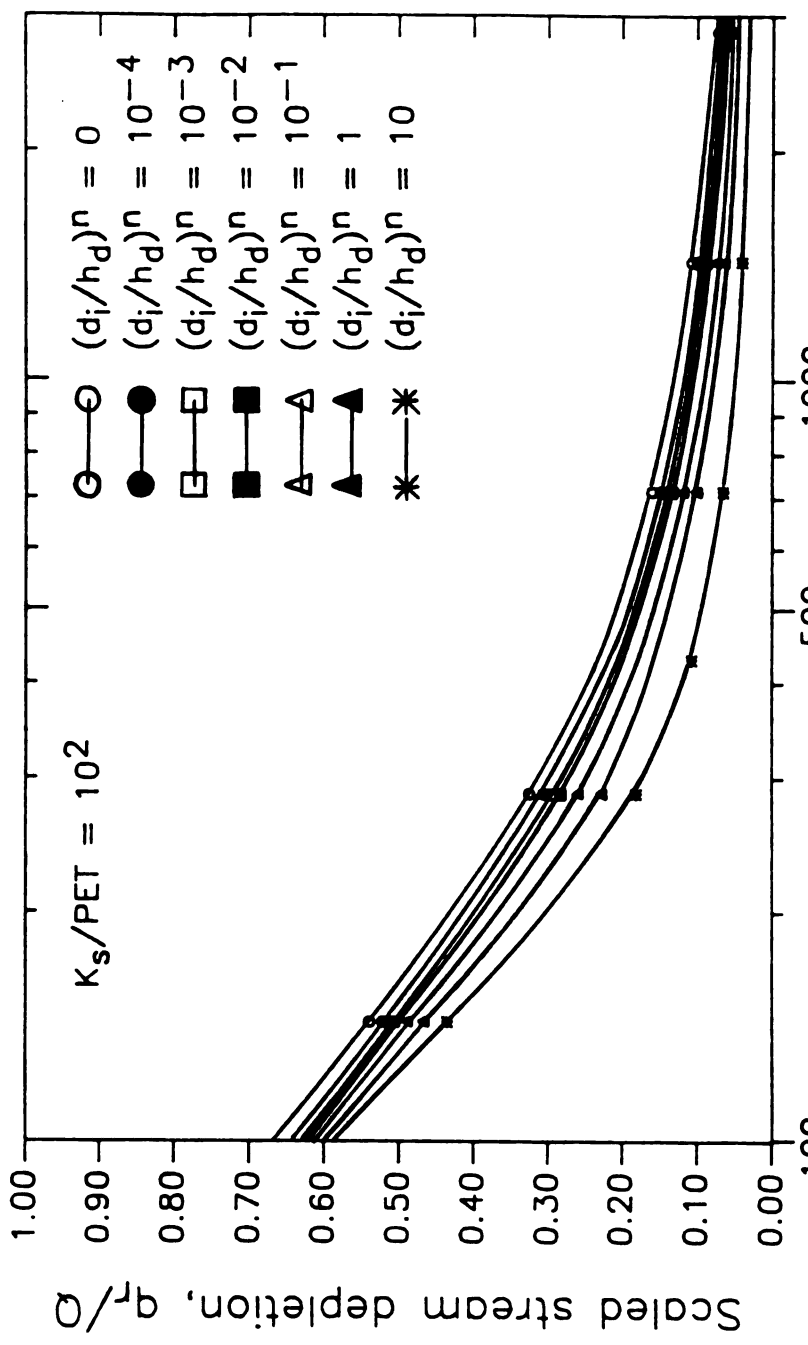

Figure 5.10. Dependence of the scaled steady state stream depletion on the scaled pumping distance and the scaled initial depth to water table when $K_s/PET = 10^2$.

As indicated above, Figures 5.8, 5.9, and 5.10 can also be used to predict the captured wetland ET since the system is at steady state. An estimate could be made based on the assumption that all pumped water is obtained from captured ET. That would result in an estimate that is at most 20 % in error when the value of a/h_d is greater than 5000 (see Figure 5.9). The scaled pumping distance decreases for the same amount of relative error caused by the assumption that all of the pumped water that is captured from the wetland ET decreases as K_s decreases, as seen in Figure 5.10. This figure shows that the maximum relative error at steady state is less than 10% if one assumes that all of the pumped water is captured from the wetland ET when $a/h_d \geq 2000$. This clearly indicates that as the value of K_s decreases while 'a' increases, the aquifer response time increases. Thus, steady state stream depletion will be low, and the major portion of the well discharge will be captured from the wetland ET.

5.4. Summary and Conclusions

In this part of the study, an investigation was conducted to develop a model that can be used to predict the steady state stream depletion rates caused by a continuous pumping well. The effects of nonlinear variation of wetland ET on the steady state stream depletion rate was investigated in the model. The model was based on combining the governing flow

equation for a water table aquifer and Anat et al's equation for nonlinear ET from the water table.

Dimensional analysis was performed to find the functional relationship between the scaled steady state stream depletion and the physical aquifer parameters. It was found that the scaled steady state stream depletion depended on five independent scaled aquifer parameters in the case where ET varies as a nonlinear function of the water table depth. It was also found that these independent parameters were reduced to three when the step ET assumption was employed to approximate the nonlinear ET assumption. The scaled parameters in the case of step ET assumption were: the scaled hydraulic conductivity, the scaled pumping distance from the stream, and the scaled initial depth to water table.

To incorporate step variation of wetland ET into the model, an explicit relationship was found for the average critical ET depth, $\bar{d}_c$, by combining Anat et al's equation with the atmospheric boundary condition. In the model it was assumed that captured ET from wetland is zero when the sum of the initial depth to water table and the drawdown is less than or equal to $\bar{d}_c$; whereas, captured ET is equal to *PET* when the sum of the initial depth to water table and drawdown is greater than $\bar{d}_c$. It was found that stream depletion rates obtained by employing this assumption were very accurate as compared to stream depletion rates obtained by incorporating the linear variation of the ET assumption.

A 2-D finite element model for saturated groundwater,

AQUIFEM-1, was modified to incorporate the nonlinear behavior of wetland ET as a function of the position of the water table and the soil hydraulic properties. The numerical model was applied to a hypothetical situation for a wide range of scaled independent aquifer parameters. The results of the numerical simulations were used to develop the families of dimensionless graphs that could be used to estimate the rate of steady state stream depletion for a practical range of scaled independent parameters. Three families of dimensionless graphs were developed between the range of values of the scaled hydraulic conductivity of 10^4 - 10^2, the scaled initial depth to water table of 0-100, and the scaled pumping distance of 100-25000.

The following conclusions were made from the analysis of the dimensionless graphs: the scaled steady state stream depletion rate approached zero as the scaled pumping distance approached infinity; whereas, the scaled steady state stream depletion approached 1 as the scaled pumping distance approached zero. When the value of the saturated hydraulic conductivity was high, the error caused by the assumption that all of the pumped water is captured from wetland ET is substantial even for large values of a/h_d. The dimensionless graphs showed that steady state stream depletion rates strongly depended on the initial position of the water table. Analysis showed that as the saturated conductivity increased, the effect of the initial position of the water table on the magnitude of stream depletion rate was more influential.

Analysis also showed, that as the value of saturated conductivity decreased, the error caused by the assumption that all of the pumped water is captured from wetland ET, decreased.

CHAPTER VI

SUMMARY AND CONCLUDING REMARKS

In the present study, three different mathematical models were developed. These models can be used to predict the stream depletion and/or captured wetland ET rates produced by a pumping well from the phreatic aquifer which is hydraulically connected to an adjacent stream. The mathematical treatment required standard use of superposition theory and the existing analytical solutions for steady, continuous pumping. The solutions obtained are appropriate only when the actual field conditions approach the assumed conditions. The study focused on the approach to dynamic equilibrium as well as conditions at dynamic equilibrium.

The first model is an analytical solution for stream depletion produced by nonuniform, cyclic pumping from a well located in a deep water table aquifer. The effects of captured wetland ET were not included in this model. An analytical expression for dimensionless volume of stream depletion (τ) was developed. This expression can be used to determine the time required to achieve a practical state of dynamic equilibrium. An analytical expression for τ was obtained (Equation 3.10) and plotted (Figure 3.8) for a

practical range of the independent variables. Equation 3.10 was obtained by recognizing that the volume of stream depletion over one cycle, from $t-t_d$ to t, is the same as the volume of stream depletion between the start of pumping and the time t by a single period of pumping (Figure 3.6). Equation 3.8 shows that τ depends on the values of α and γ but that it is independent of the value of t_d/t_a even though the stream depletion rate shows such a dependence (Equation 3.6). Analysis of the τ relationship produced Equation 3.11 which shows that time to equilibrium depends on t_a alone for small values of γ. An inspection of conditions when γ is large leads to the recognition that such wells are close enough to the stream to reach equilibrium within the first pumping period so that the nonuniform pumping pattern is an accurate representation of the stream depletion pattern.

Having obtained a consistent basis for determining the occurrence of dynamic equilibrium permitted the study of stream depletion rates at dynamic equilibrium. The β criterion (Figure 3.10) was developed to characterize the error in depletion rates estimated by assuming steady, continuous pumping at the cycle-average rate. Figure 3.10 showed that under some circumstances, the cycle-average approximation is not an adequate representation of the pumping pattern.

The second model that was developed is also an analytical model to predict the stream depletion by a steady continuous pumping well where the effects of linear variation of captured

ET were taken into account. The analytical model is based on Hantush's solution for pumping from a leaky phreatic aquifer connected to a bounding fully penetrating stream. Hantush's leakage from the lower confined aquifer was interpreted to describe a reduction in wetland ET resulting from the drawdown of the water table in a shallow phreatic aquifer. It was assumed that ET varies as a linear function of the drawdown in the phreatic aquifer so that ET is at the potential rate with zero drawdown and zero at a depth d_0. An explicit relationship was derived that showed how potential ET and d_0 were related to Hantush's leakage coefficient. Properties of unsaturated soils were incorporated into the solution by using Warrick's relationship between ET flux and depth to water table to determine d_0.

Application of the analytical model to a hypothetical situation showed that as the dimensionless distance between the well and the stream increases (increasing ϵ), the portion of the pumping well discharge captured from wetland ET increases; whereas, the portion captured from the stream decreases. This resulted from increased aquifer response time and increased area from which ET could be captured. A dimensionless graph (Figure 4.7) was developed that shows the relationship between stream depletion, water mined from aquifer storage, captured wetland ET, and time. The analysis showed that Figure 4.7 could be used to determine the time, t_e, when the system reaches a practical steady state. The analysis of Figure 4.7 also showed that as scaled pumping

distance (ϵ) increased, the system reached steady state faster than the case where the effects of captured ET was neglected.

A dimensionless graph (Figure 4.8) for the rate of stream depletion at steady state was also developed as a function of the scaled pumping distance. This graph was used to determine the stream depletion rate and captured ET rate at steady state for known value of the scaled pumping distance. The solutions obtained in this study are appropriate only when the actual field conditions approach the assumed conditions. The accuracy of the steady state stream depletion based on the assumption that the captured ET rate linearly depended on the position of the water table was investigated. The analysis indicated that this assumption could result in substantial error in stream depletion rate when d_0 was small. The analysis also indicated that the magnitude of this error could be decreased as the value of d_0 was increased. However, there was no theoretical procedure to determine the value of d_0 which could minimize the error.

Additional error could be expected from the analytical model results during the transient period as a result of a constant specific yield assumption for soils that have low hydraulic conductivity values. It was concluded from the above analysis that the analytical model is restricted significantly as a quantitative tool, but it is still valuable as a qualitative tool.

An existing finite element model was modified extensively in order to incorporate captured wetland ET as a linear

function of the depth to water table in the aquifer. Application of the finite element model and the analytical model to a hypothetical situation showed that the results obtained from the finite element model could be made to converge to the results obtained from the analytical model if the spatial discritization of the aquifer domain and time interval were made sufficiently small. Therefore, the analytical model is a valuable tool for determining the optimum finite element grid density which could produce accurate results during the transient period.

In the third model, the effects of a nonlinear variation of wetland ET was investigated on steady state stream depletion rates caused by a continuous pumping well. The model was based on combining the governing flow equation for water table aquifer and Anat et al's equation for nonlinear ET from the water table.

Dimensional analysis was performed to find the functional relationship between the scaled steady state stream depletion and the physical aquifer parameters. It was found that the scaled steady state stream depletion depended on five independent scaled parameters in the case where ET varied as a nonlinear function of the water table depth. It was also found that the number of these independent parameters was reduced to three when the step ET assumption was employed to approximate the nonlinear ET assumption. These scaled parameters were the saturated hydraulic conductivity, the pumping distance from the stream, and the initial depth to

water table.

To incorporate the step variation of wetland ET into the model, an explicit relationship was found for the average critical depth, $\bar{d}_c$, by combining Anat et al's equation with the atmospheric boundary condition. In the model it was assumed that captured ET from the wetland is zero when the sum of the initial depth to water table and the drawdown is less than or equal to $\bar{d}_c$; whereas, the captured ET is equal to *PET* when the sum of the initial depth to water table and drawdown is greater than $\bar{d}_c$. It was found that stream depletion rates obtained by employing this assumption were very accurate compared to stream depletion rates obtained by incorporating the linear variation of ET assumption.

A 2-D finite element model for saturated groundwater, AQUIFEM-1, was modified to incorporate the nonlinear behavior of wetland ET as a function of water table depth and soil hydraulic properties. The numerical model was applied to a hypothetical situation for a wide range of scaled independent aquifer parameters. The results of the numerical simulations were used to develop families of dimensionless graphs that could be used to estimate the rate of steady state stream depletion for a practical range of scaled independent parameters. Three families of dimensionless graphs were developed between the range of values of the scaled hydraulic conductivity of 10^4 - 10^2, the scaled initial depth to water table of 0 - 100, and the scaled pumping distance of 100 - 25000.

The following conclusions were made from an analysis of the dimensionless graphs: the scaled steady state stream depletion rate approached zero as the scaled pumping distance approached infinity whereas, the scaled steady state stream depletion approached 1 as the scaled pumping distance approached zero. When the value of the saturated hydraulic conductivity was high, the error caused by the assumption that all the water is captured from wetland ET is substantial even for large values of a/h_d. The dimensionless graphs showed that the steady state stream depletion rates strongly depended on the initial position of the water table. Analysis showed that as the saturated conductivity increased, the effect of the initial position of the water table on the magnitude of stream depletion rate was more influential. Analysis also showed, that as the value of the scaled saturated conductivity decreased, the error caused by the assumption that all the pumped water was captured from wetland ET, decreased.

At this point some suggestions are made for future analytical and numerical work on stream depletion and captured wetland ET rates caused by either continuous or cyclic pumping of the well.

For a more complete understanding of the physics of the problem, it is important to modify the numerical model further by incorporating the 1-D unsteady Richards' Equation between the water table and the ground surface. This would allow the specific yield to vary with the position of the water table and time.

Partial penetration of the aquifer by a stream including the presence of the clogging layer between the streambed and the aquifer is more realistic than a fully penetrating stream with no clogging layer. Although this option was already available in the numerical model, it was not used in the numerical part of the present study. The effects of these parameters on stream depletion and captured wetland ET rates can be investigated in the future study.

It is also interesting to study the effects of the partial penetration of stream with the presence of a streambed clogging layer on stream depletion caused by cyclic pumping of a well. This can be accomplished by combining Hantush's theory (1965) with the superposition principle that was used in the present study.

Also as a natural extension to the second analytical model, a theoretical development is suggested for determining the value of d_0 that improves the accuracy of the analytical model as a quantitative tool.

Finally, it is of equal importance to investigate further the possibility of obtaining an analytical solution for stream depletion by a pumping well where the effect of step variation of captured ET is accounted.

APPENDICES

APPENDIX A

SOLUTION OF EQUATION 4.8 BY LAPLACE TRANSFORMATIONS

Analytical solution of Equation 4.8 can be obtained by applying Laplace transformations (Hantush, 1964a).

$$\frac{\partial^2 Z}{\partial x^2} + \frac{\partial^2 Z}{\partial y^2} - \frac{Z}{B^2} = \frac{S}{T}\frac{\partial Z}{\partial t} \qquad \text{(A.1a)}$$

$$Z(x,y,0) = 0 \qquad \text{(A.1b)}$$

$$Z(\infty,y,t) = 0 \qquad \text{(A.1c)}$$

$$Z(x,\pm\infty,t) = 0 \qquad \text{(A.1d)}$$

Equations A.1a, A.1b, A.1c, A.1d can be written in radial coordinates.

$$\frac{\partial^2 Z}{\partial r^2} + \frac{1}{r}\frac{\partial Z}{\partial r} - \frac{Z}{B^2} = \frac{S}{T}\frac{\partial Z}{\partial t} \qquad \text{(A.2a)}$$

$$Z(r,0) = 0 \qquad \text{(A.2b)}$$

$$Z(\infty,t) = 0 \qquad \text{(A.2c)}$$

$$\lim_{r\to 0}\left(r\frac{\partial Z}{\partial r}\right) = -\frac{Q}{\pi K_s} \qquad \text{(A.2d)}$$

Here r is the radial distance from the center of a pumping well located at (x_0,y_0) to any point in the surrounding area and is equal to $[(x-x_0)^2+(y-y_0)^2]^{1/2}$. Applying Laplace transformations to Equations A.2a, A.2b, A.2c, and A.2d one can obtain,

$$\frac{\partial^2 \overline{Z}}{\partial r^2}+\frac{1}{r}\frac{\partial \overline{Z}}{\partial r}-\left(\frac{pS}{T}+\frac{1}{B^2}\right)\overline{Z}=0 \qquad \text{(A.3a)}$$

$$\overline{Z}(\infty,p)=0 \qquad \text{(A.3b)}$$

$$\lim_{r\to 0}\left(r\frac{\partial \overline{Z}}{\partial r}\right)=-\frac{Q}{\pi p K_s} \quad for \quad t>0 \qquad \text{(A.3c)}$$

In Equations A.3a, A.3b, and A.3c, p is the transformation variable. Equation A.3a is the zero order modified Bessel Equation and the general solution is (Hantush, 1964a)

$$\overline{Z}=C_1K_o(Nr)+C_2I_o(Nr) \qquad \text{(A.4)}$$

where $N^2= pS/T + 1/B^2$. In Equation A.4, I_0 and K_0 are the zero order modified Bessel functions of the first and the second kinds, respectively. Since $K_0(\infty)=0$, $I_0(\infty)=\infty$, and $\partial K_0(Nr)/\partial r=-N\ K_1(Nr)$ and as $x\to 0$, $\lim x\ K_1(x)\to 1$, (Carslaw, and Jaeger, 1959) the constants C_1 and C_2 can be obtained by evaluating Equations A.3c and A.4. K_1 in the above expression is the first order modified Bessel function of the second kind.

$$C_1 = \frac{Q}{\pi p K_s} \tag{A.5a}$$

$$C_2 = 0 \tag{A.5b}$$

Substituting Equations A.5a and A.5b into Equation A.4 yields,

$$\bar{Z} = \frac{Q}{\pi p K_s} \frac{1}{p} K_o(Nr) \tag{A.6}$$

Substituting the value of N into Equation A.6 and taking the inverse Laplace transformation of the resultant equation gives the analytical solution of boundary value problem defined by Equation A.1 (Hantush, 1964a)

$$Z = \frac{Q}{2\pi K_s} W\left(\frac{r^2 S}{4Tt}, \frac{r}{B}\right) \tag{A.7}$$

where W is the well function for leaky aquifers which is available in tabular form in the literature (Hantush, 1956; and Walton, 1962). Equation A.7 is identical to Equation 4.15 that is given in chapter 4.

The rate of stream depletion per unit with of an aquifer can be obtained by combining Equation A.7 with Darcy's Law (Hantush, 1964a)

$$q_{r_{uw}} = 0.5 K_s \left(\frac{\partial Z}{\partial x}\right)_{x=0} \tag{A.8}$$

The total rate of stream depletion then can be obtained by

integrating Equation A.8 along the stream boundary (Hantush, 1964b)

$$q_r = 0.5K_s \int_{-\infty}^{+\infty} \left(\frac{\partial Z}{\partial x}\right)_{x=0} dy \qquad \text{(A.9)}$$

and the volume of stream depletion at time t can be obtained by integrating Equation A.9 from t=0 to t (Hantush, 1964b)

$$V_r = \int_{t=0}^{t=t_0} q_r \, dt \qquad \text{(A.10)}$$

The mathematical reduction of Equations A.9 and A.10 gives Equations 4.17 and 4.18. To evaluate the infinite integral in Equation A.9 and the definite integral in Equation A.10, Laplace transformations were used (Hantush, 1964b).

APPENDIX B

LISTING OF COMPUTER PROGRAM

FOR

STREAM DEPLETION CAUSED BY CYCLIC PUMPING OF WELLS

```
C ********************************************************
C --------------------------------------------------------
C |                                                      |
C |  THIS PROGRAM CALCULATES THE IMPACT OF IRRIGATION    |
C |  WATER ON INSTERAM FLOW QUANTITY BY USING UNSTEADY   |
C |  GROUNDWATER FLOW EQUATIONS. THE PROGRAM COMPUTES    |
C |  THE IMPACTS FOR CYCLIC PUMPING.  IT IS ASSUMED  THAT|
C |  THE PUMPING RATIO Q AND AQUIFER CHARACTERISTICS      |
C |  ARE CONSTANT WITH TIME AND SPACE.                   |
C |                                                      |
C |                  WRITTEN AND DEVELOPED               |
C |                                                      |
C |                        By                            |
C |                                                      |
C |               Yakup Darama  Ph.d Candidate           |
C |                                                      |
C |                Michigan State University             |
C |                  College of Engineering              |
C |                                                      |
C |         Department of Civil and Env. Engineering     |
C |                                                      |
C |                East Lansing, Michigan 48824          |
C |                                                      |
C --------------------------------------------------------
C --------------------------------------------------------
C
      INTEGER ANSWER,MUNIT,EUNIT,OPTION,FLAG
C
      IMPLICIT REAL*8 (A-H,O-Z)
      DIMENSION RATEQ(4000)
C
      CHARACTER FLNAME*10
C
C -----------------------------------------------------
C ******** OPENING THE FILE FOR THE OUTPUT ***********
C -----------------------------------------------------
C
      WRITE(*,*) ' OUTPUT FILE NAME FOR BETA1 AND BETA2 ?'
      READ(*,'(A)')FLNAME
      OPEN(UNIT=5,FILE=FLNAME,STATUS='NEW',FORM='FORMATTED')
      WRITE(*,*) ' OUTPUT FILE NAME FOR SDF ?'
      READ(*,'(A)')FLNAME
      OPEN(UNIT=6,FILE=FLNAME,STATUS='NEW',FORM='FORMATTED')
      WRITE(*,*) ' OUTPUT FILE NAME FOR TAU ?'
      READ(*,'(A)')FLNAME
      OPEN(UNIT=7,FILE=FLNAME,STATUS='NEW',FORM='FORMATTED')
C
C ----------------------------------------
C  ************* INPUT VARIABLES *********
C ----------------------------------------
C
```

```
      DX = 1.0
      PI = 4.0*ATAN(DX)
C
10    WRITE(*,7)
7     FORMAT(/,10X,'UNIT SYSTEM FOR INPUT DATA',/
     *        ,10X,'0 = METRIC UNIT ',/
     *        ,10X,'1 = ENGLISH UNIT ',//
     *        ,10X,'PLEASE SPECIFY --> '/)
      READ(*,*)IO
      IF(IO.EQ.0) THEN
        MUNIT = 0
      ELSE
        EUNIT = 1
      ENDIF
      WRITE(*,*) ' STORATIVITY Sy ?'
      READ(*,*) STOR
C
      IF(EUNIT.EQ.1) THEN
       WRITE(*,*) ' TRANSMISSIVITY IN  ft^2/day ?'
       READ(*,*) TRANS
       WRITE(*,*) ' DISTANCE BETWEEN WELL AND RIVER IN ft ?'
       READ(*,*) DIST
       WRITE(*,*) ' PUMPING RATE Q IN ft^3/day ?'
       READ(*,*) Q
C
       ELSEIF(MUNIT.EQ.0) THEN
        WRITE(*,*) ' TRANSMISSIVITY IN  m^2/day ?'
        READ(*,*) TRANS
        WRITE(*,*) ' DISTANCE BETWEEN WELL AND RIVER IN m. ?'
       READ(*,*) DIST
       WRITE(*,*) ' PUMPING RATE Q IN  m^3/day ?'
       READ(*,*) Q
      ENDIF
C
C ---------------------------------------------
C ******* PUMPING CHARACTERISTIC DATA ***********
C ---------------------------------------------
C
      WRITE(*,*)' PUMPING PERIOD DURING ONE CYCLE TP ?'
      READ(*,*) TP
      WRITE(*,*)' CYCLE LENGTH TD in days ?'
      READ(*,*) TD
      WRITE(*,*)' TIME INCREMENT DT in days ?'
      READ(*,*) DT
      WRITE(*,*)' DLT in days FOR CONV TO TAU=0.95 ?'
      READ(*,*) DLT1
      WRITE(*,*)' NUMBER OF MAX ITERATION MAXIT ?'
      READ(*,*) MAXIT
      WRITE(*,*)' TOLERANCE FOR TAUSTR=0.95+TOL ?'
      READ(*,*) TOL
99    WRITE(*,*)' THE VALUE OF TI in days ?'
```

```
      READ(*,*) TI
C
      DLT = DLT1
C ------------------------------------------------
C **** CALCULATION OF AQUIFER RESPONSE TIME TA  ****
C ------------------------------------------------
C
      TA = ( DIST*DIST*STOR )/TRANS
C
      WRITE(5,8)TA
      WRITE(*,8)TA
8     FORMAT(10X,'AQUIFER RESPONSE TIME = ',D20.12)
C
      I = 0
      FLAG = 1
C
C ------------------------------------------------
C **** COMPUTATION OF DIMENSIONLESS VOLUME TAU *******
C ------------------------------------------------
C
50    X1 = DSQRT((TA)/(4.0*TI))
C     ----------------------
      CALL ERRFNC (X1,ERFCX)
C     ----------------------
      XX1 = X1*X1
      EXPTR1 = 1.0/(EXP(XX1))
      A = ((((TA)/(2.0*TI))+1.0)*ERFCX)
      B = (2.0*X1*EXPTR1)/(DSQRT(PI))
      VC1 = (TI/TP)*(A-B)
C
      IF(TI.GT.TP)THEN
C
        TMDIF =TI-TP
        X2 = DSQRT((TA)/(4.0*TMDIF))
C       ----------------------
        CALL ERRFNC (X2,ERFCX)
C       ----------------------
        XX2 = X2*X2
        EXPTR2 = 1.0/(EXP(XX2))
        AA = ((((TA)/(2.0*TMDIF))+1.0)*ERFCX)
        BB = (2.0*X2*EXPTR2)/(DSQRT(PI))
        VC2 = (TMDIF/TP)*(AA-BB)
        TAU = VC1-VC2
C
      ELSEIF(TI.LE.TP)THEN
       TAU = VC1
      ENDIF
C
C ------------------------------------------------
C ***** FIND THE VALUE OF te WHEN TAU = 0.95 ******
C ------------------------------------------------
```

```
C
      TAUSTR = 0.95+TOL
      IF(I.LE.MAXIT) THEN
        I = I+1
        IF((TAU.GE.0.95).AND.(TAU.LE.TAUSTR)) THEN
          TE = TI
          TTA = TE/TA
          WRITE(*,*) ' CONVERGENCE REACHED'
          GO TO 45
        ELSEIF(TAU.LT.0.95) THEN
          IF(FLAG.EQ.2) THEN
            DLT = DLT/2.0
          ENDIF
          FLAG = 1
          TI = TI+DLT
          WRITE(*,51)TAU,TAUSTR
51        FORMAT(5X,'TAU =',F20.10,5X,'TAUSTR =',F10.7)
          GO TO 50
        ELSEIF(TAU.GT.TAUSTR) THEN
          IF(FLAG.EQ.1) THEN
            DLT = DLT/2.0
          ENDIF
          FLAG = 2
          TI = TI-DLT
          GO TO 50
          WRITE(*,52)TAU,TAUSTR
52        FORMAT(5X,'TAU =',F20.7,5X,'TAUSTR =',F10.6)
        ENDIF
C
      ELSE
        WRITE(*,56)I,MAXIT
56      FORMAT(5X,I4,1X,'CONVERGENCE NOT SUCCEEDED',/,
     1         5X,'INCREASE THE VALUE OF MAXIT >',I5)
        GO TO 999
      ENDIF
C
C ------------------------------------------------
C **** COMPUTATION OF IMPACT AT ANY FUTURE TIME ******
C ------------------------------------------------
C
45    WRITE(*,46)
46    FORMAT(/,10X,'CALCULATE qmax ?',/
     *,10X,'(enter OPTION)',/
     *,10X,'TYPE  0 <---------- YES',/
     *,10X,'TYPE  1 <---------- NO',//
     *,10X,'PLEASE SPECIFY ------->',/)
      READ(*,*)OPTION
      IF(OPTION.EQ.1) THEN
        GO TO 190
      ELSEIF(OPTION.EQ.0) THEN
        WRITE(*,91)
```

```
91      FORMAT(5X,' calculating the max. q')

C
C -------------------------------------------------
C ***** COMPUTATION OF IMPACT AT TIME TAU=0.95 ******
C -------------------------------------------------
C
        N = INT(TE/TD)+1
        NN = INT(TD/DT)+5
        DO 4000 I=1,NN
           RATEQ(I) = 0.D0
4000    CONTINUE
C
      K = NN
5000  IF(K.GE.1) THEN
C
       TI = TE-((NN-K)*DT)+DT
C
       write(*,*)K
       SUM1 = 0.D0
       SUM2 = 0.D0
       I = 0
100    IF(I.LE.N) THEN
C
         ARG1 = TI-I*TD
         ARG2 = TI-TP-I*TD
C
         IF(ARG1.GT.0) THEN
           X = DSQRT((TA)/(4*ARG1))
           CALL ERRFNC (X,ERFCX)
           SUM1 = Q*ERFCX
         ENDIF
C
         IF(ARG2.GT.0) THEN
           X = DSQRT((TA)/(4*ARG2))
           CALL ERRFNC (X,ERFCX)
           SUM2 = Q*ERFCX
         ENDIF
C
         IF((ARG1.GT.0).AND.(ARG2.LE.0)) THEN
           RATEQ(K) = RATEQ(K)+SUM1
         ELSEIF((ARG1.GT.0).AND.(ARG2.GT.0)) THEN
           RATEQ(K) = RATEQ(K)+SUM1-SUM2
         ELSEIF((ARG1.LE.0).AND.(ARG2.LE.0))THEN
           SUM1 = 0.D0
           SUM2 = 0.D0
           RATEQ(K) = RATEQ(K)+SUM1-SUM2
         ENDIF
C
         I = I+1
         GO TO 100
```

```
        ENDIF
C
        WRITE(*,21)K,RATEQ(K),TI
21      FORMAT(5X,'RATEQ(',I3,')=',F12.5,5X,'t =',F10.2)
C
C -------------------------------------------------------
C **** FIND MAX IMPACT DURING THE CYCLE WHEN TAU=0.95 *****
C -------------------------------------------------------
C
        IF(K.LE.(NN-2)) THEN
         IF((RATEQ(K+1).GT.RATEQ(K)).AND.
     1                          (RATEQ(K+1).GT.RATEQ(K+2)))THEN
           QMAX = RATEQ(K+1)
           TMAX = TI+DT
           GO TO 450
         ENDIF
        ENDIF
C
C ------------------------------------------------
C ****** CHECK THE DERIVATIVE OF EQ. 3.1 *********
C ------------------------------------------------
C
        IF(K.EQ.(NN-1)) THEN
          SLOPE = (RATEQ(K)-RATEQ(K+1))/DT
          WRITE(*,22)SLOPE
22        FORMAT(5X,'SLOPE =',F15.7)
          IF(SLOPE.LT.0.D0) THEN
            K = ((NN-5)/2)+5
            GO TO 5000
          ELSE
            K = K-1
            GO TO 5000
          ENDIF
        ENDIF
C
        K = K-1
        GO TO 5000
C
        ENDIF
C
C ------------------------------------------------
C *****   CALCULATING THE STREAM DEPLETION  ********
C ***** FOR CYCLE-AVEREGE CONTINUOUS PUMPING *******
C ------------------------------------------------
C
450     X = DSQRT((TA)/(4.0*TMAX))
C
        CALL ERRFNC (X,ERFCX)
C
        QTD = Q*TP/TD
        QC1 = ERFCX*QTD
```

```
C
      X = DSQRT((TA)/(4.0*TE))
C
      CALL ERRFNC (X,ERFCX)
C
      QC2 = ERFCX*QTD
C
C ------------------------------------------
C ****** THE ERROR BETA IN EQUATION 11. ******
C ------------------------------------------
C
      BETA1 = 1.0-QC1/QMAX
      BETA2 = 1.0-QC2/QMAX
C
      TPTA = TP/TA
      TDTP = TD/TP
C
C ------------------------------------------
C ****** PRINTING THE RESULTS *************
C ------------------------------------------
C
      ENDIF
190   CONTINUE
      IF(EUNIT.EQ.1) THEN
      WRITE(5,184)TMAX,RATEQ,QC1
      WRITE(*,184)TMAX,RATEQ,QC1
184   FORMAT(10X,'At t=',F18.0,' days',2X,
     1'qmax =',D15.10,2X,'cu.ft/day'
     2,/,40X,'qc =',D15.10,2X,'cu.ft/day')
      WRITE(5,185)TE,QC2
      WRITE(*,185)TE,QC2
185   FORMAT(10X,'At te=',F18.0,' days',2X,
     1'qc =',D15.10,2X,'cu.ft/day')
      ELSEIF(MUNIT.EQ.0) THEN
      WRITE(5,186)TMAX,QMAX,QC1
      WRITE(*,186)TMAX,QMAX,QC1
186   FORMAT(10X,'At t=',F18.0,' days',2X,
     1'qmax =',D15.10,2X,'cu.m/day',
     2/,40X,'qc =',D15.10,2X,'cu.m/day')
      WRITE(5,187)TE,QC2
      WRITE(*,187)TE,QC2
187   FORMAT(10X,'At te=',F18.0,' days',2X,
     1'qc =',D15.10,2X,'cu.m/day')
      ENDIF
      WRITE(5,255)BETA1,TPTA,TDTP
      WRITE(*,255)BETA1,TPTA,TDTP
255   FORMAT(10X,'BETA1 =',F10.6,5X,'tp/ta =',F10.3,
     15X,'TD/TP =',F10.3)
      WRITE(5,256)BETA2,TPTA,TDTP
      WRITE(*,256)BETA2,TPTA,TDTP
256   FORMAT(10X,'BETA2 =',F10.6,5X,'tp/ta =',F10.3,
```

```
     15X,'TD/TP =',F10.3)
C
C ---------------------------------------------
C *********  WRITING TO SDF FILE *************
C ---------------------------------------------
C
      WRITE(6,257)TPTA,BETA2
257   FORMAT(10X,F10.4,5X,F10.5)
C
      WRITE(7,191)TP,TTA,TAU
      WRITE(*,191)TP,TTA,TAU
191   FORMAT(10X,'Tp =',F5.1,1X,'days',5X,
     1't/ta =',D20.12,5X,'TAU =',D20.12)
C
      WRITE(*,888)
888   FORMAT(/,10X,'CALCULATE THE qmax',/
     *,10X,'FOR ANOTHER TIME (enter ANSWER) ?',/
     *,10X,'TYPE  0 <---------- YES',/
     *,10X,'TYPE  1 <---------- NO',//
     *,10X,'PLEASE SPECIFY ------------->',/)
      READ(*,*)ANSWER
      IF(ANSWER.EQ.0) THEN
       WRITE(*,*)' NEW DISTANCE BETWEEN WELL AND RIVER ?'
       READ(*,*) DIST
       GO TO 99
      ELSEIF(ANSWER.EQ.1) THEN
        WRITE(*,*)' PROGRAM TERMINATED'
        GO TO 999
      ENDIF
C
999   CONTINUE
      STOP
      END
C
C
C ***********************************************
C -----------------------------------------------
C ***********************************************
C
        SUBROUTINE ERRFNC (X,ERFCX)
C       ***************************
C ***********************************************
C -----------------------------------------------
C
C ---------------------------------------------
C |-------------------------------------------
C |                                           |
C |  THIS SUBROUTINE COMPUTES THE VALUE OF ERROR
C |  FUNCTION FOR A GIVEN ARGUMENT X BY USING
C |  THE RATIONAL POLYNOMIAL APPROXIMATIONS
C |                                           |
```

```
C ------------------------------------------------
C ------------------------------------------------
C
C
      IMPLICIT REAL*8 (A-H,O-Z)
      DIMENSION CONST(5)
C
C ------------------------------------------------
C  CONSTANT TERMS IN THE APPROXIMATING FORMULA
C ------------------------------------------------
C
      NCONST = 5
      PT = 0.3275911
      CONST(1) = 0.254829592
      CONST(2) = -0.284496736
      CONST(3) = 1.421413741
      CONST(4) = -1.453152027
      CONST(5) = 1.061405429
C
C ------------------------------------------------
C
C   APPROXIMATION OF ERROR FUNCTION X (erf x) BY
C   RATIONAL APPROXIMATIONS
C
C ------------------------------------------------
C
      SUM = 0.D0
      PARM = 1.0/(1.0+PT*X)
      COEFF = EXP(-(X*X))
C
      DO 500 M=1,NCONST
         AI = FLOAT(M)
         SUM = SUM+CONST(M)*(PARM**(AI))
C
500   CONTINUE
C
      ERFX = 1.0-(SUM*COEFF)
      ERFCX = 1.0-ERFX
      RETURN
C
      END
```

APPENDIX C

LISTING OF COMPUTER PROGRAM

FOR

STREAM DEPLETION BY A PUMPING WELL INCLUDING THE EFFECTS OF LINEAR VARIATION OF WETLAND ET

```
C ------------------------------------------------------------------
C |  PROGRAM TO CALCULATE STREAM DEPLETION AND ET REDUCTION PRODUCED  |
C |  BY CONTINUOUS PUMPING WELLS LOCATED IN HOMOGENEOUS, AND          |
C |  ISOTROPIC AQUIFER.                                               |
C |                                                                   |
C |                      WRITTEN AND DEVELOPED                        |
C |                                                                   |
C |                             By                                    |
C |                  Yakup Darama  Ph.d Candidate                     |
C |                                                                   |
C |                  Michigan State University                        |
C |                    College of Engineering                         |
C |                                                                   |
C |           Department of Civil and Environmental Engineering       |
C |                                                                   |
C |                   East Lansing, Michigan 48824                    |
C |                                                                   |
C ------------------------------------------------------------------
C ------------------------------------------------------------------
C
      IMPLICIT REAL*8(A-H,O-Z)
C
      CHARACTER FLNAME*10,FLIN*10
C
C ------------------------------------------------------------------
C
C  ******************* OPENING THE FILE FOR THE OUTPUT *****************
C
C ------------------------------------------------------------------
C
      WRITE(*,*) ' INPUT FILE NAME - ?'
      READ(*,'(A)')FLIN
      OPEN(UNIT=5,FILE=FLIN,STATUS='OLD')
      WRITE(*,*) ' OUTPUT FILE NAME FOR LEAKY DEPL. - ?'
      READ(*,'(A)')FLNAME
      OPEN(UNIT=6,FILE=FLNAME,STATUS='NEW',FORM='FORMATTED')
      WRITE(*,*) ' ENTER THE OUTPUT FILE NAME FOR CAPTURED ET - ?'
      READ(*,'(A)')FLNAME
      OPEN(UNIT=7,FILE=FLNAME,STATUS='NEW',FORM='FORMATTED')
      WRITE(*,*) ' ENTER THE OUTPUT FILE NAME FOR MINED WATER - ?'
      READ(*,'(A)')FLNAME
      OPEN(UNIT=8,FILE=FLNAME,STATUS='NEW',FORM='FORMATTED')
C
C .... INPUT VARIABLES
C
      DX = 1.0
      PI = 4.0*DATAN(DX)
C
      CALL INPUT(STOR,TRANS,DIST,Q,PET,DT,SOILN,RHOB,SANDM,
     *                  SATK,DTPARM,EPS)
      CALL DEPTH(PI,SOILN,RHOB,SANDM,SATK,PET,EPS,DO)
```

```
      WRITE(*,*) 'DO =',DO
C
      TI = 0.DO
      RATEQ = 0.DO
      RATEQL = 0.DO
      RATEQS = 0.DO
      ETRATE = 0.DO
      QRQET = RATEQL + ETRATE
      TOL = 0.9999*Q
      ENDTIM = 175
15    IF(QRQET.LE.TOL) THEN
        DT = DT * DTPARM
        TI = TI + DT
        UO = SDF(DIST,STOR,TRANS,TI)
        TA = ATA(DIST,STOR,TRANS)
        ALPHA = DIST/ALEAK(TRANS,DO,PET)
C
        CALL BFLUX1(Q,TI,TA,UO,RATEQ)
        CALL BFLUX2(Q,TI,TA,UO,ALPHA,RATEQL)
        CALL REDSTO(Q,TI,UO,ALPHA,RATEQS)
        CALL ETCAP(TI,Q,RATEQS,RATEQL,ETRATE)
C
        QRQET = RATEQL + ETRATE
        WRITE(*,16)TI,QRQET
16      FORMAT(5X,F10.3,5X,F12.6)
        GO TO 15
      ENDIF
C
      STOP
      END
C
C
C ***********************************************************************
      DOUBLE PRECISION FUNCTION ALEAK(TRANS,DO,PET)
C     **********************************************
C -----------------------------------------------------------------
C  FUNCTION TO CALCULATE THE PARAMETER FOR LINEAR ET CAPTURE
C -----------------------------------------------------------------
C
      IMPLICIT REAL*8(A-H,O-Z)
C
C .... CALCULATION OF PARAMETER ALEAK FOR LINEAR ET CAPTURE
C
      ALEAK = DSQRT((TRANS*DO)/PET)
C
      RETURN
      END
```

```
C ***********************************************************************
      SUBROUTINE BFLUX1(Q,TI,TA,U0,RATEQ)
C     ***********************************
C ---------------------------------------------------------------------
C   SUBROUTINE TO CALCULATE BOUNDARY FLUXES WHEN ET CAPTURE IS NOT
C   CONCERNED.
C ---------------------------------------------------------------------
C
      IMPLICIT REAL*8(A-H,O-Z)
C
      XIN = U0
      CALL ERRFNC (XIN,ERFCX)
      RATEQ = Q * ERFCX
      TITA1 = TI/TA
C     WRITE(*,22)TI,RATEQ
C     WRITE(7,22)TI,RATEQ
C22    FORMAT(5X,F10.3,5X,F10.4)
C
      RETURN
      END
C
C
C
C ***********************************************************************
      SUBROUTINE BFLUX2(Q,TI,TA,U0,ALPHA,RATEQL)
C     ******************************************
C ---------------------------------------------------------------------
C   SUBROUTINE TO CALCULATE BOUNDARY FLUXES WHEN ET CAPTURE IS CONCERNED
C ---------------------------------------------------------------------
C
      IMPLICIT REAL*8(A-H,O-Z)
C
      BETA = U0 - ((ALPHA/2.D0)/U0)
      CALL ERRFNC (BETA,ERFCX)
      TERM1 = (1.D0/EXP(ALPHA)) * ERFCX
      ETA =  U0 + ((ALPHA/2.D0)/U0)
      CALL ERRFNC (ETA,ERFCX)
      TERM2 = EXP(ALPHA) * ERFCX
      RATEQL = (Q/2.D0) * (TERM1 + TERM2)
      TITA2 = TI/TA
      DIMQRT = RATEQL/Q
C     WRITE(*,21)TI,RATEQL
      WRITE(6,21)TI,RATEQL .
21    FORMAT(5X,F10.3,5X,F12.6)
C
      RETURN
      END
```

```
C ****************************************************************
      SUBROUTINE REDSTO(Q,TI,U0,ALPHA,RATEQS)
C     ***************************************
C ----------------------------------------------------------------
C  SUBROUTINE TO CALCULATE THE RATE OF MINED WATER FROM AQUIFER
C  STORAGE
C ----------------------------------------------------------------
C
      IMPLICIT REAL*8(A-H,O-Z)
C
      XVAL = U0
      CALL ERRFNC (XVAL,ERFCX)
      ERFU0 = 1.D0-ERFCX
      HALPU0 = - (0.5 * ALPHA/U0)**2
      RATEQS = Q * EXP(HALPU0) * ERFU0
C     WRITE(*,24)TI,RATEQS
      WRITE(8,24)TI,RATEQS
24    FORMAT(5X,F10.3,5X,F12.6)
C
      RETURN
      END
C
C
C
C ****************************************************************
      SUBROUTINE ETCAP(TI,Q,RATEQS,RATEQL,ETRATE)
C     *******************************************
C ----------------------------------------------------------------
C  SUBROUTINE TO CALCULATE THE RATE OF CAPTURED ET
C ----------------------------------------------------------------
C
      IMPLICIT REAL*8(A-H,O-Z)
C
      ETRATE = Q - (RATEQL + RATEQS)
C      AVET = Q - ETRATE
C
C     WRITE(*,26)TI,ETRATE
      WRITE(7,26)TI,ETRATE
26    FORMAT(5X,F10.3,5X,F12.6)
C
      RETURN
      END
```

```
C ***************************************************************
      SUBROUTINE DEPTH(PI,SOILN,RHOB,SANDM,SATK,PET,EPS,DO)
C     ****************************************************
C ---------------------------------------------------------------
C   SUBROUTINE TO CALCULATE DEPTH do WHERE EVAPOTRANSPIRATION FLUX IS
C   NEGLIGIBLE
C ---------------------------------------------------------------
C
C
      IMPLICIT REAL*8(A-H,O-Z)
C
C .... Soil parameters
C
      DG = SANDM
      SIGMAG = 1
C
C .... Air Entry Suction SE in cm of water
C
      PSIES = -0.5/DSQRT(DG)
      SLOPE = -2.0 * PSIES + 0.2 * SIGMAG
      POW1 = 0.67 * SLOPE
      PSI = PSIES * (RHOB/1.3)**POW1
      SE = -10.2 * PSI
      WRITE(*,121)SE
121   FORMAT(5X,' SE = ',F10.5)
      APP = PET * EPS
C
      R = APP/(SATK + APP)
C
C ...Computing the depth do where ET = 0.
C
      PIN = PI/SOILN
      COSEK = 1.D0/SIN(PIN)
      AN = (PIN * COSEK)**SOILN
      ANOM = SATK * AN
      DO = SE * ((ANOM/APP)**(1.0/SOILN) - R)
160   WRITE(*,113)DO
113   FORMAT(5X,'do =',F10.3)
C
      RETURN
C
      END
```

```
C ****************************************************************
      SUBROUTINE ERRFNC (X,ERFCX)
C     ***************************
C ----------------------------------------------------------------
C   SUBROUTINE TO EVALUATE THE VALUE OF ERROR FUNCTION AT POINT X
C ----------------------------------------------------------------
C
      IMPLICIT REAL*8(A-H,O-Z)
C
      DIMENSION CONST(5)
C
      REAL AI
C
C .... CONSTANT TERMS IN THE APPROXIMATING FORMULA
C
      NCONST = 5
      PT = 0.3275911
      CONST(1) = 0.254829592
      CONST(2) = -0.284496736
      CONST(3) = 1.421413741
      CONST(4) = -1.453152027
      CONST(5) = 1.061405429
C
C .... APPROXIMATION OF ERROR FUNCTION X BY RATIONAL APPROXIMATIONS
C
      IF(X.LT.0.DO)THEN
        Y = DABS(X)
      ELSE
        Y = X
      ENDIF
      SUM = 0.DO
      PARM = 1.0/(1.0+PT*Y)
      COEFF = EXP(-(Y*Y))
      DO 200 M=1,NCONST
         AI = FLOAT(M)
         SUM = SUM+CONST(M)*(PARM**(AI))
200   CONTINUE
      IF(X.LT.0.DO)THEN
        ERFX = 1-(SUM*COEFF)
        ERFCX = 1.0+ERFX
      ELSE
        ERFX = 1.0-(SUM*COEFF)
        ERFCX = 1.0-ERFX
      ENDIF
C
      RETURN
      END
```

```
C ***************************************************************
      SUBROUTINE INPUT(STOR,TRANS,DIST,Q,PET,DT,SOILN,RHOB,SANDM,
     *                 SATK,DTPARM,EPS)
C     *********************************
C ---------------------------------------------------------------
C  SUBROUTINE TO READ THE INPUT DATA FROM THE FILE
C ---------------------------------------------------------------
C
      IMPLICIT REAL*8(A-H,O-Z)
C
C .... AQUIFER PROPERTIES
C
      READ(5,*) STOR
      READ(5,*) TRANS
      READ(5,*) DIST
      READ(5,*) Q
      READ(5,*) DT
      READ(5,*) PET
C
C .... SOIL (MATERIAL) PROPERTIES
C
      READ(5,*) SOILN
      READ(5,*) RHOB
      READ(5,*) SANDM
      READ(5,*) SATK
C
C .... CONTROL PARAMETERS
C
      READ(5,*) EPS
      READ(5,*) DTPARM
C
      RETURN
      END
```

```
C ************************************************************
      DOUBLE PRECISION FUNCTION SDF(DIST,STOR,TRANS,TI)
C     ************************************************
C -------------------------------------------------------------
C   FUNCTION TO CALCULATE AQUIFER RESPONSE TIME
C -------------------------------------------------------------
C
      IMPLICIT REAL*8(A-H,O-Z)
C
C
      SDF = DSQRT((DIST * DIST * STOR)/(4.0 * TI * TRANS))
C
      RETURN
      END
C
C ************************************************************
      DOUBLE PRECISION FUNCTION ATA(DIST,STOR,TRANS)
C     ********************************************
C
      IMPLICIT REAL*8(A-H,O-Z)
C
C .... CALCULATION OF AQUIFER RESPONSE TIME TA
C
      ATA = DIST*DIST*STOR/TRANS
C
      RETURN
      END
```

LIST OF REFERENCES

Anat, A., H. R. Duke, and A. T. Corey, 1965, "Steady Upward Flow from Water Table", Hydrology Paper No. 7, Colorado State University, Fort Collins, Colorado.

Bedell, D. J., and R. L. van Til, 1979, "Irrigation in Michigan, 1977", Water Management Division, Department of Natural Resources, Lansing, Michigan, 41 pp.

Bouwer, H., 1978, Groundwater Hydrology, Chapter 1, p. 1-11, McGraw-Hill Inc. New York.

Bredehoeft, J. D., S. S. Papadopulus, and H. H. Cooper, Jr., 1982, "Groundwater: The Water Budget Myth", In Scientific Basis of Water Resources Management, p. 51-57, National Research Council, Geophysics Study Committee, National Academy Press, Washington D. C.

Brooks, R. H., and A. T. Corey, 1964, "Hydraulic Properties of Porous Media", Hydrology Papers, No. 3, pp. 27, Colorado State University, Fort Collins, Colorado.

Burns, A. W., 1983, "Simulated Hydrologic Effects of Possible Ground-Water and Surface-Water Management Alternatives in and Near the Platte River, South-Central Nebraska", U.S. Geologic Survey Professional Paper, 1277-G.

Campbell, G. S., 1985, Soil Physics with Basics, Transport Models for Soil-Plant Systems, Development in Soil Science 14, Elsevier Science Pub. Co. Inc. New York.

Carslaw, H. S., and J. C. Jaeger, 1959, Conduction of Heat in Solids, Second Edition, Oxford University Press, London.

Chung, S. O., 1985, Stochastic Modeling of Water Movement in the Saturated-Unsaturated Zone, Ph.D Dissertation, Iowa State University, Ames, Iowa.

Corey, A. T., 1986, Mechanics of Immiscible Fluids in Porous Media, Chapter 4, p. 131-162, Water Resources Publications, Littleton, Colorado.

Corey, A. T., 1990, "Personal communication".

Duke, H. R., 1965, Maximum Rate of Upward Flow from Water Tables, Masters Thesis, Department of Agricultural Engineering, Colorado State University, Fort Collins, Colorado.

Duke, H. R., 1972, "Capillary Properties of Soils-Influence Upon Specific Yield", Transactions of the ASAE, 15, p. 688-691

Freeze, R. A., and J. A. Cherry, 1979, Groundwater, Chapter 2, p. 29-61, Prentice-Hall, Englewood Cliffs, N.J.

Fulcher, G. W., S. A. Miller, and R. V. Til, 1986, "Effects of Consumptive Water Uses on Drough Flows on the River Raisin", Engineering-Water Management Division, Michigan Department of Natural Resources, Lansing, MI.

Gardner, W. R., 1958, "Some Steady-State Solutions of the Unsaturated Moisture Flow Equation with Application to Evaporation from a Water Table", Soil Science Vol. 85 p. 228-232.

Gardner, W. R., and Fireman, Milton, 1958, "Laboratory Studies of Evaporation from Soil Columns in the Presence of a Water Table", Soil Science, Vol. 85, No. 5.

Gillham, R. W., 1984, "The Capillary Fringe and Its Effect on Water-Table Response", Journal of Hydrology, 67: 307-324

Glover, R. E., and Balmer, C. G., 1954, "River Depletion Resulting from Pumping a Well Near a River", American Geophysical Union Trans., Vol. 35, pt. 3, p. 468-470.

Glover, R. E., 1960, "Groundwater Surface Water Relationship", A Paper at Groundwater Section of Western Resources Conference, Boulder, Colorado, Colorado State University, Paper CER60REG, 8 pp.

Hantush, M. S., 1955, "Discussion of River Depletion Resulting from Pumping a Well Near a River", Trans. American Geophysical Union, Vol. 36, p. 345-347

Hantush, M. S., and Jacob, C. E, 1955, "Non-Steady Radial Flow in an Infinite Leaky Aquifer", Trans. American Geophysical Union, Vol. 36, No. 1, p. 95-100.

Hantush, M. S., 1956, "Analysis of Data from Pumping Test in Leaky Aquifers", Trans. American Geophysical Union, Vol. 37, No. 6, p. 702-714.

Hantush M. S., 1959, "Analysis of Data from Pumping Wells Near a River", Journal of Geophysical Research, Vol. 64, No.

11, p. 1921-1932.

Hantush, M.S., 1963, "Hydraulics of Gravity Wells in Sloping Sands", Transactions of ASCE, v. 128, part 1, pp. 1423-1442.

Hantush, M.S., 1964a, Hydraulics of Wells, in Chow, Ven te, ed., Advances in Hydroscience, Vol. 1, New York, Academic Press, p. 2829-2838

Hantush, M. S., 1964b, "Depletion of Storage, Leakage, and River Flow by Gravity Wells in Sloping Sands", Journal of Geophysical Research, Vol. 69, No. 12., p. 2551-2560.

Hantush, M. S., 1965, "Wells Near Streams with Semipervious Beds", Journal of Geophysical Research, Vol. 70, No. 12, p. 2829-2838.

Hantush, M. S., 1967, "Depletion of Flow in Rigth-Angle Stream Bends", Water Resources Research, Vol.3, No.1 p. 235-240.

Hantush, Mohamed M. S. and Marino, M. A., 1989, "Chance-Constrained Model for Management of Stream-Aquifer Systems", ASCE Journal of Water Resources Planning and Management, Vol. 115, No. 3, p. 259-277.

Henningsen, F. J., 1977, "Irrigation Expansion in Michigan", Michigan State University Cooperative Extension Service, East Lansing, Michigan.

Hillel, D. 1980, Fundamentals of Soil Physics, Academic Press, New York.

Jenkins, C. T., 1968, "Computation of Rate and Volume of Stream Depletion by Wells", Techniques of Water-Resources Investigations of the U.S. Geological Survey, Book 4, Chapter D1, 17 p.

Jenkins, C. T., 1968b, "Electric-Analog and Digital-Computer Analysis of Stream Depletion by Wells", Ground Water v. 6, n. 6, pp. 27-34.

Kazmann, R. G., 1948, "The Induced Infiltration of River Water to Wells", Trans. American Geophysical Union, Vol. 29, p. 85-92.

Markar, M. S., and R. G. Mein, 1987, "Modeling of Evapotranspiration from Homogeneous Soils", Water Resources Research, Vol. 23, No. 10, p. 2001-2007.

McDonald, M. G., and A. W. Harbaugh, 1988, "A Modular Three-Dimensional Finite-Difference Groundwater Flow Model",

Techniques of Water-Resources Investigations of the USGS, Chapter A1, Book 6, Washington.

Merva, G., 1990, "Personal communication"

Moore, R. E., 1939, "Water Conduction from Shallow Water Tables", Hilgardia, Vol. 12, No. 6. p. 383-426

Moulder, E. A., and C. T. Jenkins, 1969, "Analog-Digital Models of Stream-Aquifer Systems", Ground Water, v. 7, n. 5, pp. 19-24.

Mueller, F. A., and J. W. Male, 1990, "A Management Model for Specification of Groundwater Withdrawal Permits.", Paper submitted to Water Resources Research, Department of Civil Engineering, University of Massachusettes, Amherst.

Philip, J. R., 1957, "Evaporation, Moisture and Heat Fields in the Soils", Journal of Meteorology, Vol. 14, p. 354-366.

Prickett, T. A. and C. G. Lonnquist., 1971, "Selected Digital Computer Techniques for Groundwater Resource Evaluation," Illinois State Water Survey, Urbana, Bulletin 55.

Ripple, C. D., J. Rubin, and T. E. A. van Hylckama, 1972, "Estimating Steady State Evaporation Rates from Bare Soils Under Conditions of High Water Table", U.S. Geological Survey Water Supply Paper, 2019-A.

Rorabaugh, M. I., 1956, "Groundwater in Northeastern Louisville and Kentucky with Reference to Induced Infiltration", U.S. Geological Survey Water Supply Paper, 1360-B, 169 pp.

Schleusener, R. A., and Corey, A. T., 1959, "The Role of Hysteresis in Reducing Evaporation from Soils in Contact with a Water Table", Journal of Geophysical Research, Vol. 64, No. 4, p. 469-475

Skaggs, R. W., 1975, "Drawdown Solutions for Simultaneous Drainage and ET", Journal of Irrigation and Drainage Division, ASCE, Vol. 101(IR4), p. 279-291.

Skaggs, R. W. and Y. K. Tang, 1976, "Saturated and Unsaturated Flow to Parallel Drains", Journal of Irrigation and Drainage Division, ASCE, Vol. 102(IR2), p. 221-238.

Skaggs, R. W. and Y. K. Tang, 1979, "Effects of Drain Diameter, Openings and Envelopes on Water Table Drawdown", Transactions of the ASAE, Vol. 22, n. 2 pp. 326-333.

Skaggs, R. W., 1978, A Water Management Model For Shallow Water TAble Soils, Water Resources Research Institute of the University of North Carolina, Report No. 134. 178 pp.

Spalding, C. P., and R. Khaleel, 1991, "An Evaluation of Analytical Solutions to Estimate Drawdowns and Stream Depletion by Wells", Water Resources Research, Vol. 27, No. 4, p. 597-609.

Staley, R. W., 1957, Effect of Depth of Water Table on Evaporation from Fine Sand, Masters Thesis, Colorado State University, Fort Collins, Colorado.

Taylor, O. J., 1971, "A Shortcut for Computing Stream Depletion by Wells Using Analog or Digital Models", Groundwater, Vol. 9, No. 2, p. 9-11.

Theis, C. V., 1941, "The Effect of a Well on the Flow of a Nearby Stream", Trans. American Geophysical Union, Vol. 22, pt. 3, p. 734-738.

Theis, C. V., and Conover, C. S., 1963, "Charts for Determination of the Percentage of Pumped Water Being Diverted from a Stream or Drain", U.S. Geological Survey Water Supply Paper 1545-C, p. C106-C109.

Townley, L. R., and J. L. Wilson, 1980, Description of and User's Manual for a Finite Element Aquifer Flow Model: Aquifem-1, Ralph M. Parsons Laboratory for Water Resources and Hydrodynamics, Report No. 252, Massachusetts Institute of Technology, Cambridge, Massachusettes.

Trescott, P. C., G. F. Pinder and S. P. Larson, 1976, "Finite Difference Model for Aquifer Simulation in Two Dimensions with Results of Numerical Experiments", Techniques of Water-Resources Investigations of the USGS, Chapter 1, Washington.

Walton, W. C., 1962, "Selected Analytical Methods for Well and Aquifer Evaluation", Illinois State Water Survey Bulletin, 49.

Warrick, A. W., 1988, "Additional Solutions for Steady State Evaporation from a Shallow Water Table", Soil Science, Vol. 146, No. 2, p. 63-66.

William, B. A., J. B. Miller, and W. W. Wood, 1973, "Availability of Water in Kalamazoo County, Southwestern Michigan", U.S. Geological Survey Water Supply Paper, 1972.